Studies on Genetic Engineering of Carotenoid Metabolism for Novel Flower Colour

January 2018

Watanabe Kenta

Studies on Genetic Engineering of Carotenoid Metabolism for Novel Flower Colour

A Dissertation Submitted to
the Graduate School of Life and Environmental Sciences,
the University of Tsukuba
in Partial Fulfillment of the Requirements
for the Degree of Doctor of Philosophy in Biotechnology
(Doctoral Program in Bioindustrial Sciences)

Watanabe Kenta

Table of contents

Abbreviations

ABA: abscisic acid

ADH: five-prime untranslated region of *alcohol dehydrogenase*

AMED: Agency for Medical Research and Development

AS: aureusidin synthase

BA: betalamic acid

BAC: bacterial artificial chromosome

C4'GT: chalcone 4'-*O*-glucosyltransferase

CAPS: cleaved amplified polymorphic sequence

CCD: carotenoid cleavage dioxygenase

*c*DOPA5GT: *cyclo*-DOPA 5-*O*-glucosyltransferase

CHI: chalcone isomerase

CHS: chalcone synthase

CHYB: β-ring hydroxylase

CHYE: ε-ring hydroxylase

CRISPR/Cas9: clustered regularly interspaced short palindromic repeat -associated endonuclease 9

CRTISO: carotenoid isomerase

DFR: dihydroflavonol-4-reductase

DOD: L-DOPA 4, 5-dioxygenase

DSBs: double-strand breaks

EAC: escape from adaptive conflict

EST: expressed sequence tag

GGPP: geranylgeranyl pyrophosphate

GGPS: GGPP synthase

IPI: IPP isomerase

IPP: isopentenyl pyrophosphate

LCYB: lycopene β-cyclase

LCYE: lycopene ε-cyclase

L-DOPA: L-3, 4-dihydroxyphenylalanine

MeOH: methanol

MTBE: methyl *tert*-butyl ether

NAA: α –naphthaleneacetic acid

NBRP: National BioResource Project

NBT: new plant breeding technology

NCED: 9-*cis*-epoxycarotenoid dioxygenase

NHEJ: non-homologous end joining

NPTII: Neomycin phosphotransferase II

NT: non-transgenic

Or: Orange

PAM: protospacer adjacent motif

pCmF3H: *flavanone 3-hydroxylase promoter* from *Chrysanthemum morifolium*

PDS: phytoene desaturase

PKR: polyketide reductase

pPcUbi: *ubiquitin 4-2* promoter from *Petroselinum crispum*

PSY: phytoene synthase

PYP1: pale yellow petal 1

SEF: secondary embryoid formation

sgRNA: single guide RNA

THC: 4,2',4',6'- tetrahydroxychalcone

UTR: untranslated region

VP14: viviparous14

ZDS: ξ-carotene desaturase

Z-ISO: 15-*cis*-ξ-carotenoid isomerase

Abstract

Japanese morning glory, *Ipomoea nil*, exhibits a variety of flower colours, except yellow, reflecting the accumulation of only trace amounts of carotenoids in the petals. Therefore there is no vivid yellow coloured Japanese morning glory by crossbreeding. To clarify the factor that determines carotenoid accumulation in the petals of *I. nil* and to establish a new metabolic engineering methodology of creating flowers which have yellow petals, I tried to accumulate carotenoids in the petal of *I. nil* using genetic engineering techniques.

For these purposes, firstly, to make the petal yellow with carotenoids, five carotenogenic genes (*geranylgeranyl pyrophosphate synthase*, *phytoene synthase*, *lycopene β-cyclase* and *β-ring hydroxylase* from *Ipomoea obscura* var. *lutea* and bacterial *phytoene desaturase* from *Pantoea ananatis*) were introduced to a white-flowered Japanese morning glory (*I. nil* cv. AK77) with a petal-specific promoter by *Rhizobium* [*Agrobacterium*]-mediated transformation method. I succeeded to produce transgenic plants overexpressing carotenogenic genes. In the petal of the transgenic plants, mRNA levels of the carotenogenic genes were 10 to 1,000 times higher than those of non-transgenic control. The petal colour did not visually change; however, carotenoid concentration in the petal was increased up to about ten-fold relative to non-transgenic control. Moreover, the components of carotenoids in the petal were changed, in particular several β-carotene derivatives, such as zeaxanthin and neoxanthin, were newly synthesized. This result indicated that there are some other factors contributing the low accumulation levels of carotenoids in the petals, such as carotenoid degradation. Suppression a gene related to carotenoid degradation would make petal yellow. Hence secondly, I demonstrated that clustered regularly interspaced

short palindromic repeat -associated endonuclease 9 (CRISPR/Cas9) technology, one of useful gene suppression tool, enables to disrupt a specific gene in *I. nil*. CRISPR/Cas9 technology is a versatile tool for targeted mutagenesis in many organisms, including plants. However, this technique has not been applied to the Japanese morning glory. A gene encoding dihydroflavonol-4-reductase-B (DFR-B) of *I. nil*, an anthocyanin biosynthesis enzyme, was selected as the target gene, and changes in the stem colour were observed during the early stages of plant tissue culture by *Rhizobium*-mediated transformation. Twenty-four of the 32 (75%) transgenic plants bore anthocyanin-less white flowers with bi-allelic mutations at the Cas9 cleavage site in *DFR-B*, exhibiting a single base insertion or a series of deletions of more than two bases. Thus, these results demonstrate that CRISPR/Cas9 technology enables the exploration of gene functions in this model horticultural plant.

Then thirdly, I investigated the possible involvement of carotenoid cleavage dioxygenase (CCD), which cleaves specific double bonds of the polyene chains of carotenoids, in the regulation of carotenoid accumulation in the petals of *I. nil* via CRISPR/Cas9 technology. Using bioinformatics analysis, seven *InCCD* genes were identified in the *I. nil* genome. Sequencing and expression analyses indicated that potential involvement of *InCCD4* in carotenoid degradation in the petals. Successful knockout of *InCCD4* using the CRISPR/Cas9 system in the white-flowered cultivar *I. nil* cv. AK77 caused the white petals turn to pale yellow. The total amount of carotenoids in the petals of *ccd4* plants was increased 30-fold relative to non-transgenic plants. This result indicates that in the petals of *I. nil*, not only low carotenogenic gene expression but also carotenoid degradation leads to extremely low levels of carotenoids. This is the first study, to my

knowledge, of changing the colour and component and increasing the amount of carotenoid in petals that lack ability to biosynthesis carotenoids and of concerning flower colour changes in higher plants using CRISPR/Cas9 technology.

Chapter 2. Overexpression of carotenogenic genes in the Japanese morning glory *Ipomoea nil*

2.1. Introduction

Carotenoids are yellow pigment colouring flower petals, but *I. nil* accumulates only trace amounts of carotenoids in the petal (Yamamizo et al. 2010). Contrary, there is a distant relative species that contains a high amount of carotenoids bearing a vivid yellow flower, *Ipomoea obscura* var. *lutea* (formally *Ipomoea* sp.). Previous study reported that the transcription levels of carotenogenic genes in petals of *I. nil* were remarkably lower than those in *I. obscura* var. *lutea* (Yamamizo et al. 2010). Because crossbreeding of *I. nil* and *I. obscura* is unsuccessful, I decided to transfer carotenogenic genes of *I. obscura* var. *lutea* to *I. nil* by genetic transformation to produce yellow-flowered *I. nil*. The carotenoid biosynthesis of higher plants consists of multistep reactions (Fig. 5A); isoprene units' polymerization, addition of conjugated double bonds and the conversion of *cis*- to *trans*-configuration, cyclization, hydroxylation, and/or epoxidation (Cuttriss et al. 2007) as described former. However, previous report described that the transcription levels of carotenogenic genes in petals of *I. nil* were remarkably lower than those in *I. obscura* var. *lutea* (Yamamizo et al. 2010). In addition, *PSY* and *GGPS* overexpression did not influence petal colour of *I. nil* in the previous studies (Onda unpublished, Ogata unpublished).

Hence herein this study, to increase the accumulation of carotenoid in the petal of *I. nil*, four carotenogenic genes (*GGPS*, accession number: AB499049; *PSY*, AB499050; *LCYB*, AB499055 and *CHYB*, AB499056) from *I. obscura* var. *lutea* and one [phytoene desaturase (crtI, accession number: D90087)] from bacteria were introduced to *I. nil* with *Agrobacterium*-mediated transformation method (Kikuchi et al. 2005) (Fig. 4B). The former four genes are highly expressed in the flower of *I. obscura* var. *lutea* and encode enzymes that would catalyse carotenoid biosynthesis in the chromoplast (Yamamizo et al. 2010). In

higher plants, four enzymes are involved in the biosynthesis from phytoene to lycopene, however in the plant pathogen *Pantoea ananatis* (formally *Erwinia uredovora*), it is catalysed by only one enzyme, crtI [Fig. 5A, (Misawa et al. 1990, 1994)]. The carotenoid biosynthesis pathway from IPP to zeaxanthin would be catalysed by the translational products of the five genes (hereinafter called '*GPcLC*' from five initials of transgenes; Fig. 5A, B). The previous study reported that constitutive overexpression of *PSY* in tomato caused gibberellin less and showed a dwarf phenotype because the biosynthesis pathway of carotenoid shares GGPP with that of gibberellin (Fray et al. 1995). To prevent the detrimental effect, a tissue-specific promoter is essential for metabolic engineering of carotenoid. In addition, because master regulator (or transcriptional factor) of carotenoid biosynthesis is still unknown, un-expectable regulation would occur when using carotenogenic promoter. Therefore I used petal-specific *flavanone 3-hydroxylase* promoter from *C. morifolium* (*pCmF3H*) (Noda et al. 2013).To modify petal colour of *I. nil*, a *GPcLC* overexpression construct under the control of petal-specific *pCmF3H* (Noda et al. 2013) was introduced to the white-flowered *I. nil*. Here I report the comparison of carotenoid composition and carotenogenic gene expression between transgenic and NT plants.

2.2. Materials and methods

2.2.1. Plant materials and growth conditions

The seeds of *I. nil* cv. AK77 (obtained from the NBRP "Morning glory") were used throughout the experiments in the Chapter 2. The seedlings were grown on vermiculite fertilized with 1,000-fold diluted Hyponex 6-10-5 solution (Hyponex Japan, Tokyo, Japan) once a week under continuous light (60 μmol m^{-2} s^{-1}, FL40SW lamps; NEC Lighting Ltd.,

Tokyo Japan) at 25°C for two weeks. Those plants were transferred under short-day conditions (8 h light: 16 h dark) at 25°C. Immature fruits were collected two to three weeks after flower opening (Ono et al. 2000). The immature embryos were isolated from sterilized immature fruits and cultured on an embryoid induction medium [MS medium (Murashige and Skoog 1962) with 3 mg L^{-1} α –naphthaleneacetic acid (NAA), 6% sucrose and 0.2% Gelrite® (Wako, Tokyo, Japan)] to form the somatic embryos.

2.2.2. Vector construction

The vector was provided by Dr. Oda-Yamamizo. The backbone of the binary vector was pBI121 (Jefferson et al. 1987). Five-prime untranslated region of *alcohol dehydrogenase* (*ADH*) from *Nicotiana tabacum* (Satoh et al. 2004; Matsui et al. 2015) were added to all transgenes for translational enhancer. The sequence of the transit peptide: tp from Rubisco subunit of *Pisum sativum* (Schreier et al. 1985; Misawa et al. 1993) was also added to bacterial *crtI* for plastid localization. The DNA fragments of transgenes were inserted to the *pCmF3H*::*ADH*::(*Trans gene*)::*NOSt* expression boxes, and tandemly existed the multiple cloning sites of pBI121 (Jefferson et al. 1987) one fragment each.

2.2.3. Plant transformation

Previously described *Agrobacterium*-mediated transformation using an immature embryo-derived secondary embryo was performed as previously described (Kikuchi et al. 2005). *Rhizobium radiobacter* (*Agrobacterium tumefaciens*) strain LBA4404 harbouring a ternary plasmid for *virG* N54D51 was used for transformation (van der Fits et al. 2000). The *Rhizobium radiobacter* were grown overnight at 28°C in an LB liquid medium containing

antibiotics. The bacterial cells were collected by centrifugation, washed and suspended with the secondary embryoid formation (SEF) medium (MS medium with 0.5 mg L^{-1} NAA and 6% sucrose). Somatic embryos were soaked in the bacterial suspension for 5 min and transferred to plates of an SEF medium with 0.2% Gelrite® and 10 mg L^{-1} acetosyringone. After three days of co-cultivation, the somatic embryos were washed and transferred to an SEF selection medium containing 25 mg L^{-1} kanamycin and Augmentin (125 mg L^{-1} potassium clavulanate and 250 mg L^{-1} Amoxicillin; Glaxo SmithKline K.K., Uxbridge, UK). Two to three weeks after selection, they were transferred to an embryoid maturation and germination medium [MS medium with 0.2 mg L^{-1} indoleacetic acid, 2 mg L^{-1} benzylaminopurine, 3% sucrose and 1.2% agar] contained 50 mg L^{-1} kanamycin and Augmentin. After two to six months, when the shoots were regenerated, they were transferred to a hormone-free 1/2 MS medium with 25 mg^{-1} kanamycin and Augmentin. When the roots were induced on the regenerated shoots, plantlets were transplanted to moist vermiculite for acclimatization. As the transgenic plants directly germinated from kanamycin-resistant secondary embryos, I described these plants as the T1 generation. The validity of transformation was confirmed by PCR using total DNA extracted from young leaves and primers for *Neomycin phosphotransferase II* (*NPTII*; Forward: 5' GAGGCTATTCGGCTATGACT 3', Reverse: 5' TCCCGCTCAGAAGAACTCGT 3'). Total DNA was extracted from the young leaves of plants using a previously described method (Edwards et al. 1991). PCRs were performed with GoTaq® Green Master Mix (Promega, Madison, WI, USA) on a thermal cycler, with initial denaturation at 95°C for 2 min followed by 35 cycles at 95°C for 30 s, 55°C for 30 s and 72°C for 1 min and a subsequent extension step at 72°C for 5 min. The progeny of the transformation plants (T2 and T3

generation) were also confirmed by the same DNA extraction and PCR condition using *NPTII* primers.

2.2.4. Quantitative real-time PCR (RT-qPCR) and reverse transcriptional PCR analysis

Total RNAs were isolated from petals at each stage by using the Get pure RNA Kit (Dojindo, Kumamoto, Japan). Then, cDNAs were synthesized from total RNA (1.0 μg) by the use of the SuperScriptIII First-Strand Synthesis System (Invitrogen, Thermo Fisher Scientific, Waltham, MA, USA) with oligo $(dT)_{20}$.

Transcript levels of *GGPS*, *PSY*, *LCYB*, and *CHYB* were analysed via RT-qPCR with Power SYBR™ Green PCR Master Mix (Applied Biosystems, Thermo Fisher Scientific) and Applied Biosystems 7900HT Fast Real Time PCR System (Applied Biosystems), according to the manufacturers' instructions. Each reaction (final volume, 10 μL) consisted of 5 μL 2x Power SYBR™ Green PCR Master Mix, 0.4 μM each of the forward and reverse primers, and 0.1 μL of the cDNA template (corresponding to 1 ng of total RNA). The reaction mixtures were heated to 95°C for 10 min, followed by 40 cycles at 95°C for 15 s and 60°C for 1 min. A melting curve was generated for each sample at the end of each run to ensure the purity of the amplified products. The transcript levels were calculated according to the ΔΔCt method using the *Ubiquitin* and *Actin* gene for reference (Livak and Schmittgen 2001). The primer sets were designed as which could amplify both transgenes and internal genes (Table 1). The Tukey-Kramer test was used for the statistical analysis. The results are presented as the standardized mean of three independent experiments with the SE.

The transcript level of bacterial *crtI* transgene was analysed using reverse transcription PCR (semi-quantitative RT-PCR) with BIOTAQ^{TM} (Bioline Reagents Ltd, London, UK). Reactions were carried out on a Takara PCR thermal cycler Dice (Takara Bio Inc., Shiga, Japan), starting denaturation at 95°C for 2 min followed by 25 cycles at 95°C for 30 s, 55°C for 30 s and 72°C for 30 s and a subsequent extension step at 72°C for 5 min. The *Ubiquitin* gene was used as an internal standard. The PCR products were separated on 1.5% agarose gels and then stained with ethidium bromide solution.

2.2.5. Carotenoid extraction and HPLC analysis

Carotenoids were extracted from petals and were analysed by HPLC, according to previously described method (Kishimoto et al. 2007) with slight modification. An acetone extract of frozen petals (0.5 g) was partitioned between diethyl ether and aqueous NaCl. The organic layer was washed with 5.0 mM Tris-HCl (pH 8.0), and the residue was saponified with equivalent 10% KOH–MeOH for 1 h at room temperature. The saponified matter was then extracted with diethyl ether and washed with water. The organic layer was dried and dissolved in 125 μL MeOH and subjected to HPLC analyses. The non-saponified carotenoid extract was prepared with the same method except saponification step. Each carotenoid extract was analyzed by HPLC with a Jasco MD-915 photodiode array detector (Jasco, Tokyo, Japan) under the following conditions: column, YMC Carotenoid (250 mm × 4.6 mm i.d., 5 μm; YMC, Kyoto, Japan); solvent A, MeOH/ methyl *tert*-butyl ether (MTBE)/ H_2O = 95 : 1 : 4 (v/v/v); solvent B, MeOH/ MTBE/ H_2O = 25 : 71 : 4; gradient, 0/100, 12/100, 96/0 (min/% A); flow rate, 1.0 mL·min^{-1}; column temperature, 35°C; UV/visible monitoring range, 200–600 nm. To identify carotenoids, the following carotenoid standards

have been used: violaxanthin, neoxanthin (DHI lab products, Hørsholm, Denmark), lutein, β-carotene (Sigma-Aldrich, St. Louis, MO, USA), zeaxanthin and β-cryptoxanthin (Extrasynthese, Genay, France). The total content of carotenoids was estimated from the absorbance at absorption maxima using the $E^{1\%}$ value of lutein (2550) (Britton 1995), which was defined as the theoretical absorbance of a 1% solution in a cell of 1 cm pathlength. The content of each carotenoid was calculated according to the total peak area of HPLC chromatograms at a wavelength of 450 nm, using program ChromNAV ver. 2 (Jasco). Measurements were performed in triplicate.

2.3. Results

2.3.1. Transgenic lines

More than ten lines of transgenic plants were produced from independent transformation events by *Rhizobium*-mediated transformation method. All transgenic plants grew normally and had fertility. No morphological difference between transgenic and NT plants was visually distinguished, even in the colour of the opened flower (Fig. 6A). The T3 generations of the homozygous individuals of three lines (#1-2, #5-9 and #13-11) with highest expression of *PSY* mRNA in the petals were selected for further study.

2.3.2. Analysis of carotenogenic gene expression in transgenic plants

Standard curve for PCR efficiency of each endogenous gene and transgene was independently examined. Because the PCR efficiency in all amplicons of each gene showed almost same value (Table 1), I calculated expression levels without distinction of endogenous gene and transgene. The expressions of *GGPS*, *PSY*, *LCYB*, and *CHYB* in the

petals of fully opened flowers after normalization using *Ubiquitin* and *Actin* as the reference gene were almost similar (data not shown). Both the expression levels in the petals of fully opened flowers were significantly increased in transgenic *GPcLC* plants. The expression levels of all the genes tested were about 10 to 1,000 times higher than those of NT (Fig. 6B). Bacterial *crtI* was also highly expressed in the petal of the three transgenic lines but was not present in the NT control (Fig. 6C).

2.3.3. HPLC analysis of carotenoids

HPLC chromatograms of the carotenoid extracts obtained from the petal of the three transgenic lines differ from that obtained from NT. Representative chromatograms of saponified and non-saponified carotenoid extract of NT and transgenic line #1-2 are shown in Fig. 7A, B respectively. These analyses were performed to identificate carotenoid composition and existence of esterified carotenoids, respectively (Yamamizo et al. 2010). In the petal of NT, only a trace amount of lutein and violaxanthin were detected and the other carotenoid components were below the detection limit (Table 2). On the other hand, zeaxanthin and neoxanthin were detected in the petals of three transgenic lines. Moreover, β-cryptoxanthin and β-carotene were also detected in the two transgenic lines (#1-2 and #13-11). These carotenoid components are β-carotene derivatives (Fig. 5A right side) which biosynthetic pathway is supposed to be enhanced by the transgenes. Total carotenoids in the petals of the three lines were significantly increased (Fig. 7C). Especially in #1-2 and 13-11, these carotenoid levels were about ten times higher than in NT. Although I could not observe visually yellowish petals, a novel *I. nil* flower that contains various carotenoids was established. The HPLC chromatogram of the non-saponified carotenoid extract was almost

the same as that of the saponified extract, indicating that carotenoids contained in the petals of transgenic plants were not esterified (Fig. 7A, B).

2.4. Discussion

In the present study, I succeeded to produce transgenic plants overexpressing carotenogenic genes. In the petals of fully opened flowers of the transgenic plants, transcription levels of all the transgenes were increased. The carotenoid compositions in the petal of the transgenic plants were dramatically changed. The lutein (α-carotene derivative; Fig. 5A left side) and the violaxanthin (β-carotene derivative, Fig. 5A right side) were increased as compared with NT. Moreover, zeaxanthin and β-cryptoxanthin (β-carotene derivatives) were newly detected. The possible explanation for the result is that high expression of *GGPS*, *PSY*, and *crtI* enhanced the activity of the whole biosynthetic pathway, and both α- and β-carotene derivatives were increased. Moreover, *LCYB* and *CHYB* enhanced activity of biosynthetic pathway, in particular β-carotene derivative branch. These two genes encode the enzymes that catalyze β-ring cyclization and hydroxylation, respectively, so β-carotene derivatives would be specifically produced.

In general, PSY is a rate-limiting enzyme of carotenoid biosynthesis in higher plant (Wise and Hoober 2006). In addition, previous study showed that *CHYB* is mainly responsible for the regulation of chromoplast-specific carotenoid accumulation in petals of tomato (Galpaz et al. 2006), because the CHYB catalyses the addition of hydroxyl residues required for esterification carotenoids and esterification is an important event in carotenoid accumulation in the chromoplast.

Therefore, I expected that overexpressing the genes encoding key enzymes of carotenogenesis would increase the carotenoid levels sufficient for yellow pigmentation. However, the carotenoid levels in the petal of the *GPcLC* transgenic plants were increased up to about 1 μg g^{-1}(Fig. 7C), which was not sufficient to make petals yellow visually. Carotenoid level of the petal of the fully opened flower of *I. obscura* var. *lutea* is about 100 μg g^{-1} (Yamamizo et al. 2010), so at least a hundred-fold of carotenoid accumulation would be needed to make petal colour visually yellow. The previous studies on carotenoid metabolic engineering in crops reported that only overexpressing the biosynthesis genes could increase carotenoid amount in the tissue that is almost carotenoid-free. Overexpressing only bacterial *PSY*, *crtB*, in the seeds of *B. napus* made 50-fold increase in carotenoids (Shewmaker et al. 1999) and overexpressing *PSY* and *crtI* in endosperm of *O. sativa* made total carotenoids up to 37 μg g^{-1} (Paine et al. 2005). In contrast to these previous studies (Shewmaker et al. 1999; Paine et al. 2005), in the petal of *I. nil*, only overexpressing the carotenogenic genes could not increase the level of carotenoids high enough to express yellow colour. One possible reason was postulated; carotenoids would be degraded.

Reportedly, carotenoid degradation is caused by the action of CCD4 in petals of some higher plants (Ohmiya 2009; Ahrazem et al. 2016). In *I. nil*, substantial amount of *InCCD4* are also expressed in the petal (Yamamizo et al. 2010), so it would cleave carotenoids. Suppressing the *InCCD4* would increase carotenoid accumulation. However, in the previous study in *C. morifolium*, to suppress the *CmCCD4a* expression, a single *CmCCD4a* RNAi construct were introduced, but the carotenoid amount in the petal of the transformant was below the detection limit (Ohmiya et al. 2009). Introducing two different *CmCCD4a* RNAi

constructs made petal colour from white to yellow, and its carotenoid amount was increased up to 102 μg g^{-1} but was still much less than that of yellow-flowered cultivars (Kishimoto et al. 2007; Ohmiya et al. 2009). The completely knocking out the *CmCCD4* expression might make the yellow petal colour much deeper. Also in *I. nil*, completely knocking out the *InCCD4* with the targeted mutagenesis might lead to the yellow petal. Hence the attempt of analysing and knocking out the *InCCD4* was conducted in the chapter 4 in the thesis.

Recent studies reported that the high-quality genome sequence (Hoshino et al. 2016) and the success of genome editing by CRISPR/Cas9 system (the Chapter 3) in *I. nil*. These information and technology would enable advanced carotenoid metabolic engineering so more progressive studies using *I. nil* will be conducted. If carotenoid accumulation will be enabled in a petal of *I. nil*, the range of colour variation of the flower will get almost no limitation with crossbreeding with other anthocyanin pigmented flowers, because varied colours of anthocyanin-pigmented flowers of *I. nil* were already produced in the seventeenth century. It would be the fusion of a modern genetic engineering technology and a past developing traditional breeding technique, in other words, the connection between innovation and tradition.

2.5. Tables and Figures

Table 1. Primer sets used for qRT-PCR and reverse transcriptional PCR analysis

Gene	Direction	Sequence	Product length /bp	PCR efficiency		Base mismatch count between endogenous gene & transgene
				Endogenous gene	Transgene	
GGPS	Forward	5' CGGTGGAGATGATTCACACCA 3'	65	1.015	1.044	3
	Reverse	5' CTCGCCGCAAATCGTCGTT 3'				
PSY	Forward	5' ACAGTATCCAGGTTTCCAGTTGA 3'	73	1.010	1.002	0
	Reverse	5' TCCAGAGGTCCATTCGCATT 3'				
LCYB	Forward	5' AGGCACTTAGGTATCAACGTCA 3'	127	0.975	0.985	2
	Reverse	5' GATGAACCATACCTGCAGTACCG 3'				
CHYB	Forward	5' ACAGATTCGCTTGGCAAATGGAG 3'	72	1.017	1.007	1
	Reverse	5' CGGAGAGAGCAAATGTACCGAAC 3'				
Ubiquitin	Forward	5' CTTGTCCTTCGTCTCCGTGGTG 3'	65	0.986	-	-
(qPCR)	Reverse	5' GCAGTGACACAAACATCATTGGG 3'				
Actin	Forward	5' CGTTCAGCTGAGGTTGTGAAAGA 3'	71	1.012	-	-
	Reverse	5' CGTGACCTCACTGATCATTTGATG 3'				
crtI	Forward	5' CTGTGGAGCCCGTTCTTACC 3'	136	-	-	-
	Reverse	5' GTCATCGGCTCGGCAAA 3'				
Ubiquitin	Forward	5' CTCCATCTCGTGCTCCGTTTGA 3'	363	-	-	-
(RT-PCR)	Reverse	5' GCCCTCCTTGTCCTGAATCTTG 3'				

Table 2. Concentrations of carotenoid compounds in the petals.

		Violaxanthin	Un-identified	Neoxanthin	Lutein	Zeaxanthin	β-cryptoxanthin	β-carotene
NT		0.028 ±.003	0.015 ±.002	ND	0.042 ±.007	ND	ND	ND
GPcLC	#1-2	0.188 ±.032	0.091 ±.005	0.108 ±.011	0.109 ±.007	0.306 ±.040	0.020 ±.004	0.022 ±.008
	#5-9	0.110 ±.025	0.041 ±.011	0.032 ±.011	0.073 ±.004	0.051 ±.010	ND	ND
	#13-11	0.216 ±.033	0.107 ±.002	0.075 ±.005	0.212 ±.005	0.154 ±.004	0.007 ±.004	0.020 ±.005

Values are expressed as μg g^{-1} FW; ND, not detectable; FW, fresh weight. Each value represents the mean result from triplicate ±SD.

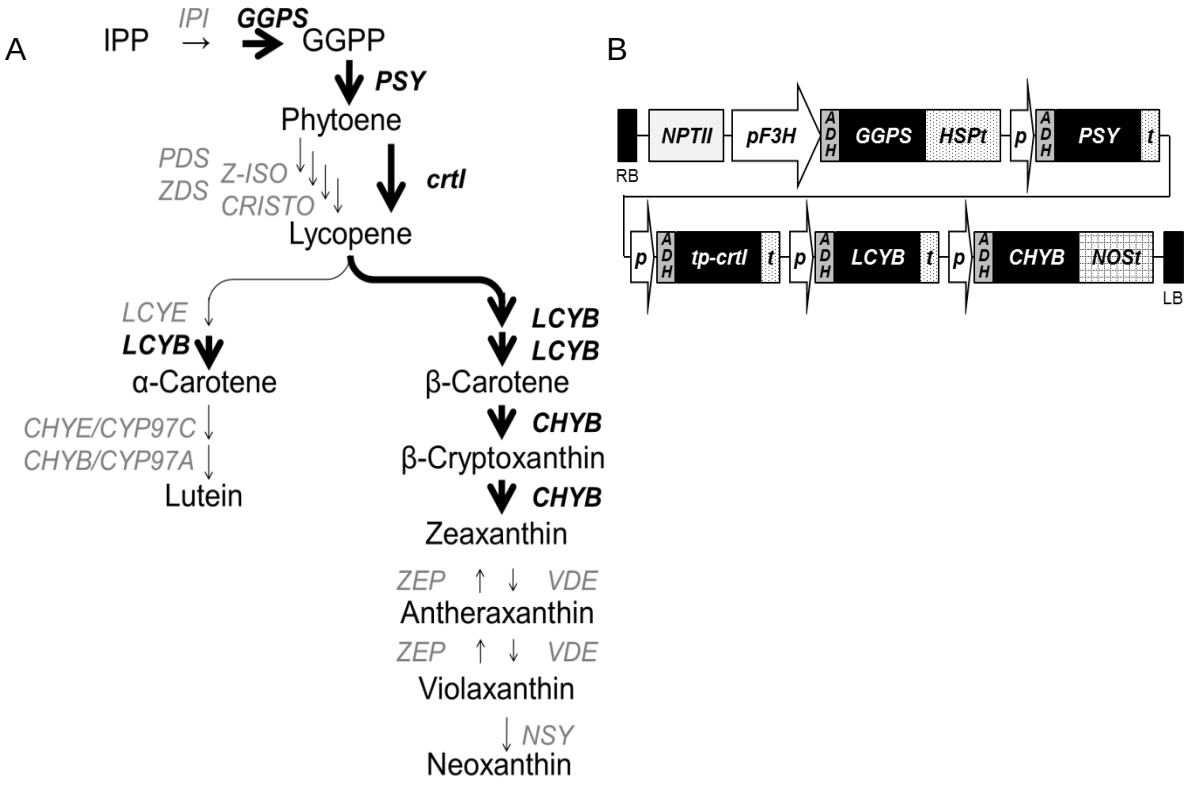

Fig. 5. Schematic of the carotenoid biosynthesis pathway in plants and the vector construct used in the present study. A: Carotenoid biosynthesis pathway. Bold arrows indicate the introduced transgenes in this study. IPP, isopentenyl pyrophosphate; *IPI*, *IPP isomerase*; GGPP, geranylgeranyl pyrophosphate; *GGPS*, *GGPP synthase*; *PSY*, *phytoene synthase*; *PDS*, *phytoene desaturase*; *Z-ISO*, *15-cis-ξ-CRTISO*; *ZDS*, *ξ-carotene desaturase*; *CRTISO*, *carotenoid isomerase*; *crtI*; *phytoene dehydrogenase* from plant pathogen (*P. ananatis*), *LCYE*, *lycopene ε-cyclase*; *LCYB*, *lycopene β-cyclase*; *CHYE*, *ε-ring hydroxylase*; *CHYB*, *β-ring hydroxylase*, *ZEP*, *zeaxanthin epoxidase*; *VDE*, *violaxanthin deepoxidase*; *NSY*, *neoxanthin synthase*. **B:** T-DNA region of the construct (*GPcLC*). RB: right border, *NPTII*: *neomycin phosphotransferase II*, *pF3H* [*p*]: promoter of *flavanone 3-hydroxylase* of *Chrysanthemum morifolium* (petal specific promoter), *ADH*: 5'UTR region of *alcohol dehydrogenase* (translational enhancer), *HSPt* [*t*]: terminator of *heat shock protein*, *tp*: *transit peptide*, *NOSt*: terminator of *nopaline synthase*, LB: left border.

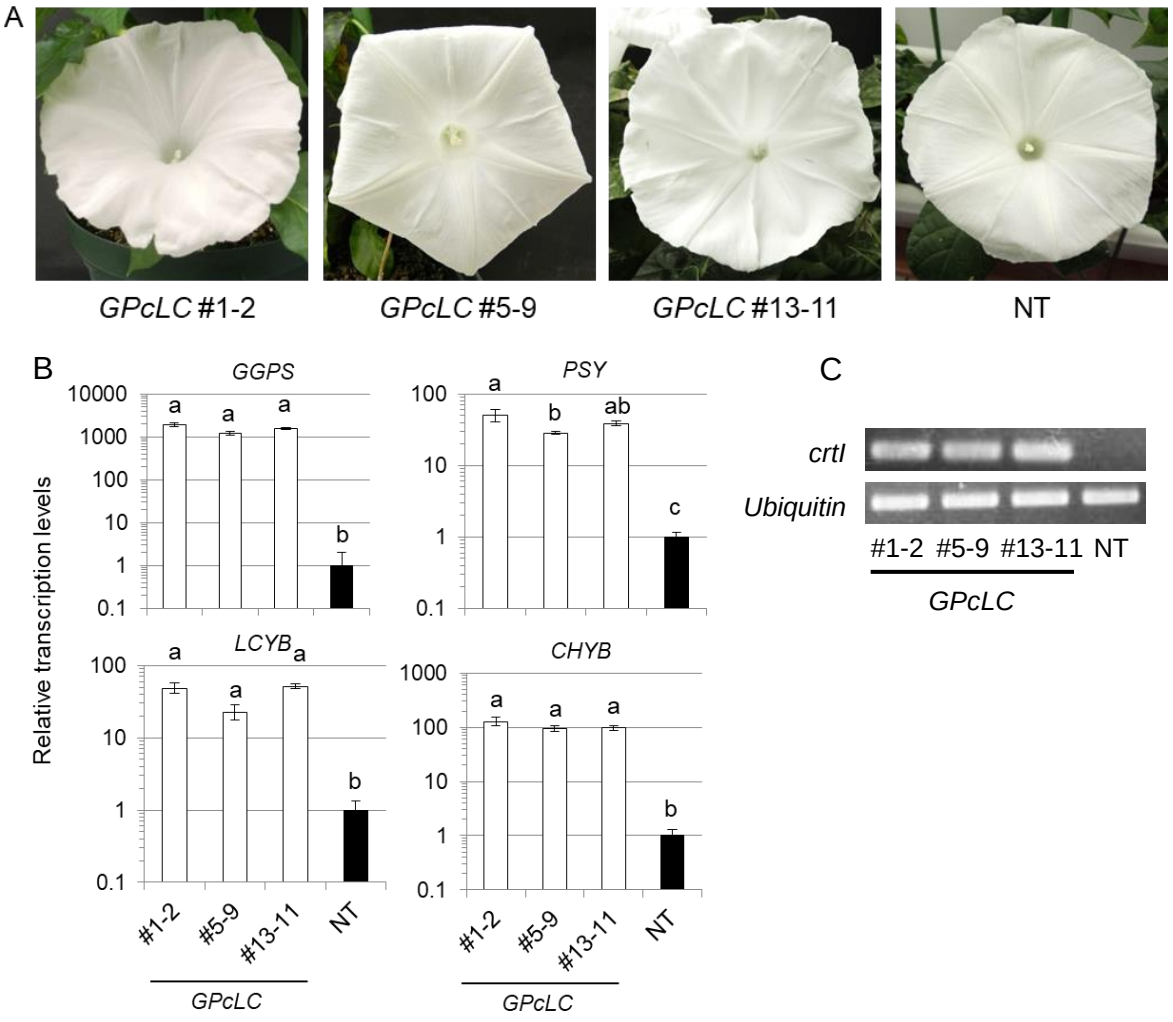

Fig. 6. Carotenogenic genes expression levels in the transgenic plants. A: Appearance of *GPcLC* #13-11 and non-transgenic (NT) flowers. **B:** Relative expression levels of the botanical transgenes in opened flower of the transgenic *GPcLC* plants detected by RT-qPCR analyses (white bars). The primer sets used for the analysis were designed as which could amplify both transgenes and internal genes. *I. obscura* (grey bars): *I. obscura* var. *lutea*; The expression levels were normalized against mRNA levels of *Actin*. Different letters indicate significant differences by Tukey-Kramer test (P <0.01). Error bars indicate standard error (SE, n = 3). **C:** Expression levels of the bacterial *crtI* genes in opened flower of the transgenic *GPcLC* plants detected by Semi-quantitative reverse transcriptional PCR analysis. The constitutively expressed gene for the *Ubiquitin* in *I. nil* was used as an internal control.

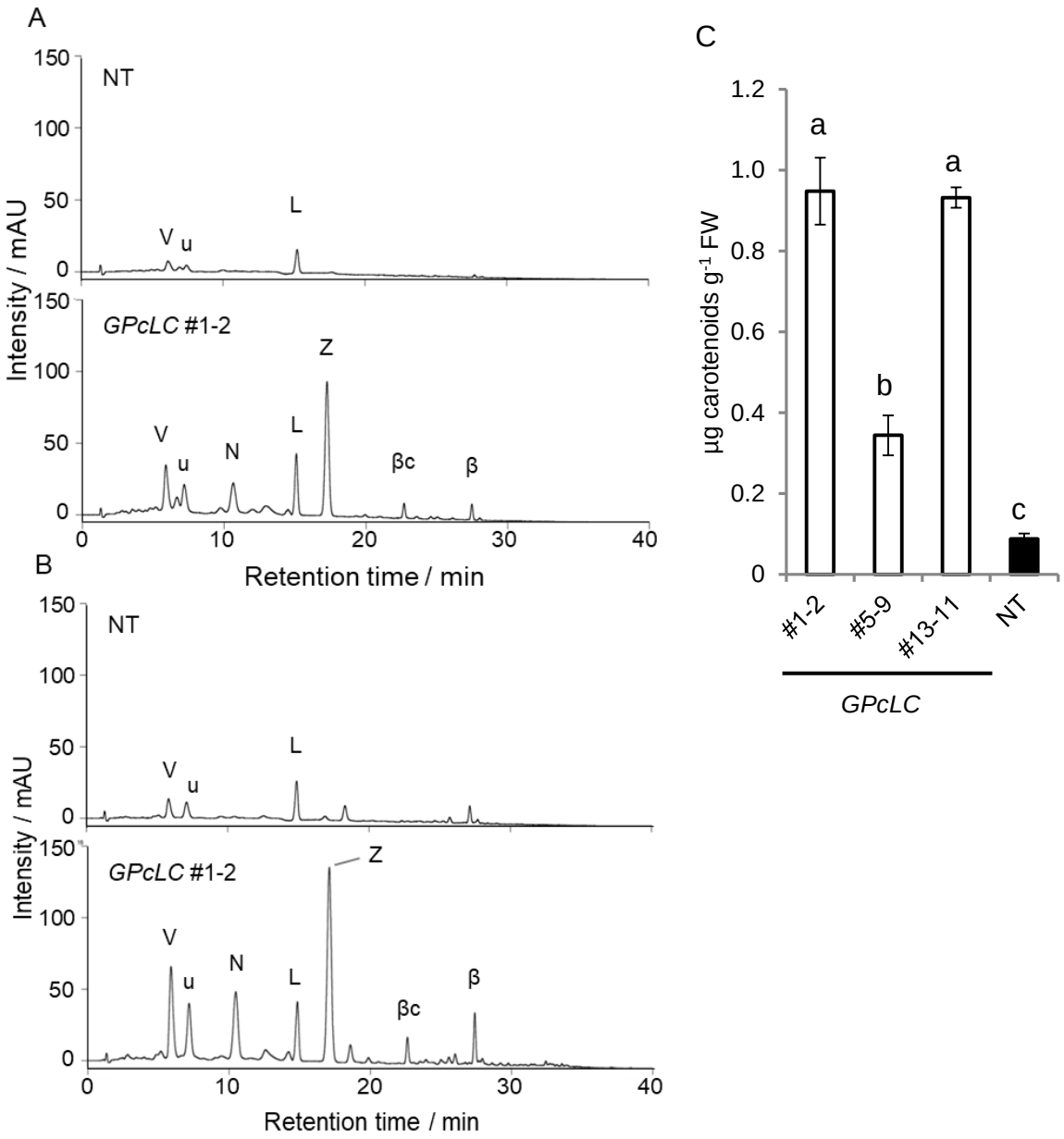

Fig. 7. HPLC chromatograms and total carotenoid concentration of flowers of non-transgenic (NT) and transgenic *GPcLC* plant. A, B: HPLC elution profiles of saponified and non-saponified carotenoids extracted from petals of opened flower, respectively. Upper: NT; lower, *GPcLC* #1-2. V, violaxanthin; u, un-identified carotenoid; N, neoxanthin; L, lutein; Z, zeaxanthin; βc, β-cryptoxanthin; β, β-carotene. **C**: Total carotenoid contents in open flower of the NT and *GPcLC*, as determined by HPLC analysis after saponification. All experiments were biologically repeated three times. Different letters indicate significant differences by Tukey-Kramer test (P <0.05). Error bars indicate standard error (SE, n = 3).

Chapter 3. CRISPR/Cas9-mediated mutagenesis of the *dihydroflavonol-4-reductase-B* (*DFR-B*) locus in the Japanese morning glory *Ipomoea nil*

3.1. Introduction

Methods for targeted mutagenesis have rapidly been developed, and their applications to exotic plants are gradually advancing (Shan et al. 2013; Zhang et al. 2016b). Several systems have been developed to induce DNA double-strand breaks (DSBs) at specific genome sites. Such breaks provide increased opportunities to induce site-directed mutations through DNA repair systems, such as non-homologous end joining (NHEJ) (Puchta and Fauser 2014). Among engineered nuclease systems for DSBs, the CRISPR/Cas9 system can be applied more readily than other systems because of its simple experimental design and high specificity (Puchta 2017). The CRISPR/Cas9 system has been successfully utilized for targeted mutagenesis in a variety of organisms, including plants, and will increase reverse genetic studies, particularly for plants with good transformation systems and high-quality genome sequences.

However, this technique has not been applied to the Japanese morning glory. Here in this Chapter, to confirm the applicability of the CRISPR/Cas9 system to *I. nil*, I selected *DFR-B* (*difydroflavonol-4-reductase -B*), the gene encoding an enzyme in the anthocyanin biosynthesis pathway (Dooner et al. 1991), and CRISPR/Cas9 system-mediated changes in the stem colour were observed during the early stages of plant tissue culture via *Rhizobium*-mediated transformation. Moreover, in morning glories, including *I. nil*, *DFR* is present as a small, tandemly arrayed three-gene family (*DFR-A*, *DFR-B* and *DFR-C*), although most *Solanaceae* species, the relatives of *Convolvulaceae*, including *Ipomoea*, have a single copy of the *DFR* gene (Inagaki et al. 1999). In the common morning glory, *Ipomoea purpurea*, all three genes are expressed, but *DFR-B* is the main gene and is interpreted as EAC. Moreover, in *I. nil*, these three genes are structurally normal, but *I. nil*

DFR-B (*InDFR-B*) is the genetically dominant gene responsible for pigmentation in the stems and flowers, as several spontaneous mutants of *InDFR-B* have shown the null phenotype (Inagaki et al. 1996). Thus, it remains unknown whether the targeted mutagenesis of *InDFR-B* located between *InDFR-A* and *InDFR-C* causes the null phenotype. Additionally, to confirm the accuracy of the CRISPR/Cas9 system, potential off-target modifications on the two orthologous genes, namely, *DFR-A* and *DFR-C*, were examined. These observations reconfirm the importance of the protospacer adjacent motif (PAM) in targeted mutagenesis using the CRISPR/Cas9 system in *I. nil*. The Cas9 protein is an endonuclease functioning with single guide RNA (sgRNA). The Cas9, sgRNA complex scans double-stranded DNA to detect DNA sequences complementary to the 20 nt target sequence in the sgRNA and the NGG motif, referred to as the PAM, located immediately after the target sequence. The PAM is essential for the binding of CRISPR/Cas9 to the DNA target (Nishimasu et al. 2014; Sternberg et al. 2014).

The first spontaneous white flower mutant in *I. nil* was painted in 1631 in Japan, approximately 850 years after the initial import of the blue wild-type flower plants from China. Using the CRISPR/Cas9 system, within a year, white flower mutants were generated several at the same locus but affecting different alleles, indicating the strength of this system and its future prospects. To my knowledge, this study is the first to establish changing flower colour in higher plants using the CRISPR/Cas9 system.

3.2. Materials and methods

3.2.1. Plant materials and growth conditions

The seeds of *I. nil* cv. Violet (obtained from the NBRP "Morning glory") were used for the experiments. The growth conditions and were same as former described conditions in the Chapter 2.

3.2.2. Vector construction and transformation

An all-in-one binary vector (Mikami et al. 2015) harbouring sgRNA, *Friedrich Fauser's Cas9* (*FFCas9*) and *NPTII* expression loci was constructed as previously described (Ito et al. 2015). Briefly, two complementary oligo DNAs for the *DFR-B* target sequence (Forward: 5' ATTGAAGCATCATACCACCACTAG 3'; Reverse: 5' AAACCTAGTGGTGGTATGA-TGCTT 3') were annealed at 95°C for 5 min. The target sequence-cloning vector, pUC19_AtU6oligo, was digested with restriction enzyme *Bbs*I and ligated to the annealed oligo DNA. The cloning vector and binary vector, pZD_AtU6gRNA_FFCas9_NPTII, were digested with the restriction enzyme I-*Sce*I, and the sgRNA expression cassettes of each vector were subsequently exchanged. The transformation method was same as the former described method in the Chapter 2.

3.2.3. Cleaved amplified polymorphic sequence (CAPS) analysis

DNA fragments of *InDFR*s were PCR-amplified using total DNA of transformants with GoTaq® Green Master Mix (Promega) and the specific primers (*InDFR-A* Forward: 5' CATAAAACCATTAGACCTG 3', *InDFR-A* Reverse: 5' AAATAACATATTGAATTCTGC 3'; *InDFR-B* Forward: 5' TGCGGTTACCAAGCTAACGAA 3', *InDFR-B* Reverse: 5'

GTGATCATGTCCGCTAAACCA 3'; *InDFR-C* Forward: 5' TTGCGGATTTCCCTAT-TGGAT 3', *InDFR-C* Reverse: 5' GTTCCCTATAGAGACCGGACA 3', *InPSY*: Forward: 5' GTGCAGAGTATGCAAAGACG 3', *InPSY* Reverse: 5' GCCTAGCCTCCCATCTATCC 3'). The thermal cycles of the reaction were same as the *NPTII* reactions in *InDFR-B*, InDFR-C and *InPSY*. The PCR cycles for *InDFR-A* were as follows: initial denaturation at 95°C for 2 min followed by 35 cycles at 95°C for 30 s, 50°C for 30 s and 72°C for 1 min and a subsequent extension step at 72°C for 5 min. The amplified DNA fragments were digested with *Spe*I and analysed via agarose gel electrophoresis.

3.2.4. Sequencing analysis

The total DNAs and *InDFR-B* primers were the same as those used in the CAPS analysis. Primer sets for candidates of off-target mutation were listed in Table 3. The PCRs were performed using Advantage® 2 Polymerase Mix (BD Biosciences Clontech, Palo Alto, CA, USA) on a thermal cycler, with an initial denaturation at 95°C for 1 min followed by 35 cycles of 95°C for 30 s and 68°C for 1 min and a subsequent extension step at 68°C for 1 min. The PCR products were cloned into the pGEM®-T Easy Vector (Promega) and were sequenced using a CEQ8000 automated DNA sequencer with a DTCS Quick Start Kit (Beckman Coulter, Fullerton, CA, USA). Nucleotide and amino acid sequences were analysed using GENETYX-MAC (Software Kaihatsu Co., Tokyo, Japan). The *I. nil* genome sequence was analysed using the NCBI BLAST system 2.2.26 (DNA Data Bank of Japan, Mishima, Shizuoka, Japan) (Altschul et al. 1997) to detect potential off-target sequences.

3.3. Results

3.3.1. Selection of the target gene and the sgRNA for CRISPR/Cas9

To examine whether the CRISPR/Cas9 system could be applied to *I. nil*, the *InDFR-B* gene [accession number: AB006793 (Inagaki et al. 1999)] was selected as the target of Cas9 endonuclease. Because null mutations in *InDFR-B* lead to anthocyanin-less stems, leaves and flowers, I visually distinguished the bi-allelic mutants during transformation. For the sgRNA sequence, 20 bp in the fourth exon of the *InDFR-B* gene encoding a catalytic site of the DFR enzyme (Fig. 8A) (Trabelsi et al. 2008) was selected. The sgRNA sequence of *InDFR-B* shows high homology to those of *InDFR-A* and *InDFR-C*, with 19/20 and 18/20 matches in the nucleotide sequences, respectively, but only *InDFR-B* has the PAM next to the sgRNA sequence (Fig. 8A). Potential off-target sites of *InDFR-B* were searched with GGGenome (http://gggenome.dbcls.jp/) allowing no mismatch in seed sequence which is the most critical determinant of target specificity (Fu et al. 2013; Cong et al. 2013) and 3 bp mismatches in 20 bp sequence. Additional twelve sites were searched as potential off-target sites (Table 4). However two seed sequence matching sites showed five and eight mismatches to the target site. Moreover, three of the off-target candidates had no PAM sequence and other seven had mismatches in seed sequence.

3.3.2. Construct for the CRISPR/Cas9 system and transformation

An Arabidopsis codon-optimized *Streptococcus pyogenes* Cas9 expression cassette (Fauser et al. 2014), an sgRNA expression cassette, and a selective marker (*NPTII*) were combined into a single plant binary vector to form an all-in-one vector for plant transformation (Fig. 8B). *Cas9* was driven by the constitutive *Ubiquitin 4-2* promoter from *Petroselinum*

crispum (*pPcUbi*) (Kawalleck et al. 1993; Fauser et al. 2014). The *AtU6* promoter was used to express the sgRNA (Waibel and Filipowicz 1990; Li et al. 2007). The construct was introduced to secondary embryos to make stable transgenic *I. nil* using the *Rhizobium* (*Agrobacterium*) method (Ono et al. 2000; Kikuchi et al. 2005). A total of 32 transgenic plants (T1) showing kanamycin resistance with the T-DNA insertion in the genome were obtained.

3.3.3. Identification of the mutants by appearance, CAPS analysis and DNA sequencing

Initially, visual screening based on the appearance of pigmentation with anthocyanin was performed. Non-transgenic cv. Violet plants exhibited violet-coloured stems; however, more than one-third of the regenerated plants showed anthocyanin-less stems, typical of the phenotype of null mutations in *InDFR-B* (Fig. 8C). Notably, I never observed a shift in colouring, namely, violet to green/green to violet within a single plantlet and its stems during growth.

Subsequently, I conducted a CAPS analysis to detect mutations in the target region. I designed the expected cleavage site of CRISPR/Cas9 overlapping with the recognition sequence of the restriction enzyme *Spe*I (Fig. 8A). If the CRISPR/Cas9 cleaved target sequence and NHEJ occurred, then this restriction site would collapse, and the PCR-amplified DNA fragment would not be digested using *Spe*I. To detect mutations, total DNA was extracted from the transgenic leaves and PCR-amplified, and the resulting PCR products were subjected to *Spe*I digestion and analysed via agarose gel electrophoresis. The non-mutated PCR fragment of *InDFR-B* is 537 bp in length, and *Spe*I digestion produced

303- and 234-bp fragments; however, the mutated PCR fragments were not digested (Fig. 8D). Ten kanamycin-resistant transgenic plants showed *Spe*I-resistant single DNA bands, indicating that these plants are candidates of the bi-allelic mutants. Seventeen plants had both undigested and digested bands (Fig. 8D). Among these mutants, the #36-2 plants showed a shorter DNA fragment approximately 400 bp in length prior to *Spe*I digestion, suggesting a larger deletion in the locus (Fig. 8D). I also analysed the two orthologous loci, namely, *InDFR-A* and *InDFR-C*, using CAPS analysis and detected no mutations (Fig. 9).

Moreover, the DNA sequences of the mutated sites in *InDFR-B* were determined. The error-free PCR-amplified fragments of the mono-allelic mutants, #8-1 and 36-2, and the bi-allelic mutants, #9-1 and 39-1, were cloned and subjected to DNA sequencing. All plants showed mutations in the predicted cleavage site (Fig. 8E). The detected insertion was one bp, whereas the deletions ranged from two to 98 bp. Interestingly, the L2 chimaeric plant #8-1 showed three patterns of DNA sequences in *InDFR-B* (two different mutations and one non-mutation), despite the diploid genome. The L1 chimaeric plant #36-2 had the longest deletion (98 bp), as predicted in the CAPS analysis (Fig. 8D, E and Fig. 10).

I also analysed nine off-target candidates' sites having a PAM site with DNA sequencing in plant #9-1 and 39-1, and found there was no mutation in candidate sites (Fig. 11).

3.3.4. Phenotype and genotype of the targeted mutagenesis

Bi-allelic mutants lost anthocyanin, resulting in green stems and white flowers (Fig. 12A). Non-mutated plants showed violet stems and flowers, similar to NT plants (Fig. 12B). Most of the mono-allelic mutants also showed violet stems and flowers, similar to non-mutated plants. Notably, plants #8-1 and #36-2, considered mono-allelic mutants based on CAPS

analysis, showed green stems with violet flowers and violet stems with pale flowers, respectively (Fig. 12C, D). These two plants were considered periclinal chimaeras, as these phenotypes were the same as periclinal chimaeras resulting from transposon mutagenesis (Inagaki et al. 1996). In *I. nil*, the L1 layer is responsible for most of the flower colour, whereas the L2 layer determines the stem colour and the genotype of gamete cells (Inagaki et al. 1996). Therefore, plant #8-1 was considered an L2 chimaeric plant with a targeted mutation in *DFR-B* in the L2 layer, and plant #36-2 was considered an L1 chimaeric plant with a targeted mutation in *DFR-B* in the L1 layer. Because the L2 layer slightly contributed to the petal colour, the flowers of plant #36-2 were pale violet, as previously reported (Inagaki et al. 1996). Then I checked the indel mutation and T-DNA existence at the root, stem, leaf and petal of #36-2. The root tissue does not contain L1 and L2 layers, because L3 forms the central tissues including the pith and roots (Aida et al. 2016). The root of #36-2 had no mutation and no T-DNA insertion (Fig. 13). Therefore, I concluded that at least plant #36-2 was L1 periclinal chimaera.

I observed few somaclonal changes in anthocyanin pigmentation during cultivation. Periclinal chimaeric plants #8-1 and #36-2, considered L2 and L1 chimaeras, respectively, bore sectorial flowers only once during each life time, baring more than 30 flowers in total (Fig. 14A, B). Sectors of chimaeric plants were extensively studied using transposon mutants in the *DFR-B* locus in *I. nil* (Inagaki et al. 1996), and two potential causes were considered: somaclonal mutations and invasion of cells from an adjacent layer. I examined the total DNA extracted from sector cells using CAPS analysis and confirmed that these white sectors consisted of bi-allelically mutated cells (Fig. 14C).

3.3.5. Inheritance of CRISPR/Cas9 system-induced mutations in subsequent generations

I observed the progeny (T2) of the transformed plants, and all results were essentially as expected. For example, the progeny of plant #9-1, bi-allelic mutants, showed green stems (24 plants), indicating that plant #9-1 (T1) was a perfect bi-allelic-targeted mutant of *InDFR-B*. Among the offspring of #9-1, targeted mutants without T-DNA insertions were observed, suggesting that the targeted mutations at *InDFR-B* and T-DNA were not co-inherited in #9-1. These plants are targeted mutants and are considered transgenic plants based on process-based definitions and NT plants based on product-based definitions (Araki and Ishii 2015; Sprink et al. 2016).

I also observed the progeny (T2) of the L2 chimaeric mutant #8-1 and the L1 chimaeric mutant #36-2. The progeny of plant #8-1 showed green stems (16 plants), and the progeny of plant #36-2 showed violet stems (50 plants). I examined the T-DNA retention of the 24 progenies of the L1 chimaeric mutant #36-2 using PCR amplification to detect a fragment of the NPTII gene. None of the T2 plants of #36-2 progeny had T-DNA insertions in their genomic DNA (Fig. 15). Because gamete cells originated from L2 cells (Inagaki et al. 1996), these results reconfirmed that plant #8-1 was an L2 chimaeric plant and that plant #36-2 was an L1 chimaeric plant.

3.4. Discussion

These data provide the first demonstration that the CRISPR/Cas9 system can generate targeted mutagenesis in *I. nil*. Approximately one-third of the stable transgenic plants were bi-allelic mutants at the *DFR-B* locus in one generation. This high efficiency indicates that

the CRISPR/Cas9 system is a highly applicable technique for next-generation breeding in *I. nil* and other horticultural plants.

I successfully visually selected targeted mutagenesis in the early stage during transformation, as the loss of function of the target gene *DFR-B* prevents the synthesis of stem pigmentation with anthocyanin. In the present study, the gene disruption was detected only at the *InDFR-B* locus, whereas no mutations were observed in the two orthologous loci, namely *InDFR-A* and *InDFR-C,* despite their high homology. These data confirmed the validity of target specificity and the indispensability of PAM for the CRISPR/Cas9 system, avoiding potential off-target mutagenesis. In a recent study, the bi-allelic mutation rate was 31% (10/32), and the total mutation rate was 84% (27/32). The mutation rate of this study was relatively high among higher plants (Zhang et al. 2016b, a). Moreover, a low tendency of obtaining 6% (2/32) chimaeric plants was observed. Because the transformation and regeneration system in *I. nil* uses secondary embryogenesis from secondary embryos induced on immature embryos, I consider that the consequent plant transformant primarily originated from a single cell of the secondary embryo (Ono et al. 2000) except chimaeric plant #8-1 and #36-2. This unique character of the transformation and regeneration system might affect the low tendency of obtaining chimaeric plants. Because growth rate of secondary embryo had an individual difference slightly, some secondary embryos rarely reached to the regeneration step and could be multi-cell embryo rarely, so the chimaeric mutants were obtained at a low tendency. Despite the high efficiency of obtaining bi-allelic mutations, the overall tendency of the results, 1 bp insertions or short deletions of less than 100 bp, was similar to those in other plants, for example, Arabidopsis (Feng et al. 2014) and rice (Zhang et al. 2014). Furthermore, the efficiency of editing depends on sgRNA (Zhang

et al. 2014, 2016b) and the optimization of sgRNA design to maximize activity is advancing (Doench et al. 2016). By selecting a target sequence with optimization program and software (Lei et al. 2014; Naito et al. 2015), the editing efficiency will increase more in *I. nil*.

In *I. nil*, *DFR*s are present as a small three-gene family (*DFR-A*, *DFR-B* and *DFR-C*). This gene duplication and evolution is the best example of the escape from adaptive conflict (EAC) (Des Marais and Rausher 2008). In the present study, I successfully inactivated *DFR-B* without modification in *DFR-A* and *DFR-C* genes, although these three genes are tandemly arrayed within a 17-kb DNA region (Inagaki et al. 1999). I reconfirmed that *DFR-B* is the main gene for pigmentation among these three duplicated genes and the EAC in this locus. Using a transposable insertion mutant, a-3' line of the *DFR-B* locus and its somaclonal revertants, extensive genetic experiments were conducted in 1930s and 1990s (Imai 1931, 1938; Inagaki et al. 1996; Iida et al. 1999). I revisited the same locus in the opposite direction, generating null mutants. This direction, the reverse genetic approach to these legacy phenomena, represents one of the important purposes of targeted mutagenesis.

Plants #8-1 and #36-2, initially classified as mono-allelic mutants as determined by CAPS analysis, showed colour combinations of stems and flowers that differed from those of the other mono-allelic mutants (Fig. 12C, D). Therefore, I considered these plants to be periclinal chimaeric mutants. The shoots of many angiosperms, including *I. nil*, consist of three cell layers: the epidermal cell layer, L1; the sub-epidermal cell layer, L2; and the internal tissues, L3, in the shoot meristems (Fig. 12, below) (Satina et al. 1940; Huala and Sussex 1993). In wild-type *I. nil*, flower pigmentation occurs mostly in L1 and slightly in L2, whereas stem pigmentation is restricted to L2 (Inagaki et al. 1996). I concluded that

these plants were periclinal chimaeric mutants, initially using the results of the comparison of the phenotype with the literature and later using CAPS analysis (Fig. 8D and Fig. 9), sequence determination (Fig. 8D and Fig. 10), and observation of inheritance in the T2 generation (Fig. 15). These results demonstrated plant #8-1 was a periclinal chimaera that had bi-allelic mutation in L2; in contrast, plant #36-2 was also a periclinal chimaera with a bi-allelic mutation in L1 (Fig. 12C, D). Periclinal chimaeric mutations of *DFR-B* in *I. nil* were extensively studied by Imai (Imai 1931, 1938) with genetic analyses and reanalysed by Inagaki et al. in molecular and biochemical studies (Inagaki et al. 1996). The plants #8-1 and #36-2 exactly followed their reports, particularly regarding the pale flower colour of the L1 chimaera (Fig. 12D). Moreover, plants #8-1 and #36-2 bore sectorial flowers (Fig. 14). Because these sectorial flowers were rare events and difficult to analyse, I could not decide whether these sectors resulted from somaclonal-targeted mutagenesis or the invasion of the cells in the adjacent layer. However, invasion from neighbouring cell layers to make a sector in a flower has been described for chimaeric mutants by transposons (Inagaki et al. 1996), and I did not observe any somaclonal-targeted mutagenesis or secondary mutagenesis, suggesting that sectors in a flower of plants #8-1 and #36-2 are caused by the invasion.

The nucleotide sequencing of the mutated region revealed variable mutations in the *InDFR-B* region, ranging from one bp insertion to deletions of up to 98 bp (Fig. 8E and Fig. 10). In general, random NHEJ occasionally generates mutations without losing gene function, such as in-frame mutations (multiple of 3 nt deletions) or silent mutations (without changes in the amino acid sequence). In the present study, bi-allelic mutations of 3-bp deletions resulted in the leucine 197 deletion, observed in two independent plants (#9-1 and #39-1). The fact that neither mutant could produce anthocyanin suggested that leucine 197

is indispensable for the enzymatic activity of InDFR-B. In the grape DFR (Trabelsi et al. 2008), crystallization analysis revealed that the conserved proline 190 (corresponding to proline 195 in InDFR-B, next to the deleted leucine 197) is used for the interaction of flavonol with nicotinamide adenine dinucleotide phosphate ($NADP^+$) to form the catalytic complex (Fig. 16) (Trabelsi et al. 2008). The deletion of this amino acid leucine 197 might result in the failure of forming stacked saturated and aromatic rings, with lost enzyme activity. In this case, I successfully increased the efficiency of the targeted mutagenesis by selecting the CRISPR/Cas9 target sequence at the active site encoding the sequence of the target enzyme.

In the present study, I successfully applied a CRISPR/Cas9 system in *I. nil* for targeted mutagenesis in one generation. To my knowledge, this report is the first to examine changing flower colour using the CRISPR/Cas9 system. The successful results of the present study will facilitate the modification of flower colours and shapes with targeted mutagenesis in *I. nil* and other ornamental flowers or vegetables. Moreover, in the present study, I obtained T2 plants with targeted mutagenesis at the *InDFR-B* locus but without T-DNA. These plants are biologically non-transgenic and could not be distinguished from other spontaneous mutants (Araki and Ishii 2015; Sprink et al. 2016). I propose that these plants will attract the attention of the public and will improve understanding of NBT.

3.5. Tables and Figures

Table 3. Primer sets used for sequence analysis for potential off-target sites in the plant #9-1 and 39-1 in the present study. Nested PCR was used to amplify the candidate #1.

off-target candidate name	Direction	Sequence
off-target candidate 1 for 1st PCR	Forward	5' ATATATTTTCTGTTGTGACC 3'
	Reverse	5' TCTTCTCCTGGCTTTTGA 3'
off-target candidate 1 for 2nd PCR	Forward	5' AATATTTATCTTAATTGCAG 3'
	Reverse	5' TACCAAATCAAAATGCTC 3'
off-target candidate 2	Forward	5' CCTTAGGGAATGAATTGAGC 3'
	Reverse	5' TAGGCAGAGTAATCAGTCCA 3'
off-target candidate 3	Forward	5' ATAAGTGCTTGTTTCACCA 3'
	Reverse	5' GTAATGTTATTTTGGACCCT 3'
off-target candidate 4	Forward	5' GCCTATTCCGTGAACCAA 3'
	Reverse	5' GTTGTGAAACTGCGTCCA 3'
off-target candidate 5	Forward	5' TGATTTGCGAGAACAAGCTG 3'
	Reverse	5' GTACAACTTTAGAAGCGTGGA 3'
off-target candidate 6	Forward	5' TCAGCCGGGTTCAAATCGTC 3'
	Reverse	5' TACCGTAGTACTCGCTTCACC 3'
off-target candidate 7	Forward	5' ATAACTGCTTGTTTCACCA 3'
	Reverse	5' TTTTCATGTTCAAAGGTGAC 3'
off-target candidate 8	Forward	5' CATATATGCTCTAGAAAGACG 3'
	Reverse	5' TGAAACCCTTTGAGGTGA 3'
off-target candidate 9	Forward	5' GAAGCAGTAAGCTATTCCCA 3'
	Reverse	5' ATAATTTGTATATTGCCGGAT 3'

Table 4. Potential off-target sites in *InDFR-B* in the present study. The off-target sequences except *DFR*s were searched with GGGenome (http://gggenome.dbcls.jp/) against *I. nil* cv. TKS whole genome. Blue letters indicate PAM sequence. Red lower case letters show mismatches and gaps to the on-target (*DFR-B*) sequence. Green letters indicate the 12 bp seed sequences. Search conditions used were 12 bp seed: 12 bp seed sequence allowing no mismatch, and <3 bp Mismatch: allowing less than 3 bp mismatches within 23 bp. Only sequences having a PAM sequence were selected. Candidate sites were numbered 1 to 9 for further analysis.

	candidate number	scaffold	strand	potision	sequence	PAM	mismatch(es) initial 8 bp	mismatch(es) total
DFR-B		805	+	1966837	AAGCATCATACCACCACTAGTGG	o	0	0
DFR-A		805	+	1959514	cAGCATCATACCACCACTAGTca	x		
DFR-C		805	+	1971365	cAGtATCATACCACCACTAGTca	x		
12 bp seed	1	875	+	640822	tgcacctcTACCACCACTAGTGG	o	0	8
	2	2036	+	2396563	ggGCccCgTACCACCACTAGGGG	o	0	5
<3 bp Mismatch	3	875	+	1857780	AAGCATaATACCACCACTAGTGG	o	1	3
	4	2690	+	1189128	AA-tATCATACCACCAtTAGAGG	o	1	2
	5	2704	+	1868233	AAtCATCATACCACCAC-AGTGG	o	1	3
	6	3195	+	433510	AAGCcTCtTACCA-CACTAGCGG	o	1	3
	7	465	-	1708179	AAGCATaATACCACCACTAGTGG	o	1	3
	8	1026	-	3378314	AA-CA-CATACCACCtCTAGCGG	o	1	3
	9	3054	-	232458	AAt-ATCATACCACCAtTAGAGG	o	1	2

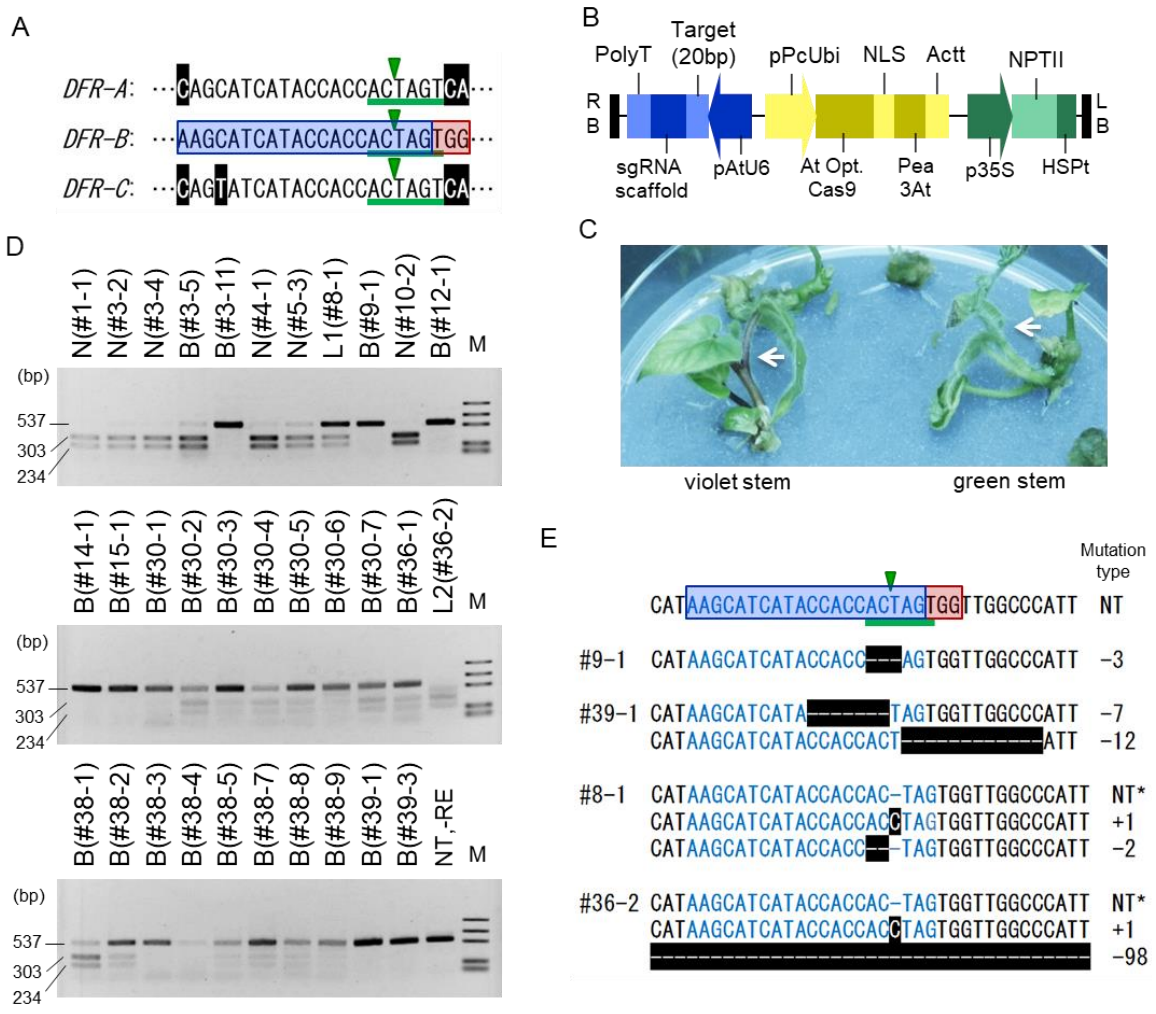

Fig. 8. CRISPR/Cas9-mediated targeted mutagenesis in *InDFR-B*.

Fig. 8. (continued). **A**: Schematic representation of *InDFR-A, -B,* and *-C* target sequences. In *InDFR-A* and *-C,* the white letters in black highlight indicate mismatches with *InDFR-B*. In *DFR-B,* the 20-bp target-specific sequence is shown in blue highlight, and the PAM sequence (TGG) is shown in red highlight. *Spe*I restriction enzyme sites (ACTAGT) are underlined with green. The green triangles indicate the expected cleavage site of the CRISPR/Cas9 system. **B**: T-DNA region of the all-in-one vector, pZD_AtU6gRNA_FFCas9 _NPTII. **C**: Kanamycin-resistant regenerated shoots of plants transf-ormed with the CRISPR/Cas9 system. Without targeted mutations, stems were coloured violet (left), whereas bi-allelically mutated stems remained green (right). **D**: CAPS analysis of the target region in the *InDFR-B* locus. Total DNA was extracted from the leaves of transgenic plants and amplified by PCR. The PCR products were digested with the *Spe*I restriction enzyme, except -RE. M: marker (1,000, 700, 500, 200 and 100 bp); NT-RE: PCR product of a NT plant without restriction enzyme digestion. Numerals after # indicate independent T1 plants. N, B, L1, and L2 represent the phenotype of each plant. N: Violet stem and violet flower (same as NT); B: Green stem and white flower; L2: Green stem and violet flower; L1: Violet stem and pale-violet flower. **E**: Sequences of targeted mutations in the *InDFR-B* locus. The NT type sequence is shown at the top and is designated **A**. Deleted nucleotides are shown in dashes with black highlight (-). The inserted cytidine residue is shown with black highlight. NT sequences were detected using CAPS analysis (*) in chimaeric plants (#8-1 and 36-2).

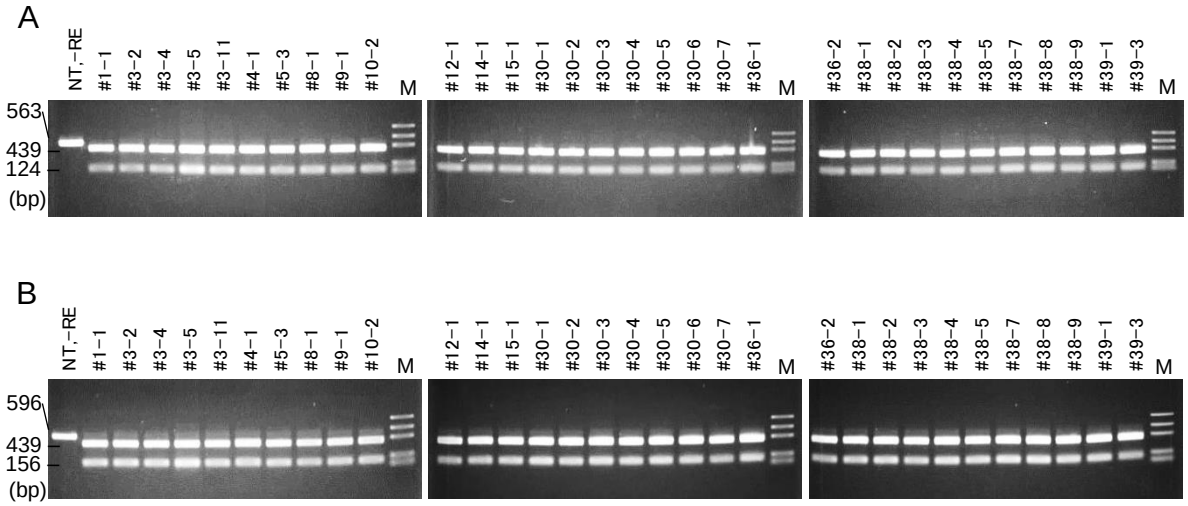

Fig. 9. CAPS analysis of the *InDFR-A* and -*C* locus in transformed plants using CRISPR/ Cas9 system. Total DNAs were extracted from the leaves of the transformed plants and amplified by PCR reaction. PCR products were digested by *Spe*I restriction enzyme except NT, -RE. **A**: All the PCR fragments of *InDFR-A* of 563 bp in length were cleaved into 439 bp and 124 bp fragments by digestion with *Spe*I. **B**: All the PCR fragments of *InDFR-C* of 596 bp in length were cleaved into 439 bp and 156 bp. Those results indicates that there were no off-target mutation in *InDFR-A* and –*C* using gRNA of *InDFR-B*. M: marker (1,000, 700, 500, 200 and 100 bp); NT, -RE: PCR product of NT without restriction enzyme digestion.

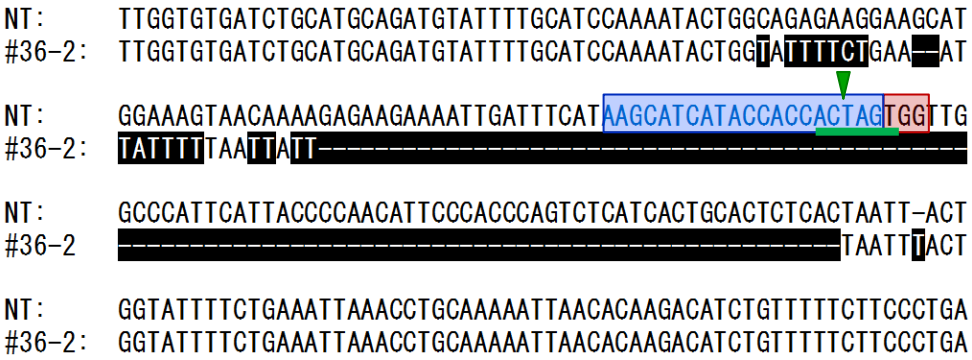

Fig. 10. DNA Sequence of *InDFR-B* with a long deletion identified from plant #36-2. The non-transgenic type sequence is shown above. The red box indicates PAM sequence, the blue box indicates target sequence and *Spe*I restriction enzyme site (ACTAGT) is shown on green underline. The green triangle indicates the expected cleavage site by CRISPR/Cas9 system. Deletions, insertions and point mutations are shown with black highlight.

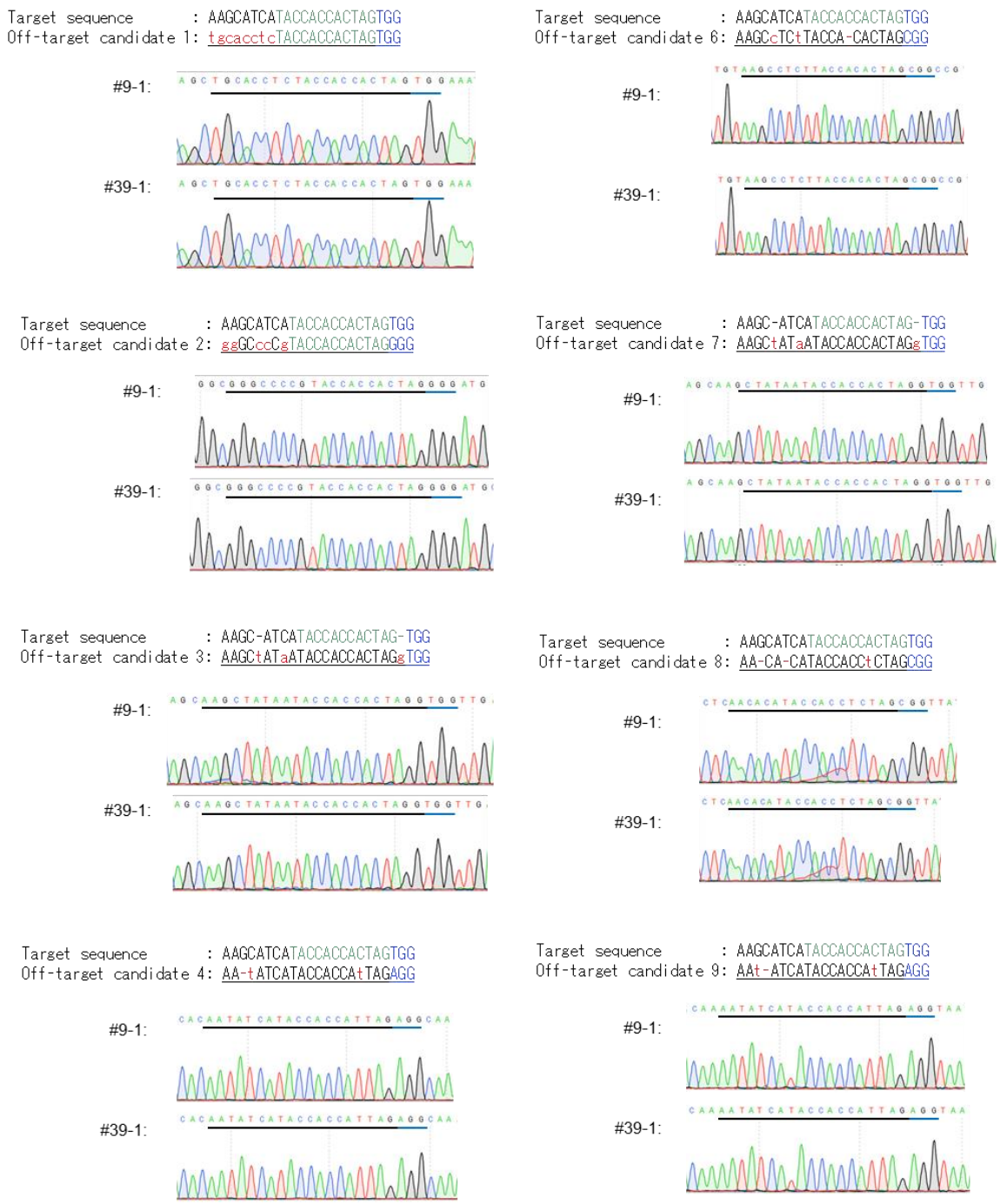

Fig. 11. Sequence analysis for the off-target mutation candidates in the plant #9-1 and #39-1. There was no altered sequence. I concluded that these sites are no more candidates of off-target mutation at least in these plants.

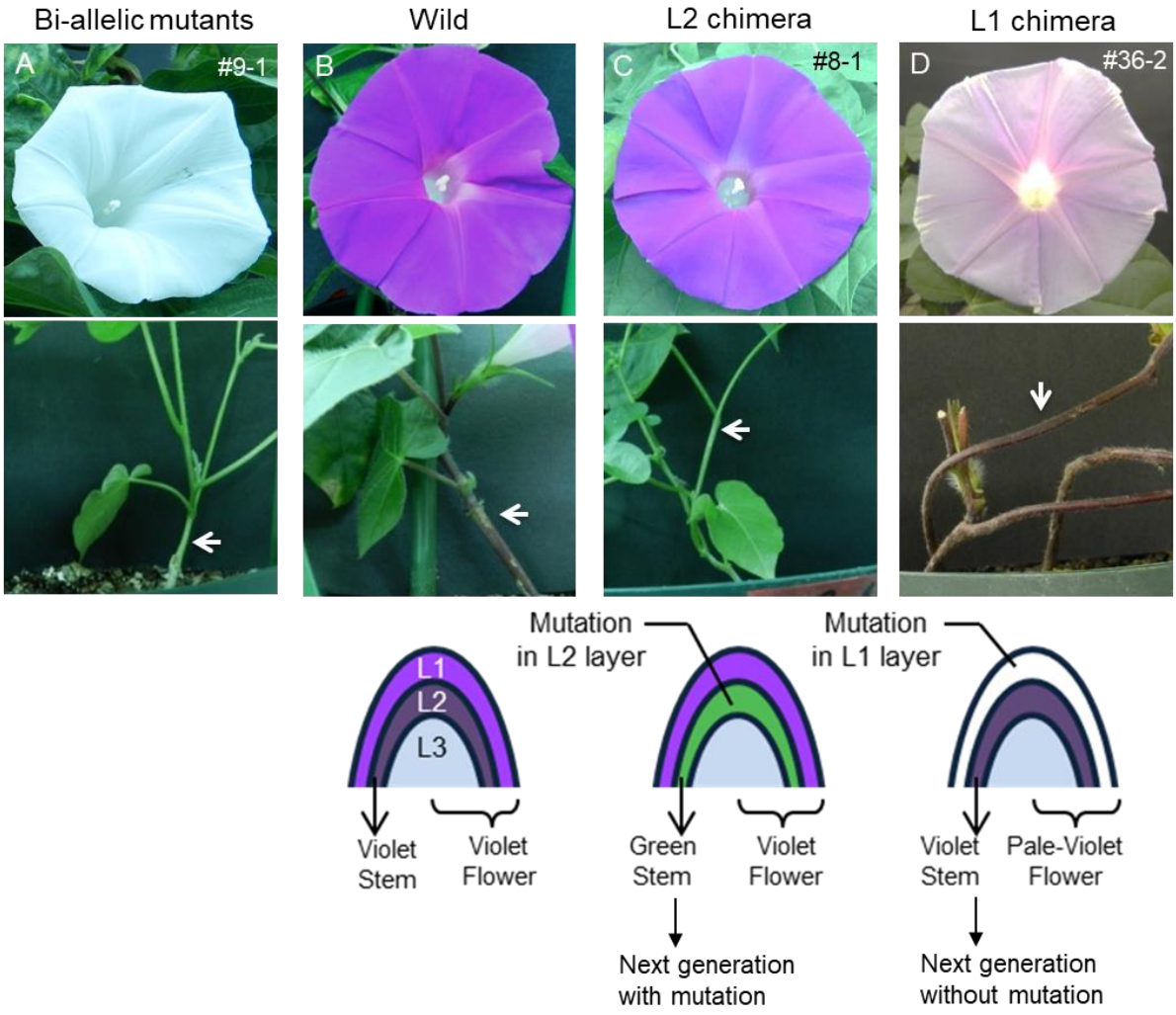

Fig. 12. Flowers of CRISPR/Cas9-mediated *dfr-b* mutants. The appearances of flowers (top) and stems (middle) and a schematic drawing of the meristem layers and their functions (bottom). L1: epidermal layer; L2: sub-epidermal layer; L3: internal tissues. **A**: A flower and stem of #9-1, a bi-allelic-mutant plant. **B**: A flower and stem of *I. nil* cv. Violet, an NT plant. **C**: A flower and stem of #8-1, an L2 periclinal chimaera plant and a representation of the meristem layers of the L2 chimaera showing bi-allelic mutation only in the L1 layer. **D**: The flower and stem of #36-2, an L1 periclinal chimaera plant and a representation of the meristem layers of the L1 chimaera showing bi-allelic mutation only in the L2 layer.

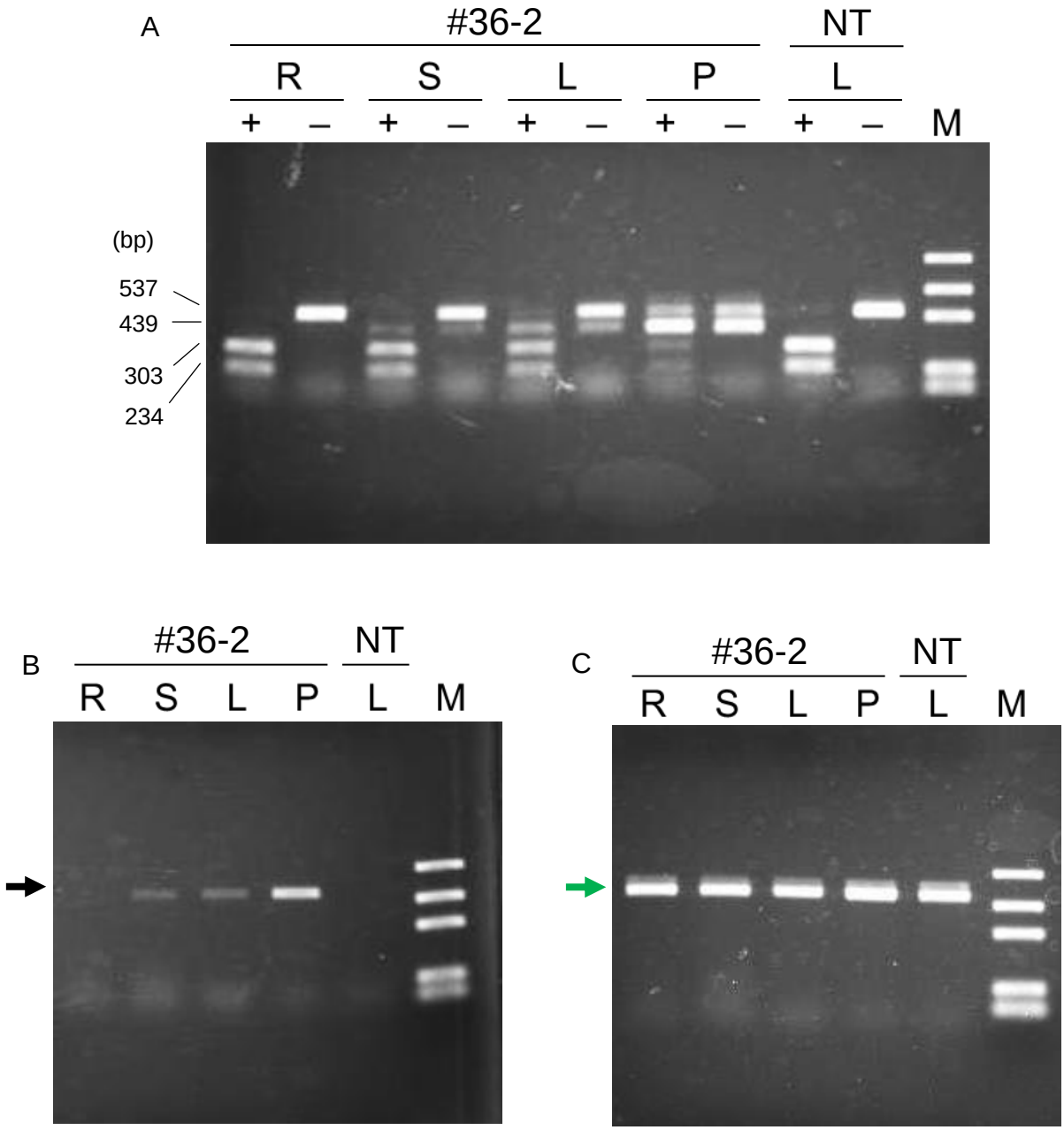

Fig. 13. Tissue specific CAPS analysis of the *InDFR-B* and genotype check of chimeric plant #36-2.

Fig. 13. (continued). Total DNAs were extracted from the root (R), stem (S), leaves (L) and petal (P) of the transformed plants #36-2 and leaf of NT plant, and amplified by PCR reaction. **A**: The PCR fragments of *InDFR-B.* The PCR products were then digested using the *Spe*I restriction enzyme (+). -: without *Spe*I restriction enzyme digestion. **B, C**: The PCR fragments of *NPTII* (black allow) and *phytoene syntase* (green arrow; internal control) respectively. M: marker (1,000, 700, 500, 200 and 100 bp).

The root of #36-2 did not show mutated *dfr-b* [**A**, 537 (+) and 439 bp] and *NPTII* (**B**, black arrow) bands. Moreover, the stem, leaf and petal showed these bands, however, the bands of the stem and leaf were weaker than that of petal, while the bands of internal control gene (**C**, green arrow) were almost same levels. The band depth of mutated *dfr-b* and *NPTII* reflected the ratio of L1 derived tissue per total tissue used for DNA extraction. The root is completely L3 derived while the stem and leaf component is mainly pith (L3 derived) and the petal component is mainly epidermal layer (L1 derived). Therefore, I concluded that at least plant #36-2 is chimeric mutant.

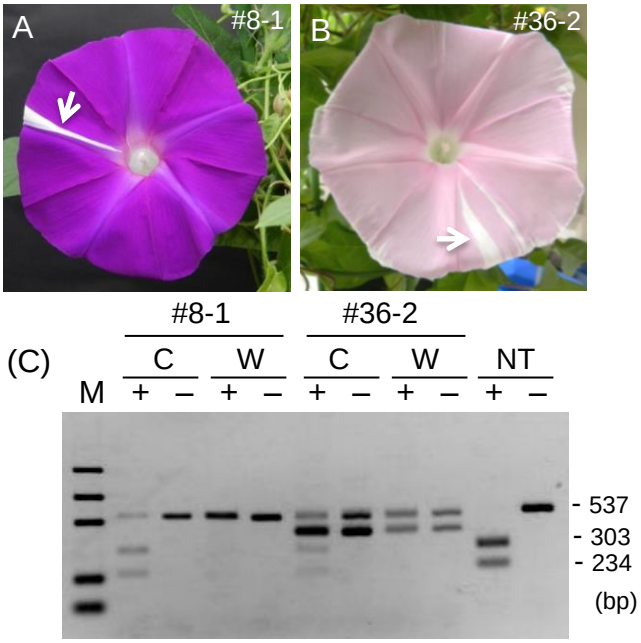

Fig. 14. Phenotypes and genotypes of sectorial chimaeric flowers. **A**: A sectorial flower of the L2 chimaeric plant #8-1. **B**: A sectorial flower of the L1 chimaeric plant #36-2. **C**: CAPS analysis of the *InDFR-B* loci in sectorial chimaeric flowers shown in **A** and **B**. Total DNA was extracted from the sectorial white tissues of the petals indicated by arrows (W) and other coloured tissues of the petal (C), which were subsequently used for PCR amplification. The PCR products were then digested using the *Spe*I restriction enzyme (+). -: without *Spe*I restriction enzyme digestion; M: marker (1,000, 700, 500, 200 and 100 bp); NT: Total DNA of an NT plant.

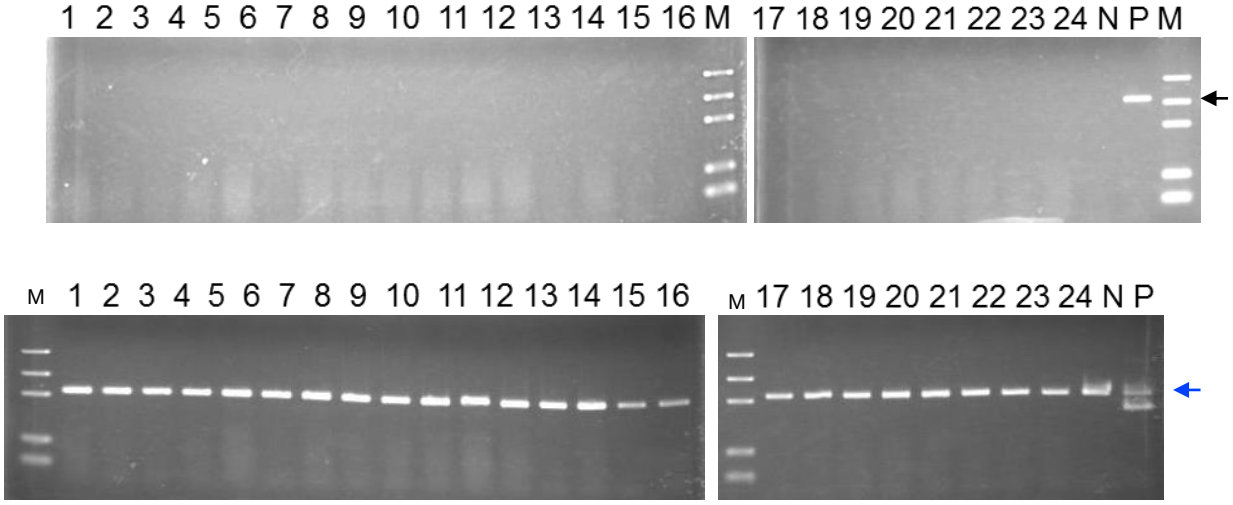

Fig. 15. Genotype check of T2 progeny of chimeric plant #36-2. The *NPTII* gene was PCR-amplified and analyzed by electrophoresis. N: non-transgenic *I. nil* cv. Violet. P: parental transgenic plant line #36-2 (T1 generation). Black and blue arrows indicate the amplified fragment of *NPTII* and *DFR-B* (without mutations) genes respectively. Non of the twenty-four progenies (T2) showed the band of the transgene.

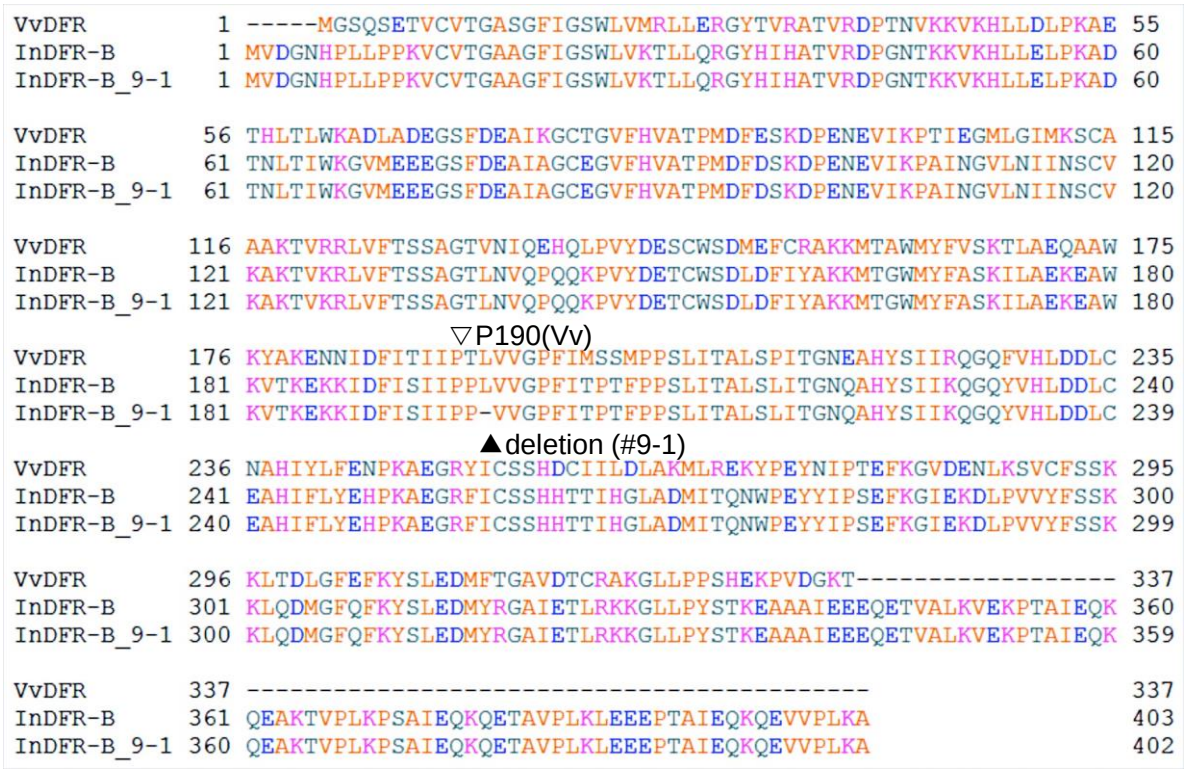

Fig. 16. Deletion of a single amino acid (L197) abolished enzymatic activity. A multiple sequence alignment of dehydroflavonol-4-reductase (DFR) amino-acid sequence. Amino-acid residues are presented with single letter that are colored by means of similarity. VvDFR: DFR protein of grape *Vitis vinifera* (Genbank accession X75964; Sparvoli *et al*., 1994). InDFR-B: DFR-B wild type protein of *I. nil* (DDBJ accession AB006793; Inagaki *et al*., 1999). InDFR-B_9-1: A mutated DFR-B protein of plant #9-1 in this study. The black triangle shows the deletion of the leucine 197 (L197). The open triangle shows the conserved proline 190 (P190) of VvDFR essential to form DFR–$NADP^+$–flavonol complex (Trabelsi *et al*., 2008).

Chapter 4. Alteration of flower colour in *Ipomoea nil* through CRISPR/Cas9-mediated mutagenesis of *carotenoid cleavage dioxygenase 4*

4.1. Introduction

Several strategies for controlling carotenoid accumulation in floral tissues have been reported, involving the synthesis, sink capacity, esterification, and suppression of the degradation of carotenoids [reviews: (Tanaka and Ohmiya 2008; Li and Yuan 2013)]. For example, in marigold, *Tagetes erecta*, different levels of carotenoid accumulation lead to differences in petal colour, ranging from pale yellow to dark orange (Moehs et al. 2001). A previous study showed that the carotenoid content correlates well with the transcript levels of carotenogenic genes such as *PSY* and *1-deoxy-D-xylulose 5-phosphate synthase* (Moehs et al. 2001). This finding suggests that the carotenoid content depends on the mRNA transcript levels or stability of carotenogenic genes in tissues (Moehs et al. 2001). Previous study reported that the transcription levels of carotenogenic genes such as *PSY* and *CHYB* in the petals of *I. nil* were extremely low compared with those of *I. obscura* var. *lutea*, which exhibits high levels of carotenoids and bears vivid yellow petals (Yamamizo et al. 2010). Subsequently, carotenoid biosynthetic pathway in the floral tissue of *I. nil* was enhanced by introducing multiple carotenogenic genes of which expression levels are relatively low in the petals of *I. nil* than that of *I. obscura* var. *lutea*; however, the petal colour did not change (Chapter 2). I concluded that the trace amounts of carotenoids in the petals of *I. nil* were not due solely to low expression levels of carotenogenic genes but that another mechanism must prevent carotenoid accumulation.

In higher plants, CCD enzymes contribute to carotenoid degradation and cleave specific double bonds of the polyene chain of carotenoids. CCD was first identified through the analysis of a viviparous abscisic acid-deficient mutant of maize (*Zea mays*) and was designated *viviparous14* (*VP14*) (Schwartz et al. 1997; Tan et al. 1997). Based on studies

focussing on *VP14*, many CCD homologous enzymes in different plant species and other organisms have been identified and characterized [reviews: (Ohmiya 2009; Walter et al. 2010; Ahrazem et al. 2016)]. Analysis of the genome sequence of *Arabidopsis thaliana* led to the definition of nine clades of dioxygenases (Tan et al. 2003), which are classified into the *9-cis-epoxycarotenoid dioxygenase* (*NCED*) and *CCD* subfamilies based on sequence similarities. NCEDs are related to the production of viviparous abscisic acid but not to petal colour formation (Schwartz et al. 1997, 2003; Tan et al. 1997). However, the functions of CCDs differ between clades (Ahrazem et al. 2016). CCD7 and CCD8 are related to the production of strigolactones, which act as a branching signal (Gomez-Roldan et al. 2008; Umehara et al. 2008). CCD1 plays roles in the formation of volatile compounds responsible for flavour and aroma and in carotenoid turnover (Schwartz et al. 2001; Auldridge et al. 2006; Ilg et al. 2010). The functions of CCD4 are similar to those of CCD1, but some CCD4s are involved in the degradation of carotenoids and prevent carotenoid accumulation in the petals. In chrysanthemum, *C. morifolium*, the expression levels of carotenogenic genes show no significant difference between white and yellow petals. However, *CmCCD4a* is expressed in white petals but not in yellow petals (Kishimoto and Ohmiya 2006; Ohmiya et al. 2006). Furthermore, loss-of-function mutation of CmCCD4a in white chrysanthemum petals resulted in a drastic increase in carotenoids (Ohmiya et al. 2012). Similarly, transposon mutagenesis of *BnaC3.CCD4*, an orthologue of *CCD4* in *B. napus*, converts petal colour from white to yellow (Zhang et al. 2015). These results indicate that CCD4 cleaves carotenoids and prevents carotenoid accumulation in the white petals of chrysanthemum and *B. napus*. However, although *CCD4*s are expressed in the petals of rose (Huang et al. 2009), tomato (Wei et al. 2016) and Arabidopsis (Winter et al. 2007) (eFP

browser; http://bbc.botany.utoronto.ca/efp/cgi-bin/efpWeb.cgi), the involvement of CCD4 in petal colour formation has not been clearly elucidated in these plants. In *I. nil*, a substantial amount of InCCD4 is expressed in the petals (Yamamizo et al. 2010). However, in a previous study, only the petal-specific expression of InCCD4 was examined based on a partial sequence (Yamamizo et al. 2010); thus, the contribution of InCCD4 remains unknown, and a comprehensive study of InCCDs is needed.

Previous attempts to change flower colour by suppressing *CCD4* expression using RNAi methods have been reported (Ohmiya et al. 2006, 2009). In *C. morifolium*, the introduction of a *CmCCD4a* RNAi construct into a white-flowered cultivar successfully reduced the level of *CmCCD4a* expression in the petals. The carotenoid content in the petals of the RNAi transformants increased to 102 μg g^{-1} but was still much lower than in yellow-flowered cultivars because *CmCCD4a* expression remained at low levels (Kishimoto et al. 2007; Ohmiya et al. 2009). Thus, completely knocking out *CCD4* expression might be necessary to obtain a deeper yellow petal colour. Recently developed methods for targeted mutagenesis (or genome editing) can completely knock out gene function. In particular, the CRISPER/Cas9 system can be utilized more easily than other systems because of its simple experimental design and high specificity (Puchta 2017), and the CRISPR/Cas9 system has already been successfully applied in *I. nil* (Chapter 3).

In the present study, I comprehensively analysed all the predicted *CCD* homologous genes according to the whole-genome sequence of *I. nil* (Hoshino et al. 2016). The sequencing and expression analyses suggested potential involvement of *InCCD4* in carotenoid degradation in the petals. Therefore, I knocked out *InCCD4* using targeted mutagenesis with CRISPR/Cas9 system. The *ccd4* knockout plants exhibited pale yellow

petals with up to 30-fold-increased carotenoid accumulation in the midribs of the petal. Subsequently, I revealed that *InCCD4* is also related to petal colour formation in *I. nil*, similar to what has been found in chrysanthemum and Brassica.

4.2. Materials and methods

4.2.1. Plant materials and growth conditions

Seeds of *I. nil* cv. AK77 (obtained from the NBRP "Morning glory") were used in the experiments. The growth conditions and were same as former described conditions in the Chapter 2. For RT-qPCR, roots, stems and cotyledons were collected at one week after sowing. Leaves were collected at two weeks after sowing. Petals were collected at each developmental stage, 96, 48, and 12 h before flowering, and immediately after opening (referred to as S1, S2, S3 and S4, respectively). For transformation, immature embryos of *I. nil* cv. AK77 were collected at two weeks after flower opening (Ono et al. 2000).

4.2.2. Identification of CCD genes in plants

A tBLASTn (DNA Data Bank of Japan) (Altschul et al. 1997) search was performed using the amino acid sequences of the Arabidopsis *CCD* genes as the query against the predicted transcript sequence from the *I. nil* genome and the EST sequence database (Hoshino et al. 2016), using an e-value of 1e-20. *InCCD4* was also detected in the EST database (http://ipomoeanil.nibb.ac.jp/; Contig11866d).

4.2.3. Phylogeny analysis

Multiple alignments of amino acid sequences were produced using GENETYX-MAC

(Software Kaihatsu). The phylogenetic tree was calculated using the neighbour-joining method (Saitou and Nei 1987) and bootstrap analysis (1,000 replicates) with MEGA7 software (Kumar et al. 2016). Missing sequence data were treated via pairwise deletion of gaps. Branch lengths were assigned utilizing pairwise calculations of genetic distances.

4.2.4. Quantitative real-time PCR (RT-qPCR) analysis

Total RNA was isolated from each tissue and petals from each stage using the Get Pure RNA Kit (Dojindo). Subsequently, cDNA was synthesized from total RNA (1.0 µg) using the SuperScriptIII First-Strand Synthesis System (Invitrogen) and oligo(dT)20. The transcript levels of C*CD*s were analysed via RT-qPCR with Power SYBR™ Green PCR Master Mix (Applied Biosystems) and the Applied Biosystems 7900HT Fast Real-Time PCR System (Applied Biosystems), according to the manufacturers' instructions. Transcript levels were calculated according to the ΔΔCq (formerly ΔΔCt) method (Livak and Schmittgen 2001) using the *Actin 4* (accession number: AB054978) and *Ubiquitin 3-3* (AB265782) genes as references (Higuchi et al. 2007; Yamada et al. 2007). The primers used in this experiment are listed in Table 5. Statistical significance of the differential expression levels was assessed as previously described for three independent experiments (with mean centring and autoscaling) (Willems et al. 2008; Bustin et al. 2009). The Tukey-Kramer test at the 1 and 5% level were used for the tissue- and developmental stage-specific expression analysis and the analysis of carotenoid biosynthesis-related genes, respectively. The results are presented as the standardized mean of three independent experiments with the SE.

4.2.5. Vector construction

The backbone of the vector used for targeted mutagenesis was pDeCas9-Kan [modified form pDeCas9 (Fauser et al. 2014), where the *Bialaphos resistance* gene is replaced with *Neomycin phosphotransferase II* (*NPTII*)]. Briefly, three pairs of complementary oligo DNAs for the *InCCD4* target sequences (Table 6) were annealed at 95°C for 5 min. The guide RNA (gRNA) and the target sequence-cloning vectors pMR203 (pENTR _L1L4_AtU6gRNA), pMR204 (pENTR_R4R3_AtU6gRNA) and pMR205 (pENTR _L3L2_AtU6gRNA) were digested with the restriction enzyme *Bbs*I and ligated to the annealed oligo DNA. The cloning vectors were verified by sequencing. The three gRNA expression cassettes were merged with the binary vector via an LR reaction. The destination vector was verified by *Eco*RI digestion.

4.2.6. Plant transformation

Rhizobium [*Agrobacterium*]-mediated transformation using an immature embryo-derived secondary embryo was performed as described previously (Kikuchi et al. 2005). For transformation, *Rhizobium radiobacter* (formerly *Agrobacterium tumefaciens*) strain LBA4404 harbouring a ternary plasmid for *virG* N54D (van der Fits et al. 2000) was used. As the transgenic plants were directly germinated from kanamycin-resistant secondary embryos, I described these plants as the T1 generation. The validity of the transformation was confirmed by PCR using total DNA extracted from young leaves and primers for *NPTII* (Table 6). Total DNA was extracted from the young leaves of plants as previously described (Edwards et al. 1991). PCR was performed using GoTaq® Green Master Mix (Promega) in a thermal cycler, with initial denaturation at 95°C for 2 min, followed by 30 cycles at 95°C

for 30 s, 55°C for 30 s and 72°C for 1 min, with a final extension step at 72°C for 5 min.

4.2.7. Detection of mutants

First, I conducted a CAPS analysis to detect mutations in the target region using the restriction enzyme *Acl*I and *InCCD4*-specific primers (Table 6) as previously described (Chapter 3). Subsequently, the mutations were confirmed via DNA sequencing. DNA fragments of *InCCD4* were PCR-amplified using total DNA from transformants and the Advantage® 2 Polymerase Mix (BD Biosciences Clontech) and the *InCCD4*-specific primers (Table 6). PCR was performed using a thermal cycler, with initial denaturation at 95°C for 1 min, followed by 30 cycles of 95°C for 15 s and 68°C for 30 s, and an additional 10 min extension step at 70°C for incorporation and preservation of 3' A-overhangs. The PCR products were cloned into the pGEM®-T Easy Vector (Promega) and sequenced using an ABI 3130 Genetic analyzer (Applied Biosystems) with the BigDye Terminator v3.1 Cycle Sequencing Kit (Applied Biosystems). Nucleotide and amino acid sequences were analysed using GENETYX-MAC (Software Kaihatsu Co.).

4.2.8. Carotenoid extraction and HPLC analysis

Carotenoids were extracted from petals and leaves, and analysed via HPLC as previously described (Kishimoto et al. 2007), with slight modifications. An acetone extract of frozen petals (0.3 g) and leaves (0.1 g) was partitioned between diethyl ether and aqueous NaCl. The organic layer was washed with 5.0 mM Tris-HCl (pH 8.0), and the residue was saponified with an equivalent amount of 10% KOH–MeOH for 1 h at room temperature. The saponified matter was then extracted with diethyl ether and washed with water. The

organic layer was then dried and dissolved in 125 μL of MeOH and subjected to HPLC analyses. A non-saponified carotenoid extract was prepared according to the same method except for the saponification step. The total content of carotenoids was estimated from the absorbance at absorption maxima using the $E^{1\%}$ value of lutein (2550) (Britton 1995), defined as the theoretical absorbance of a 1% solution in a cell with a 10 mm path length. The content of each carotenoid was calculated according to the total peak area of HPLC chromatograms at a wavelength of 450 nm.

4.3. Results

4.3.1. Genome-wide identification of *I. nil CCD* genes

Searches for putative *CCD* homologous genes in the predicted transcripts from the *I. nil* genome sequence (Hoshino et al. 2016) and EST clones (http://ipomoeanil.nibb.ac.jp/) revealed a total of seven sequences representing the *I. nil CCD* gene subfamily. These *CCD* genes were designated *InCCD1a*, *InCCD1b*, *InCCD4*, *InCCD7*, *InCCD8*, *InCCD-like-a*, and *InCCD-like-b* based on their homology to tomato and Arabidopsis genes (Table 5). The numbers of pseudo-chromosomes, putative gene length, intron numbers and amino acid length are also listed in Table 1. Predicted amino acid sequences were used for phylogenetic analysis (Fig. 17).

4.3.2. Tissue- and developmental stage-specific expression of *InCCD*

Next, I analysed the tissue- and developmental stage-specific transcriptional levels of seven *InCCD*s via RT-qPCR (Fig. 18 and Fig. 19). *InCCD1a*, *1b*, *like-a* and *like-b* were expressed almost constitutively, and their levels showed no significant difference between the different

developmental stages of petals. In the roots, *InCCD7* and *8* were expressed at relative high levels, and no significant difference existed between the stages of petal development. The expression level of *InCCD4* was significantly higher in the cotyledons, leaves, and opened flowers than in the roots, stems and S1-S3 stages of petals. Moreover, among the tested *CCD* genes, only the expression of *InCCD4* increased significantly with floral tissue development, while carotenoid levels decreased with floral tissue development, as previously reported (Yamamizo et al. 2010). Therefore, I conducted a detailed analysis of InCCD4 amino acid sequence.

4.3.3. Amino acid sequence of InCCD4

Comparison of CCD4 sequences revealed that the InCCD4 protein contained four highly conserved His residues that have been previously described as typical ligands of a non-haem iron cofactor required for dioxygenase activity (Schwartz et al. 1997) (Fig. 20). Additionally, conserved Glu or Asp residues, which are used to fix iron-ligating His (Kloer and Schulz 2006), were also found in the InCCD4 protein sequence. Based on the results of amino acid sequence and tissue-specific gene expression analyses, I assumed that InCCD4 might exhibit conserved carotenoid cleavage activity and play some role in the petals of *I. nil* in the absence of carotenoids. Subsequently, *InCCD4* was knocked out through targeted mutagenesis to investigate InCCD4 function.

4.3.4. Knocking out *CCD4* and identification of mutants

To completely inactivate InCCD4 in *I. nil*, I constructed CRISPR/Cas9 and gRNA vector for *InCCD4* (Fig. 21A) and introduced this construct into *I. nil* cv. AK77 using

Rhizobium-mediated transformation. I designed three gRNAs (gRNA1, gRNA2, and gRNA3) with a target sequence within the first exon of the *InCCD4* gene in the genome to introduce mutations (Fig. 21B). I designed the expected cleavage site of gRNA3 overlapping with the recognition sequence of the restriction enzyme *Acl*I to perform CAPS analysis. I searched the whole *I. nil* genome sequence to detect potential off-target sequences using the Web-based program GGGenome (http://gggnome.dbcls.jp/) and concluded that there were no potential off-target sites.

Nine lines of transgenic Cas9/gRNA plants were produced from independent transformation events (Fig. 21C). CAPS analysis showed that five lines exhibited bi-allelic mutations in *InCCD4* alleles, because the PCR fragment of non-digested and digested fragment were identical (Fig. 21D, E). All the bi-allelic *CCD4* mutants (*ccd4*) showed pale yellow midribs, whereas no differences in petal colouration were observed between mono-allelic (or chimeric) mutants and NT plants. Subsequently, two independent *ccd4* lines were selected for further study. Sequence analysis showed that *ccd4* plants exhibited a frame-shift mutation in both alleles (Fig. 22), and the putative amino acid sequences of the *ccd4* plants were truncated and incomplete (Fig. 23).

4.3.5. Phenotypes and the amount and composition of carotenoids in *ccd4* mutant lines

Representative flower phenotypes of NT and the *ccd4* mutant line #11-1 and #14-1 are shown in Fig. 24A-F. The midribs of the flower petals of both *ccd4* plants showed pale yellow colouration (Fig. 24A-F). Apart from this petal colour change, no other morphological differences between NT and *ccd4* were visually distinguishable. The fertility

of both mutants was normal, and unlike maize *vp14*, these plants did not show viviparity (Schwartz et al. 1997; Tan et al. 1997).

Subsequently, I compared the amount and composition of carotenoids in the petals of the *ccd4* mutant lines (#14-1) and NT. Representative HPLC chromatograms of saponified and non-saponified carotenoid extract are shown in Fig. 24G and Fig. 25, respectively. These analyses enabled detection of the carotenoid composition and the existence of esterified carotenoids, respectively (Yamamizo et al. 2010). The total amount of carotenoids in the petals of the two *ccd4* lines was significantly increased (Fig. 24H). The carotenoid levels in the mutant lines were approximately 20 times higher than those in NT. However, the carotenoid components detected in the *ccd4* lines were almost the same as those in NT (Fig. 24G). Lutein accounted for the majority of the carotenoid components in both NT and the *ccd4* mutant lines. The HPLC chromatogram of the non-saponified carotenoid extract was almost identical to that of the saponified extract, indicating that the carotenoids present in the petals of transgenic plants were not esterified (Fig. 24G and Fig. 25). In addition, only trace amount of chlorophyll a was detected in both NT and the *ccd4* mutant lines (Fig. 25).

I also analysed the amount and composition of carotenoids in the leaves of progeny of the *ccd4* mutant lines and NT (Fig. 26). The carotenoid components were almost same and no significant difference was detected in the carotenoid total amounts in the leaves. In addition, chromatograms of non-saponified extracts have peaks of chlorophylls (Fig. 26).

4.3.6. Expression of carotenoid biosynthetic genes in the petals of *ccd4* mutant lines

To investigate whether knockout of *InCCD4* affected the carotenoid biosynthesis pathway and related factors, I performed RT-qPCR to compare the expression levels of two

carotenogenic and three genes involved in the carotenoid accumulation (*PSY*: AB499050, *CHYB*: AB499056, *Orange* (*Or*): LC314594, *Pale yellow petal 1* (*PYP1*), LC314595 and *Chromoplast-specific carotenoid-associated protein* (*CHRC*), LC314596] in the petals of opened flowers in the *ccd4* mutant lines (Fig. 27). *Or*, *PYP1*, and *CHRC* encode a post-translational stabilizer of PSY (Zhou et al. 2015; Park et al. 2016), a carotenoid esterase (Ariizumi et al. 2014), and a carotenoid-binding protein (Vishnevetsky et al. 1996; Leitner-Dagan et al. 2006), respectively. The expression levels of these genes showed no significant differences between the NT and *ccd4* plants; thus, I concluded that the increase in carotenoid levels was due solely to the loss-of-function of InCCD4.

4.4. Discussion

According to previous studies, the genome sequences of *CCD1*s, *CCD4*s, *CCD7*s, and *CCD8*s generally exhibit 11–13, 0–2, 5–6 and 6–7 introns, respectively (Ahrazem et al. 2010). The detected *CCD* sequences of *I. nil* nearly matched these patterns (Table 5), suggesting that the *InCCD*s were correctly detected based on genomic information.

The expression level of *InCCD4* was significantly increased during floral tissue development (Fig. 18 and Fig. 19), similar to what has previously been reported for *CmCCD4a* of chrysanthemum (Ohmiya et al. 2006). However, *InCCD4* was not exclusively expressed in floral tissue but also highly expressed in cotyledons and leaves (Fig. 18 and Fig. 19). In a previous study, flower colour was found to be controlled by the *CCD4* family, which includes multiple *CCD4* genes, and at least one *CCD4* member is highly and exclusively expressed in flowers (Ohmiya et al. 2006; Rodrigo et al. 2013; Zhang et al. 2015). Moreover, only one homologous gene of *CCD4* was detected in the genomic

sequence of *I. nil* (Table 5). In most plants, the number of *CCD4* genes is variable between different species, with at least two genes being identified per species (Ahrazem et al. 2010; Vallabhaneni et al. 2010). The presence of a single *CCD4* gene has only been reported in a limited number of plant species with available genome sequences, such as Arabidopsis, papaya (*Carica papaya)*, peach (*Prunus persica*) and sorghum (*Sorghum bicolor*) (Ahrazem et al. 2016), and *I. nil*. The results of the present study showed that it is not only *CCD4*s (which are exclusively expressed in petals) but also *InCCD4* (whose expression is not restricted to petals) that may contribute to flower colour.

According to previous studies in Arabidopsis, loss of AtCCD4 function alone does not affect carotenoid homeostasis; however, it is not only AtCCD4 but also AtCCD1 that contributes to carotenoid turnover (Gonzalez-Jorge et al. 2013; Lätari et al. 2015). Additionally, the observation that *InCCD4* showed relatively high expression in the cotyledons and leaves of *I. nil* indicates that InCCD4 might affect carotenoid turnover together with InCCD1a and/or InCCD1b. However, as the carotenoid amounts and components in the leaves of the *ccd4* mutants were almost the same as those in NT (Fig. 26), to analyse the effect of InCCD4 on carotenoid turnover, it will be necessary to knock out *InCCD1a* and *InCCD1b* and construct a double mutant, which is beyond the scope of the present study.

To elucidate the function of InCCD4, I generated *InCCD4* knockout mutants using the CRISPR/Cas9 system and obtained homozygous mutant lines (Fig. 21 and Fig. 22). The putative amino acid sequence of InCCD4 in the *ccd4* plants was shortened and incomplete (Fig. 23). Moreover, this sequence lacked the highly conserved His, Glu, and Asp residues (Tan et al. 2003; Kloer and Schulz 2006), indicating that the carotenoid cleavage activity of

InCCD4 was lost in *ccd4* plants. The colour change of the midribs of the flowers of *ccd4* plants was very noticeable (Fig. 24A-F). Because the expression levels of carotenoid accumulation related genes showed no significant differences (Fig. 27), loss of InCCD4 function increased carotenoid accumulation in the petals. Hence, I concluded that it is not only low carotenogenic gene expression (Yamamizo et al. 2010) but also the cleavage activity of InCCD4 that contributes to the control of carotenoid accumulation in floral tissues of *I. nil*.

Carotenoid levels were significantly increased in the petals of *ccd4* mutant lines and chlorophyll levels were almost identical in ccd4 mutants and NT, so we concluded that yellow colouration was due to carotenoid accumulation. However, these components did not differ from NT (Fig. 24G, H). The majority of the carotenoid components found in both NT and the *ccd4* mutants consisted of non-esterified (free form) lutein, violaxanthin, and β-carotene, although the β-carotene level was below the detection limit in NT, reflecting the fact that the level of carotenoid accumulation related genes expression in the petals of the *ccd4* mutants was the same as in NT, which was still lower than that in *I. obscura* var. *lutea* (Yamamizo et al. 2010). In the Chapter 2, I successfully changed the components and increased the total amount of carotenoids after overexpressing genes encoding carotenoid biosynthesis enzymes, including the rate-limiting enzyme PSY (Giuliano et al. 1993; Moehs et al. 2001) and key enzymes responsible for the addition of hydroxyl residues required for the esterification of carotenoids (CHYB) (Galpaz et al. 2006; Yamamizo et al. 2010). Thus, the combination of *InCCD4* mutagenesis and overexpression of carotenoid accumulation related genes sufficiently would increase the carotenoid content in the petals of *I. nil* to produce yellow petals.

The carotenoids contained in the petals of *ccd4* plants were not esterified and existed in the free form (Fig. 25). Esterified carotenoids are the dominant chemical form for the storage of these compounds within chromoplasts. In the petals of *I. obscura* var. *lutea*, β-carotene derivatives (β-carotene, β-cryptoxanthin, and zeaxanthin) have been shown to account for approximately 85%, and xanthophylls such as β-cryptoxanthin and zeaxanthin exist in esterified forms (Yamamizo et al. 2010). I assume that low levels of carotenoids observed in the petals of the *ccd4* mutant lines partially reflect the absence of esterification activity. Therefore, promotion of esterification activity will increase carotenoid accumulation. Overexpression of *PYP1*, which encodes the enzyme that esterifies carotenoids (Ariizumi et al. 2014), may enhance esterification activity and could increase carotenoid accumulation.

In the present study, I focused on the function of the InCCD4 enzyme in the petals of *I. nil*, which can store only trace amounts of carotenoids. Then I successfully increased carotenoid accumulation in the petals changed their colour. These results suggest that the low carotenoid levels observed in the floral tissues of *I. nil* are due to not only low carotenogenic gene expression but also carotenoid degradation through InCCD4. Thus, knocking out *CCD4* will produce novel flower colours and contribute to the development of nutritionally improved agricultural crops and fruits with high economic value, such as peaches and bananas (Brandi et al. 2011; Bai et al. 2016; Buah et al. 2016). The present study represents an important milestone towards the application of the CRISPR/Cas9 system to modify flower colour via increasing the amounts of carotenoids in petals lacking the ability to accumulate carotenoids and to further carotenoid metabolic engineering.

4.5. Tables and Figures

Table 5. The *InCCD* genes and properties of the deduced proteins.

Name	Description	Pseudo Chromosome	Gene length (bp)*	number of intron	Predicted protein length (AA)	Accession number
CCD1a	*Carotenoid cleavage dioxygenase 1a*	4	13279	13	603	BR001460
CCD1b	*Carotenoid cleavage dioxygenase 1b*	12	7270	14	578	BR001461
CCD4	*Carotenoid cleavage dioxygenase 4*	15	3373	1	591	BR001462
CCD7	*Carotenoid cleavage dioxygenase 7*	9	3009	6	614	BR001463
CCD8	*Carotenoid cleavage dioxygenase 8*	10	6411	5	561	BR001464
CCDlike a	*Carotenoid cleavage dioxygenase like a*	10	12085	10	509	BR001465
CCDlike b	*Carotenoid cleavage dioxygenase like b*	15	33696	13	604	BR001466

*Number of nucleotides from predicted transcription start site to end site, including intron(s), in base pairs (bp).

Table 6. Primer sets used in the present study.

Purpose	Target gene	Direction	Sequence	Amplified length (bp)
RT-qPCR (*CCD*s)	*CCD1a*	Forward	5' GCAGTAGCATTACCTCAGATTCCA 3'	66
		Reverse	5' ATTCTCAGAGTGCAGAACAGGTAG 3'	
	CCD1b	Forward	5' TCGGTAGTACGTTGTTAGGGTCT 3'	56
		Reverse	5' ACTTAGGTTTATAACTTTGCCGGAT 3'	
	CCD4	Forward	5' TTTTCCGGCAACCGCTTT 3'	65
		Reverse	5' GGCGATGTAAGCCGGATTG 3'	
	CCD7	Forward	5' TCCCAGCCATTCATCCAGACT 3'	66
		Reverse	5' CGGAAGAAGTTGCAGCATAAACA 3'	
	CCD8	Forward	5' GAGACCCTGCAACTTTCCCAAT 3'	61
		Reverse	5' CTTTGCCTTCTTCCCAACCAA 3'	
	CCDlike-a	Forward	5' AGCATCAGTCTCGGCGATGA 3'	70
		Reverse	5' GGGTCTCAGAGAGGGCATACTTCT 3'	
	CCDlike-b	Forward	5' AACCACCGACCCAGTTAACGA 3'	70
		Reverse	5' GAACATCATCTGCCTGACCATTG 3'	
	Actin	Forward	5' CGTTCAGCTGAGGTTGTGAAAGA 3'	71
		Reverse	5' CGTGACCTCACTGATCATTTGATG 3'	
	Ubiquitin	Forward	5' CTTGTCCTTCGTCTCCGTGGTG 3'	65
		Reverse	5' GCAGTGACACAAACATCATTGGG 3'	
Vector Construction	gRNA1	Forward	5' ATTGCTTTCATTGATCCGCCGCTC 3'	-
		Reverse	5' AAACGAGCGGCGGATCAATGAAAG 3'	
	gRNA2	Forward	5' AAACGTCGACGAGCTCCCGCCGGC 3'	-
		Reverse	5' ATTGGCCGGCGGGAGCTCGTCGAC 3'	
	gRNA3	Forward	5' ATTGTGAAACCGGAGAAAACGTTG 3'	-
		Reverse	5' AAACCAACGTTTTCTCCGGTTTCA 3'	
Genotyping	*NPTII*	Forward	5' GAGGCTATTCGGCTATGACT 3'	751
		Reverse	5' TCCCGCTCAGAAGAACTCGT 3'	
CAPS & Sequencing	*CCD4*	Forward	5' TCGAAGAAAAGACGGTAACCAC 3'	600
		Reverse	5' CCAAGCTGGTGTTCGCTA 3'	
RT-qPCR (carotenogenic genes)	*PSY*	Forward	5' GTGCAGAGTATGCAAAGACG 3'	168
		Reverse	5' GCCTAGCCTCCCATCTATCC 3'	
	CHYB	Forward	5' CCTATCGCCGACGTACCTTA 3'	134
		Reverse	5' TCGTTTAGCCCACCAACTTC 3'	
	Or	Forward	5' ATCTCTGCCTTGATGGTAGTTGA 3'	65
		Reverse	5' TACTTGCACCTCTTATGCTCCT 3'	
	PYP1	Forward	5' CTGAATATGCCAATTCCCGTCT 3'	69
		Reverse	5' TGTCCATTCCACTAGCAAGCAC 3'	
	CHRC	Forward	5' AACCCTCTGTATTTCCGGTGA 3'	58
		Reverse	5' CTCAATGCGGCCATTTTCGAT 3'	

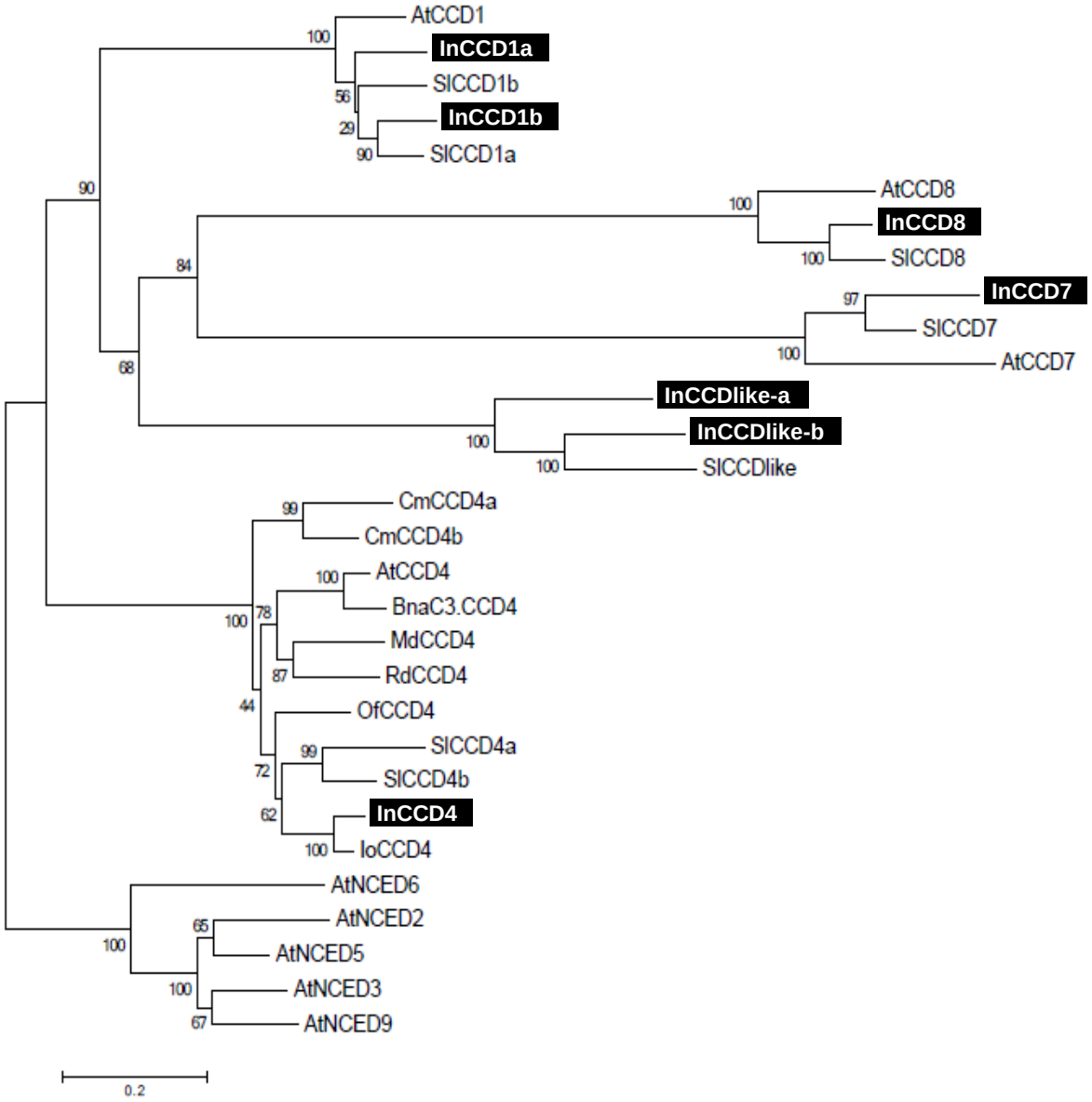

Fig. 17. Phylogenetic tree of CCDs of various plant species.

Fig. 17. (continued). The neighbor-joining phylogenetic tree (Saito and Nei, 1987) was generated based on the alignment of deduced protein sequences from CCD homologs in *I. nil* (black highlighted) and from various plant species. The horizontal branch length is proportional to the estimated number of amino acids substitutions per residue (Bar = 0.2 aa substitution per residue). Number at the branch points represents the bootstrap values for percentage of 1,000 replicate trees. This is an unrooted tree. AtCCD1 (accession number: At3g63520), AtCCD4 (At4g19170), AtCCD7 (At2g44990), AtCCD8 (At4g32810), AtNCED2 (At4g18350), AtNCED3 (At3g14440), AtNCED5 (At1g30100), AtNCED6 (At3g24220), and AtNCED9 (At1g78390) are CCDs and NCEDs of Arabidopsis. SlCCD1a (Solyc01g087250), SlCCD1b (Solyc01g087260), SlCCD4a (Solyc08g075480), SlCCD4b (Solyc08g075490), SlCCD7 (Solyc01g090660), SlCCD8 (Solyc08g066650) and SlCCD-like (Solyc08g066720) are CCDs of tomato. CmCCD4a (AB247158) and CmCCD4b (AB247160) are CCDs of chrysanthemum. Other include IoCCD4 of *Ipomoea obscura* var. *lutea* (AB499059), MdCCD4 of apple (*Malus* × *domestica*, EU327777), OfCCD4 of osmanthus (*Osmanthus fragrans*, EU334434), RdCCD4 of rose (*Rosa* × *damascena*, EU334433) and BnaC3.CCD4 of rapeseed (*Brassica napus*, KP658825).

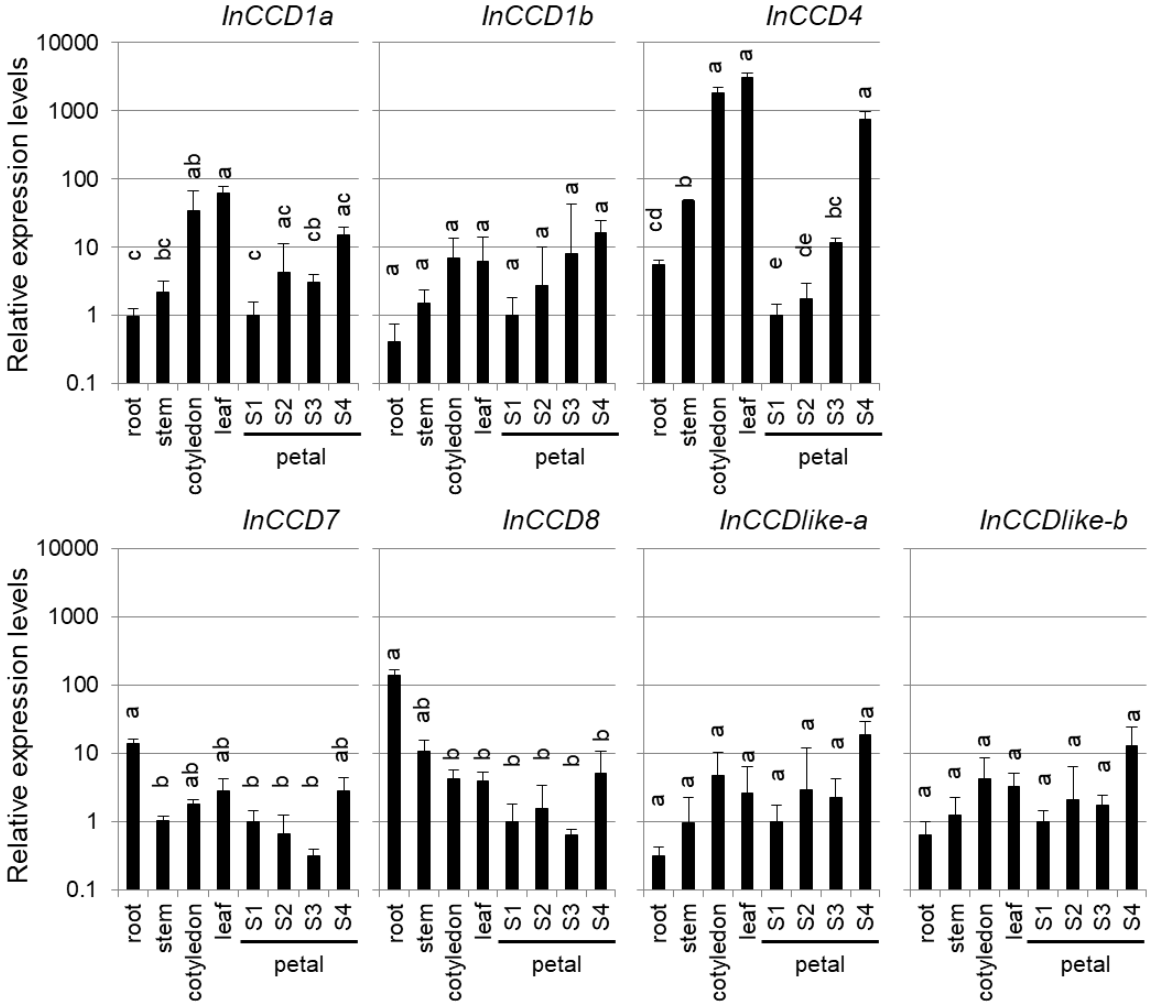

Fig. 18. Tissue and developmental stage specific expression levels of *InCCDs*. Quantitative real-time RT-PCR analysis was performed in biological triplicate using each *InCCD*-specific primers, and the expression levels were normalized against *actin* levels; mean values ±SE are shown (n = 3). Different letters within each tissue and stage indicate significant differences by Tukey-Kramer test (P <0.01).

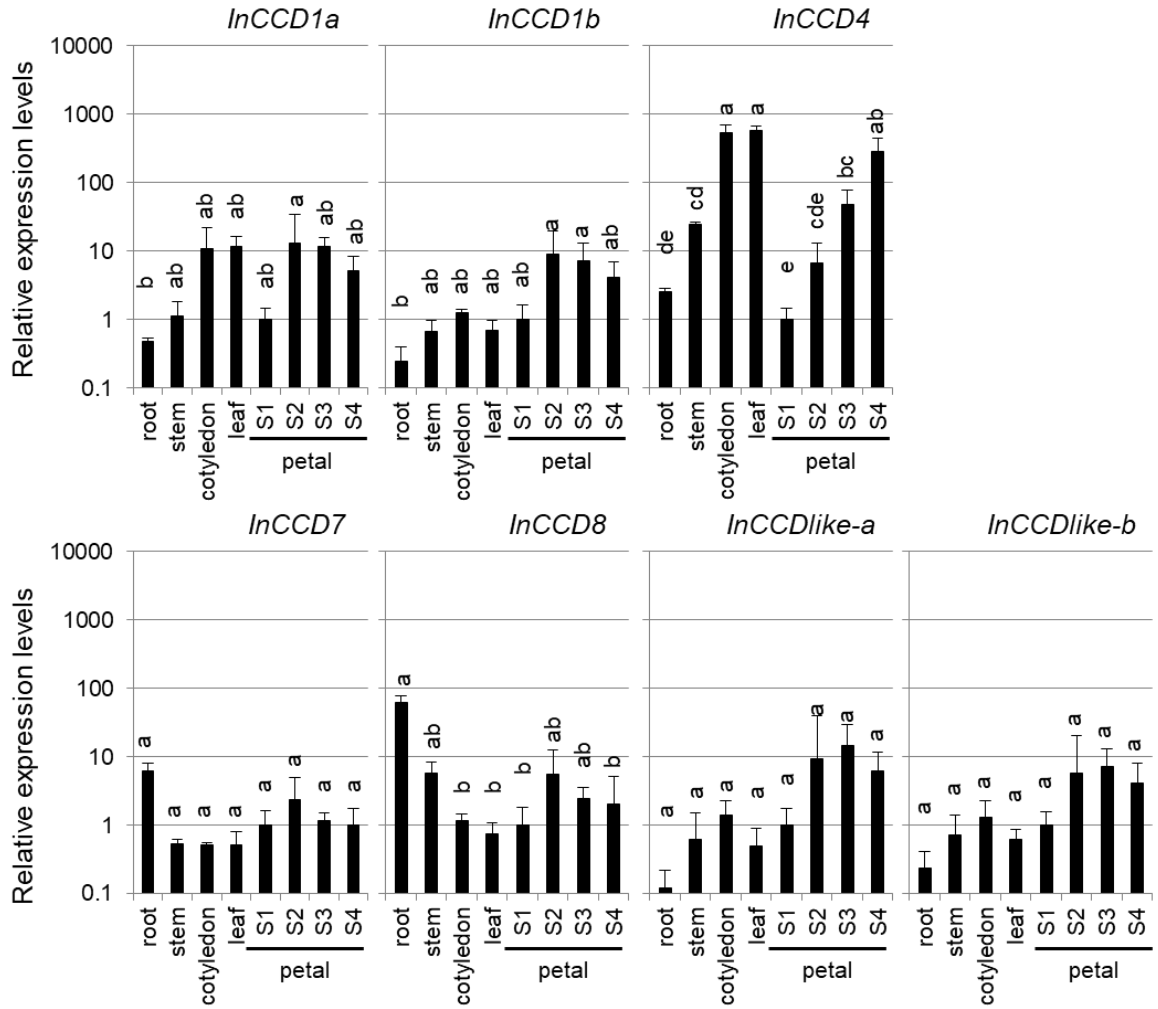

Fig. 19. Tissue and developmental stage specific expression levels of *InCCDs* normalized against *Ubiquitin* levels. RT-qPCR analysis was performed in biological triplicate using each *InCCD*-specific primers, and the expression levels were normalized against *Ubiquitin* levels; mean values ±SE are shown (n = 3). Different letters within each tissue and stage indicate significant differences by Tukey-Kramer test ($P < 0.01$).

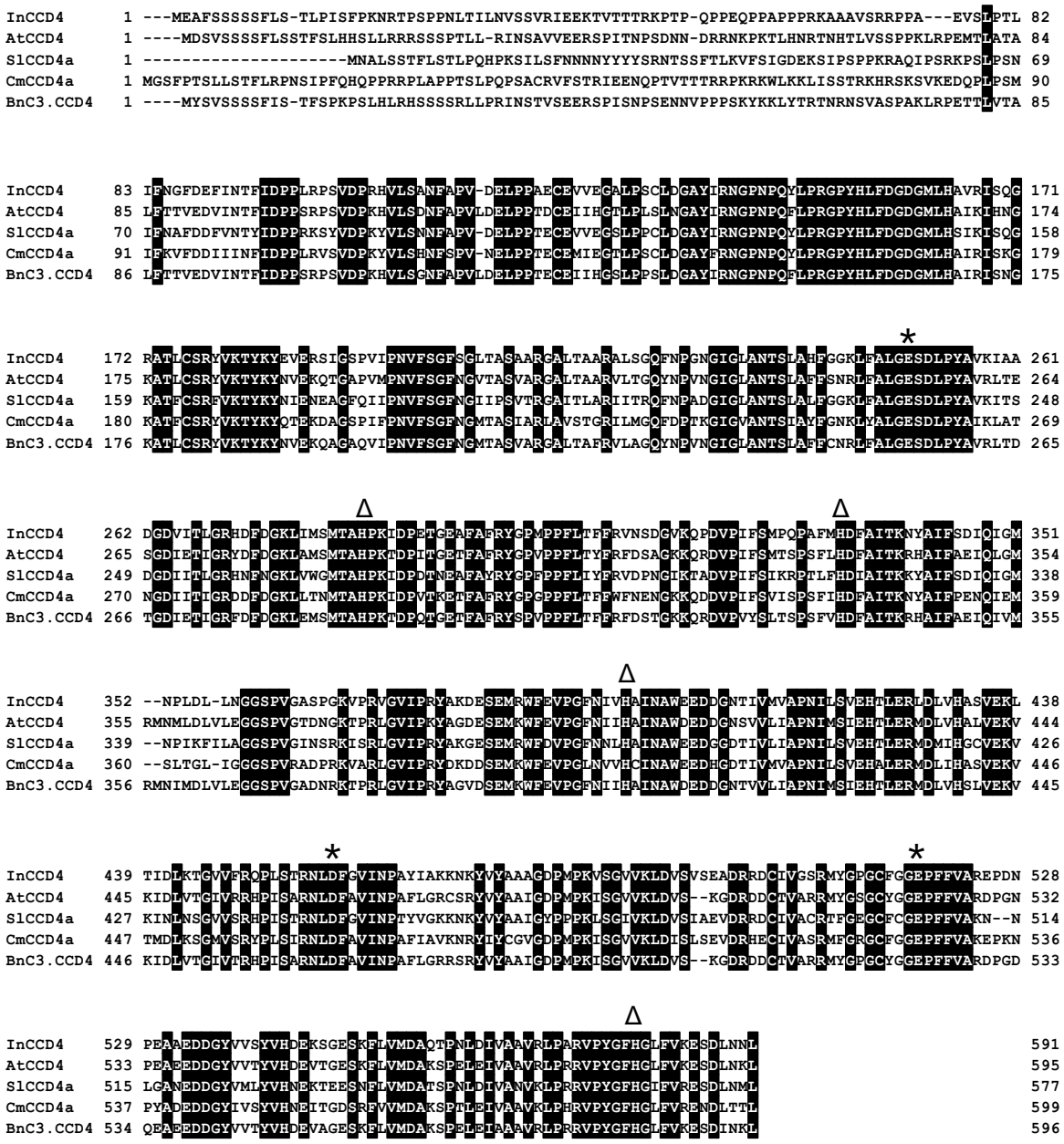

Fig. 20. Sequence comparison of CCD4 of various plant species. The amino acid sequences are given in the one-letter code and have been aligned, with the introduction of gaps (---), to maximize possible homology. Identical amino acids are indicated with black backgrounds. Conserved four His and three Glu or Asp residues are marked with asterisks and triangles respectively.

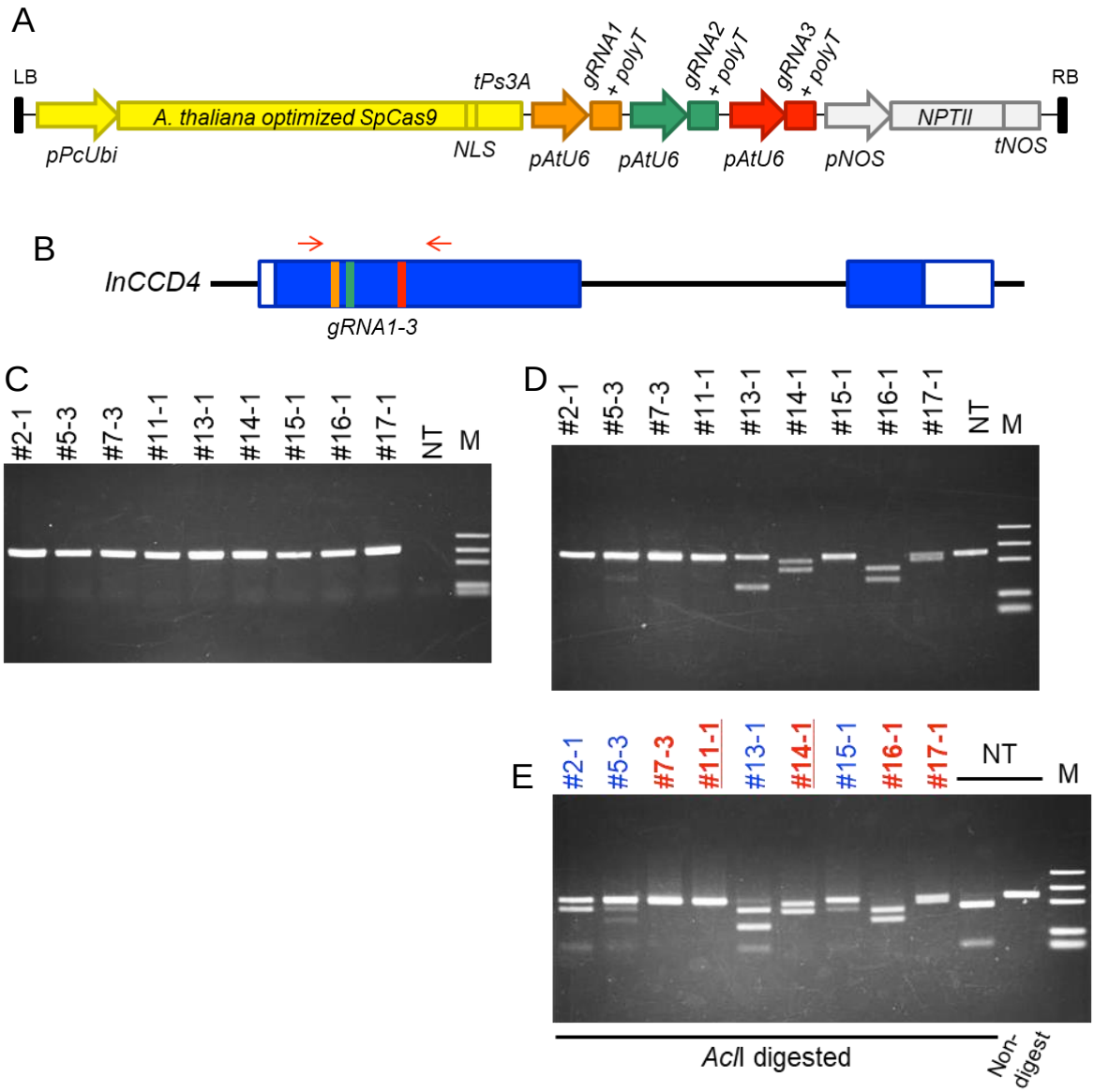

Fig. 21. Identification of *InCCD4* mutant lines. A: Schimetic representation of the construct used in the study. **B**: The gene structure of *InCCD4* along with the sites of mutation. The coding sequences, untranslated regions, intron and gRNA positions are indicated with blue boxes, white boxes, a black bar and orange lines, respectively. Red arrows indicate the primers used for CAPS and sequence analysis. **C**: PCR fragments of *NPTII* from transgenic Cas9/gRNA plants. M: marker (1,000, 700, 500, 200 and 100 bp). **D**, **E**: CAPS analysis of transgenic Cas9/gRNA plants. The PCR products shown in **D** were non-digested, and in **E** were digested using the *Acl*I restriction enzyme, except for the NT control, shown on the right side in **E**. Blue letters indicate mono-allelic (and/or chimeric) mutants and red bold letters indicate bi-allelic mutants. Two bi-allelic mutants (#11-1 and #14-1; underlined) were used for further study. M: marker.

Fig. 22. Partial DNA sequences of *InCCD4* in the two mutant lines, *ccd4* #11-1 and 14-1, were aligned with those in NT. As these lines are bi-allelic mutants containing two different alleles, two sequences were obtained and designated with _1 and _2. Guide RNAs and protospacer adjacent motif (PAM) sequences are indicated by pale blue and pale red boxes, respectively. The hyphens with black background indicate deleted nucleotide bases by the CRISPR-Cas9 system.

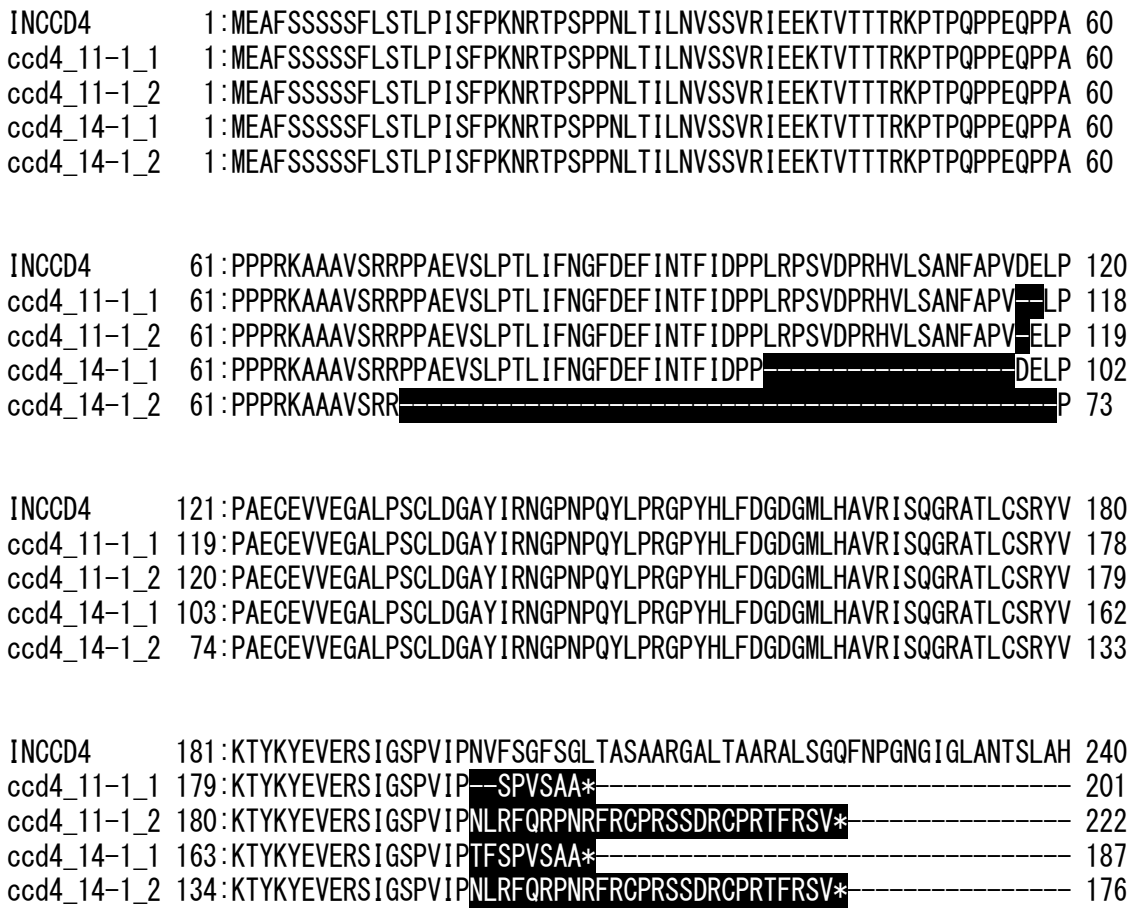

Fig. 23. Putative amino-acid sequences of *InCCD4* mutant lines. As these lines are bi-allelic mutants containing two different alleles, two amino-acid sequences were predicted and designated with _1 and _2. The white letters with black background indicate deleted residues or flame-shifted amino-acid sequences by the CRISPR-Cas9 system. Please note, the four conserved His and the three conserved Glu and Asp residues among CCD4 family proteins shown in Fig. 3. are located after 250 aa.

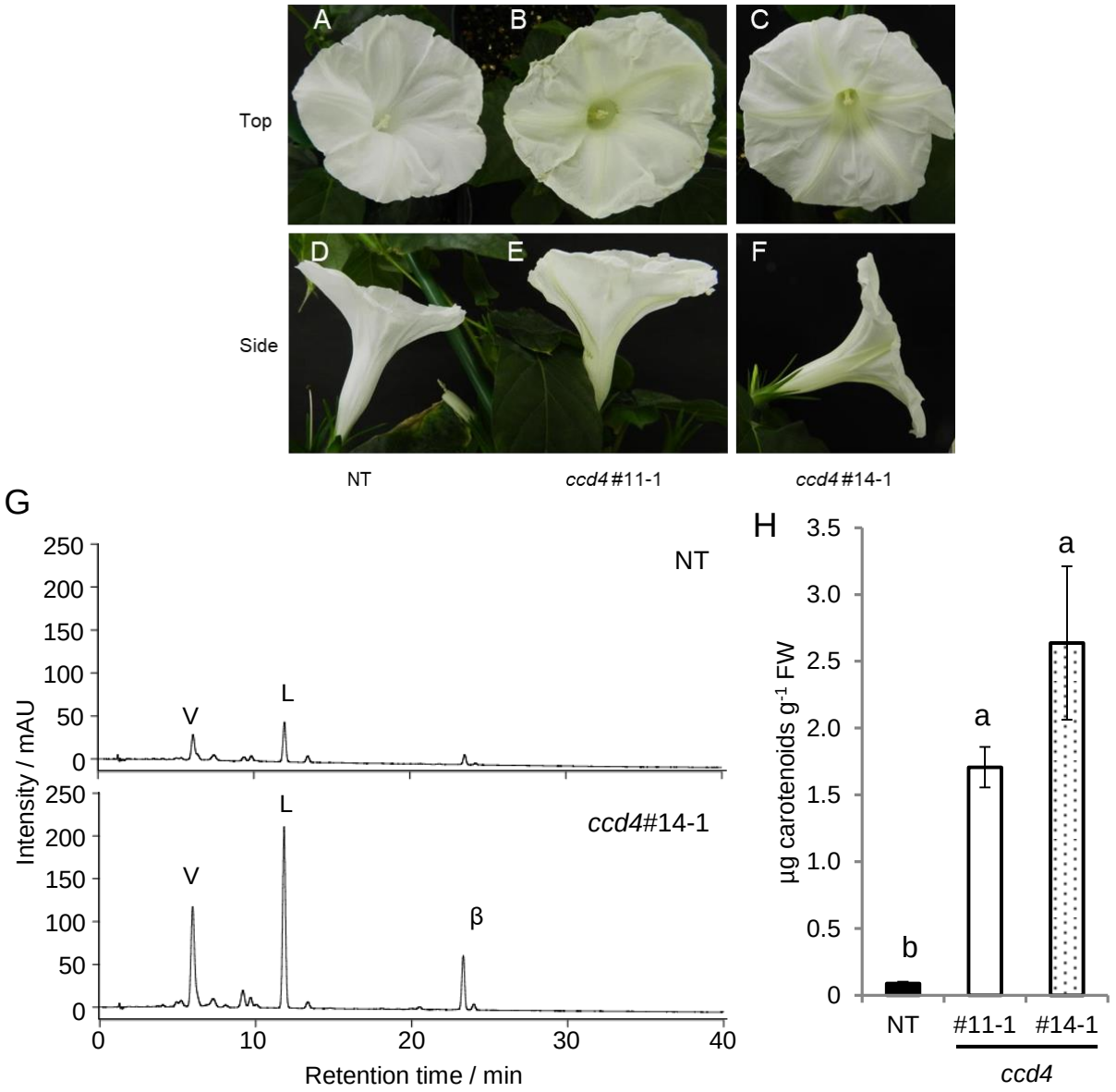

Fig. 24. HPLC chromatograms and total carotenoid concentration of flowers of non-transgenic (NT) and *ccd4* plant. A: Appearance of *ccd4* #11-1; **B, E**: *ccd4* #14-1; **C, F**: NT; **A, D**: opened flowers. Top: top view; Side: side view. **G**: Representative HPLC elution profiles of non-saponified carotenoids extracted from petals of opened flower. V, violaxanthin; L, lutein; β, β-carotene. **H**: Total carotenoid contents in the petal of opened flower of the NT and *ccd4*, as determined by HPLC analysis after saponification. All experiments were biologically repeated three times. Different letters indicate significant differences by Tukey-Kramer test (P <0.05). Error bars indicate ± SE (n = 3).

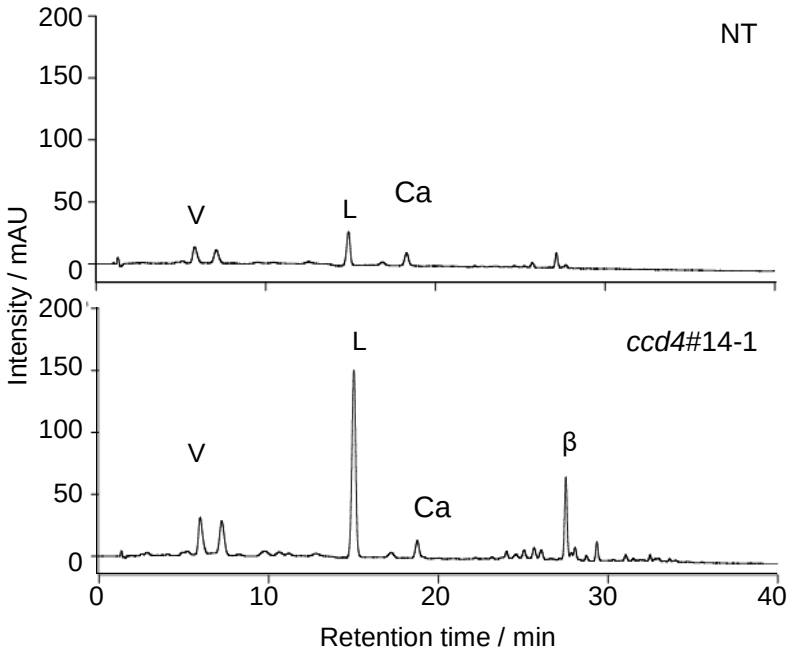

Fig. 25. Representative HPLC elution profiles of non-saponified carotenoids of flowers of NT and *ccd4* plant. Carotenoids were extracted from petals of opened flower without saponification. V, violaxanthin; L, lutein; β, β-carotene; Ca, chlorophyll a. Upper: non-transgenic plant (NT); lower: *ccd4*#14-1 mutant.

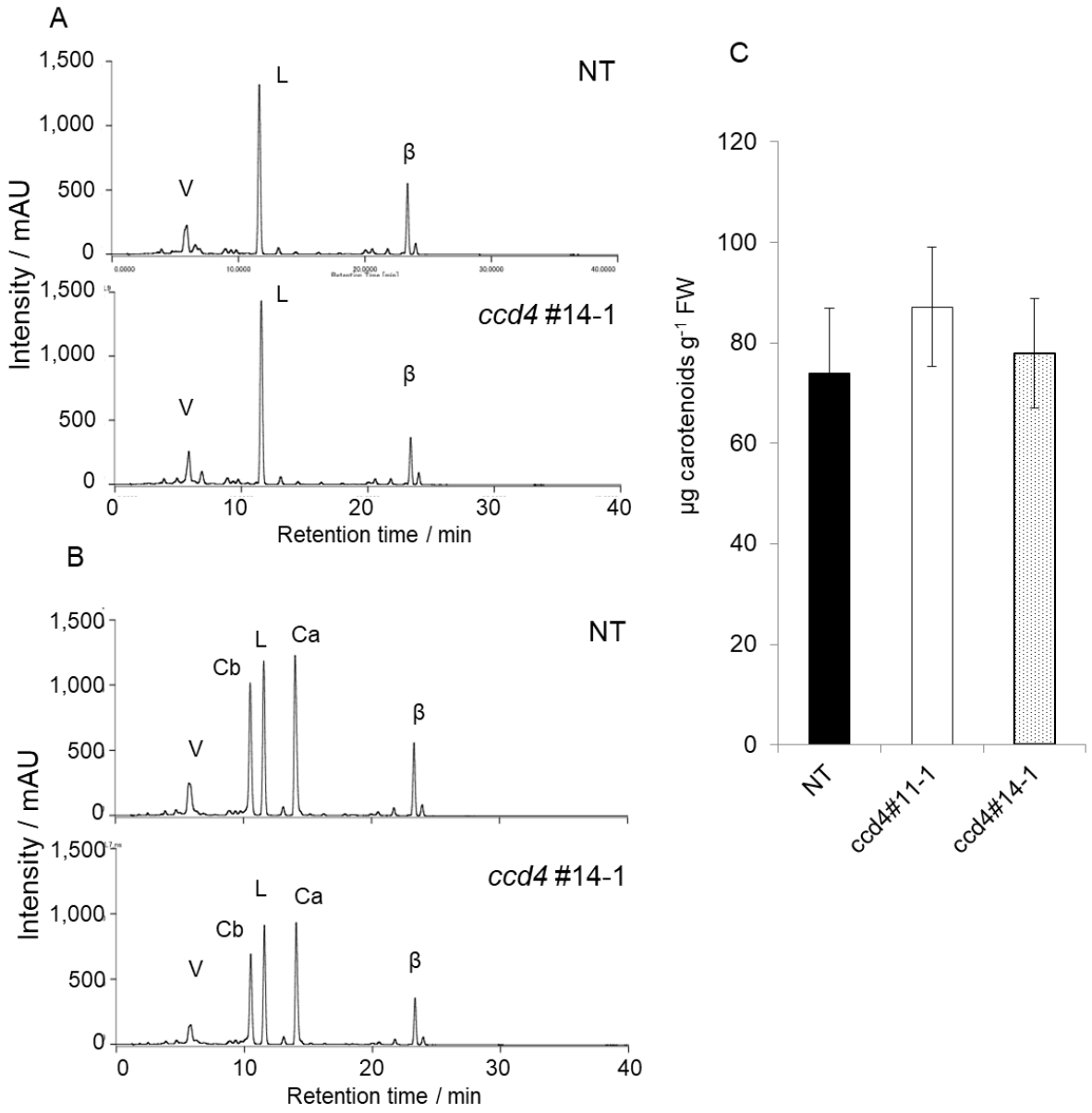

Fig. 26. HPLC chromatograms and total carotenoid concentration of leaves of non-transgenic (NT) and progeny of the *ccd4* plants. **A**, **B**: Representative HPLC elution profiles of saponified **A** and non-saponified **B** carotenoids extracts, respectively. The carotenoids were extracted from the leaves collected at two weeks after sowing. V, violaxanthin; L, lutein; β, β-carotene; Cb, chlorophyll b; Ca, chlorophyll a. **C**: Total carotenoid contents in the leaves of the NT and *ccd4*, as determined by HPLC analysis after saponification. All experiments were biologically repeated three times. The Tukey-Kramer test was used to determine statistical significance, and no significant difference were detected ($P > 0.05$). Error bars indicate ± SE ($n = 3$).

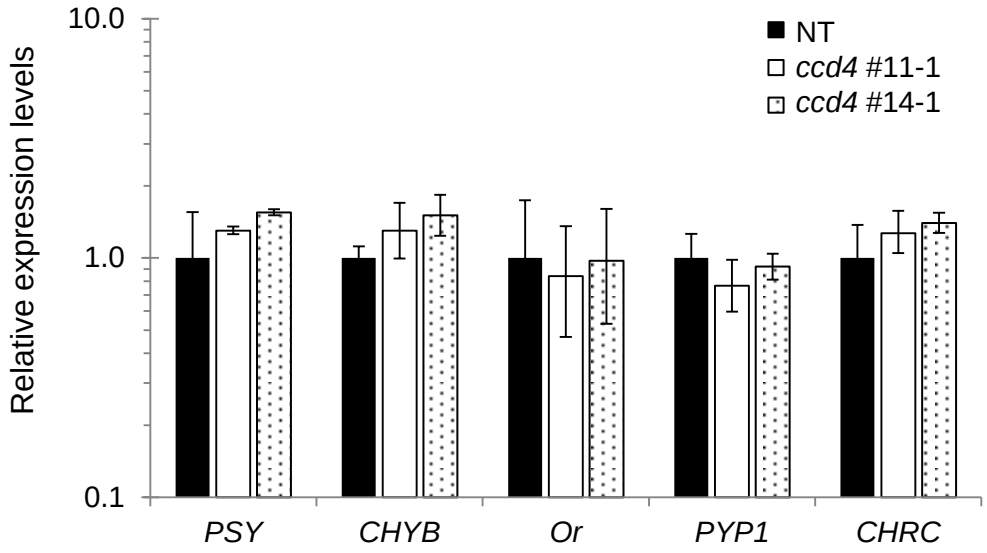

Fig. 27. The expression levels of carotenoid biosynthetic and accumulation related genes in the fully opened petal. Quantitative real-time RT-PCR analysis was performed in biological triplicate using each gene-specific primers, and the expression levels were normalized against *actin* levels; mean values ± SE are shown (n = 3). There was no significant difference ($P > 0.05$).

Chapter 5. General discussion

5.1. Discussion

Here in the present study, I tried to produce yellow-flowered Japanese morning glory with genetic engineering by accumulating carotenoids, besides retrospectively accomplished with flavonoid. The summary of the present study illustrated in Fig. 28. In the Chapter 2, I succeeded to produce transgenic plants overexpressing five carotenogenic genes in the petal of *I. nil*. Then carotenoid concentration in the petal was increased up to about ten-fold relative to NT. Moreover, the components of carotenoids in the petal were changed, in particular several β-carotene derivatives, such as zeaxanthin and neoxanthin, were newly synthesized. Nevertheless, the petal colour did not visually change. This result indicated that there are some other factors contributing the low accumulation levels of carotenoids in the petals.

In the Chapter 3, the applicability of the recent developed CRISPR/Cas9 system to *I. nil* was confirmed. I also investigated traits of off-targeting, chimaeras and inheritances, and concluded that these traits would not be barriers for genome editing in *I. nil*.

Hence in the Chapter 4, I investigated the possible involvement of CCD which cleaves specific double bonds of the polyene chains of carotenoids, using the CRISPR/Cas9 method established in the Chapter 3. The total amount of carotenoids in the petals of *ccd4* plants was increased 30-fold relative to NT plants, caused the white petals to turn pale yellow. This result indicates that in the petals of *I. nil*, not only low carotenogenic gene expression but also carotenoid degradation leads to extremely low levels of carotenoids.

Thirty-fold carotenoid made petal yellow, but it was still slight pale. One possible strategy for more accumulation is applying traditional or conventional breeding techniques, such as selective breeding and crossbreeding. If transformed plants produced in this study

will be used for the traditional breeding, the flower would get more yellowish colour. Changing a host cultivar or transgene source of transformation can also increase the carotenoid accumulation. In the attempts of producing blue rose, delphinidin, a blue anthocyanin, accumulation rate and its colouration were depending on host cultivars (Katsumoto et al. 2007). Fortunately, *I. nil* have a lot of cultivars and there would be cultivars which can accumulate high carotenoid in a petals when carotenogenic genes overexpression (Chapter 2) and/or *InCCD4* knocking out (Chapter 4). As in case golden rice (Paine et al. 2005), changing the transgene source also has potential to increase the accumulation of carotenoids. Moreover, there would be still other factors to make petal bright yellow. I will discuss about two candidates of the other factors, esterification and chromoplast development.

The esterified carotenoids are the dominant chemical form for storage of this compound within chromoplasts. In the petal of *I. obscura* var. *lutea*, β-carotene, β-cryptoxanthin and zeaxanthin occupy about 85% of carotenoids. Among them, xanthophylls such as β-cryptoxanthin and zeaxanthin existed in the esterified form (Yamamizo et al. 2010). However, in the present study, carotenoids contained in the petals of transgenic plants were not esterified and existed in the free form. Absence of esterification activity would be the reason why total amount of carotenoid was not high enough to express yellow colour in spite of carotenogenic genes overexpressed. Promoting esterification activity by, for example, overexpressing the *PYP1* which encodes the enzyme that esterifies carotenoids (Ariizumi et al. 2014) would increase the carotenoid accumulation.

In yellowish tissue of higher plants, such as flowers and fruits, carotenoid is stored in the chromoplast. The edible tissues of crops are endosperms and/or tubers, and full filled

with amyloplast which is one of the plastid forms that stores starch (Solymosi and Keresztes 2012). Because plastids can convert each other, amyloplast to chromoplast conversion would naturally occur in amyloplast-rich tissues. Hence the simple overexpression of the carotenogenic genes in the seeds of *B. napus* and endosperm of *O. sativa* can increase the carotenoids accumulation (Shewmaker et al. 1999; Paine et al. 2005). On the other hand, in the petal of *I. nil*, over-expressions of carotenogenic genes could not cause plastid to chromoplast conversion in floral tissue simply, unlike amyloplast to chromoplast conversion in crops. Otherwise the plastids might be absent in the petal. Induction of the chromoplast differentiation would increase carotenoids sufficient to express yellow colour. Although little is known about the mechanisms of chromoplast differentiation, some factors that affect the event have been reported. One of the factor is Or which is firstly isolated in mutant of cauliflower, *Brassica oleracea* var. *Botrytis* (Crisp et al. 1975; Li et al. 2006; Lu et al. 2006) and recent studies showed that Or is post-translational stabilizer of PSY (Zhou et al. 2015; Park et al. 2016). Moreover, previous studies showed that some mutations increased carotenoid accumulation levels (Kim et al. 2013; Tzuri et al. 2015; Yuan et al. 2015a). Overexpression of modified *Or*, or introducing the mutations with the genome editing tools would cause potential of chromoplast differentiation and facilitate more accumulation of carotenoids.

I hope that the present study will help to produce novel flower colours, to contribute to the development of nutritionally improved agricultural crops, and to improve understanding of NBT.

5.2. Figure

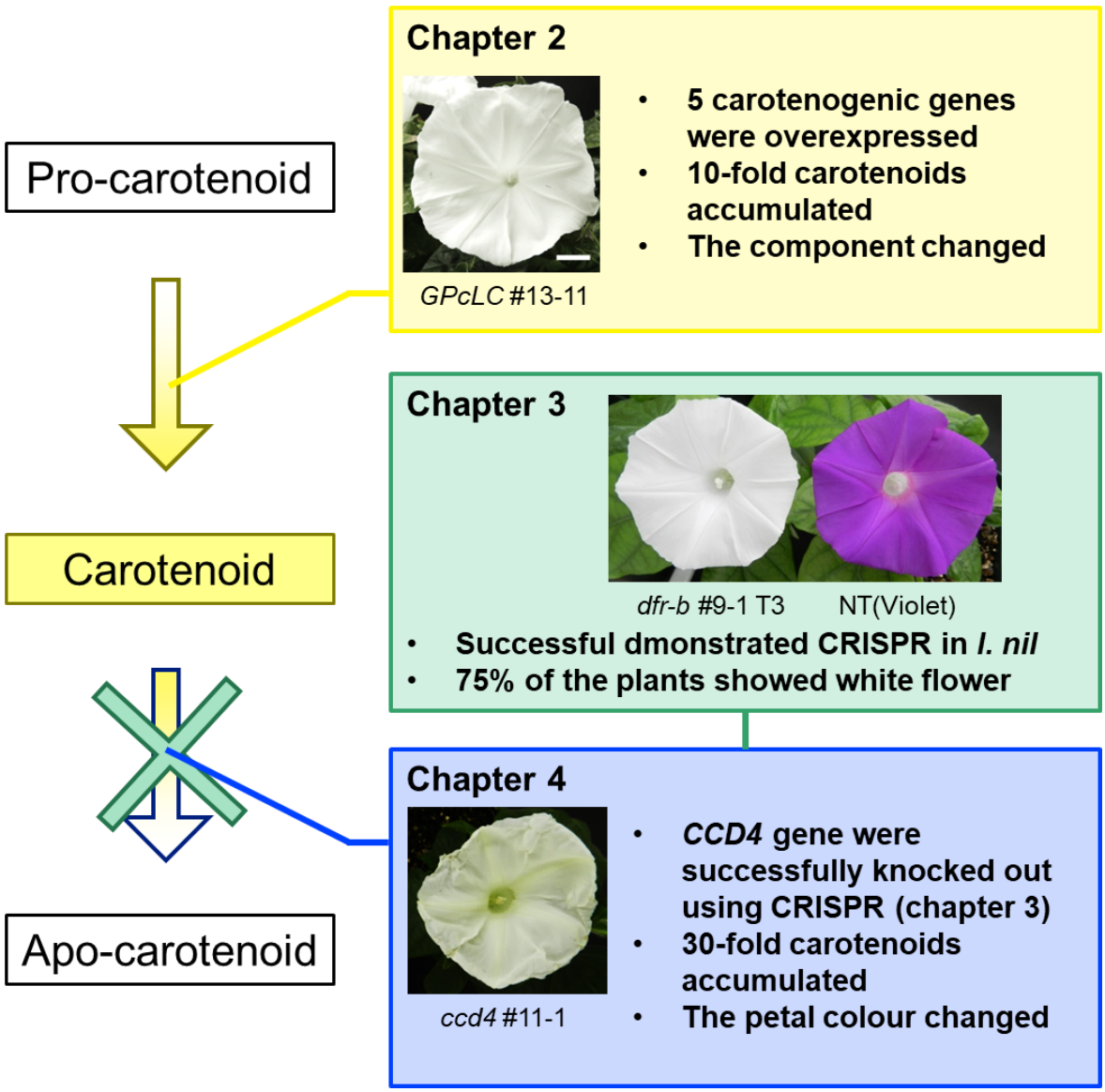

Fig. 28. Summary of the present study. In the Chapter 2, I succeeded to produce transgenic plants overexpressing five carotenogenic genes in the petal of *I. nil*. The carotenoid concentration in the petal was increased up to about ten-fold relative to NT and the components changed. In the Chapter 3, the applicability of the recent developed CRISPR/Cas9 system to *I. nil* was confirmed. In the Chapter 4, the total amount of carotenoids in the petals of *ccd4* plants was increased 30-fold relative to non-transgenic plants, caused the white petals to turn pale yellow.

References

Ahrazem O, Gómez-Gómez L, Rodrigo MJ, Avalos J, Limón MC (2016) Carotenoid cleavage oxygenases from microbes and photosynthetic organisms: Features and functions. *Int J Mol Sci* **17**: 1781. doi: 10.3390/ijms17111781

Ahrazem O, Trapero A, Gómez MD, Rubio-Moraga A, Gómez-Gómez L (2010) Genomic analysis and gene structure of the plant carotenoid dioxygenase 4 family: A deeper study in *Crocus sativus* and its allies. *Genomics* **96**: 239–250. doi: 10.1016/j.ygeno.2010.07.003

Aida R, Sasaki K, Ohtsubo N (2016) Production of chrysanthemum periclinal chimeras through shoot regeneration from leaf explants. *Plant Biotechnol* **33**: 45–49. doi: 10.5511/plantbiotechnology.15.1127a

Altschul SF, Madden TL, Schäffer AA, Zhang J, Zhang Z, Miller W, Lipman DJ (1997) Gapped BLAST and PSI-BLAST: A new generation of protein database search programs. *Nucleic Acids Res* **25**: 3389–3402. doi: 10.1093/nar/25.17.3389

Aoki T, Akashi T, Ayabe S (2000) Flavonoids of Leguminous plants: Structure, biological activity, and biosynthesis. *J Plant Res* **113**: 475–488. doi: 10.1007/PL00013958

Araki M, Ishii T (2015) Towards social acceptance of plant breeding by genome editing. *Trends Plant Sci* **20**: 145–149. doi: 10.1016/j.tplants.2015.01.010

Ariizumi T, Kishimoto S, Kakami R, Maoka T, Hirakawa H, Suzuki Y, Ozeki Y, Shirasawa K, Bernillon S, Okabe Y, et al. (2014) Identification of the carotenoid modifying gene *PALE YELLOW PETAL 1* as an essential factor in xanthophyll esterification and yellow

flower pigmentation in tomato (*Solanum lycopersicum*). *Plant J* **79**: 453–465. doi: 10.1111/tpj.12570

Auldridge ME, McCarty DR, Klee HJ (2006) Plant carotenoid cleavage oxygenases and their apocarotenoid products. *Curr Opin Plant Biol* **9**: 315–321. doi: 10.1016/j.pbi.2006.03.005

Azadi P, Otang NV, Chin DP, Nakamura I, Fujisawa M, Harada H, Misawa N, Mii M (2010) Metabolic engineering of *Lilium* × *formolongi* using multiple genes of the carotenoid biosynthesis pathway. *Plant Biotechnol Rep* **4**: 269–280. doi: 10.1007/s11816-010-0147-y

Bai S, Tuan PA, Tatsuki M, Yaegaki H, Ohmiya A, Yamamizo C, Moriguchi T (2016) Knockdown of Carotenoid Cleavage Dioxygenase 4 (CCD4) via virus-induced gene silencing confers yellow coloration in peach fruit: Evaluation of gene function related to fruit traits. *Plant Mol Biol Report* **34**: 257–264. doi: 10.1007/s11105-015-0920-8

Brandi F, Bar E, Mourgues F, Horváth G, Turcsi E, Giuliano G, Liverani A, Tartarini S, Lewinsohn E, Rosati C (2011) Study of "Redhaven" peach and its white-fleshed mutant suggests a key role of CCD4 carotenoid dioxygenase in carotenoid and norisoprenoid volatile metabolism. *BMC Plant Biol* **11**: 24–37. doi: 10.1186/1471-2229-11-24

Britton G (1995) UV/visible spectroscopy. In: Britton G, Liaaen-Jensen S, Pfander H (eds) Carotenoids, Volume 1B: Spectroscopy. Birkhäuser Verlag, Basel, pp 13–62

Brockington SF, Yang Y, Gandia-Herrero F, Covshoff S, Hibberd JM, Sage RF, Wong GKS, Moore MJ, Smith SA (2015) Lineage-specific gene radiations underlie the evolution of novel betalain pigmentation in Caryophyllales. *New Phytol* **207**: 1170–1180. doi: 10.1111/nph.13441

Buah S, Mlalazi B, Khanna H, Dale JL, Mortimer CL (2016) The quest for Golden Bananas: Investigating carotenoid regulation in a Fe'i group *Musa* cultivar. *J Agric Food Chem* **64**: 3176–3185. doi: 10.1021/acs.jafc.5b05740

Bustin SA, Benes V, Garson JA, Hellemans J, Huggett J, Kubista M, Mueller R, Nolan T, Pfaffl MW, Shipley GL, et al. (2009) The MIQE guidelines: minimum information for publication of quantitative real-time PCR experiments. *Clin Chem* **55**: 611–622. doi: 10.1373/clinchem.2008.112797

Cazzonelli CI, Pogson BJ (2010) Source to sink: regulation of carotenoid biosynthesis in plants. *Trends Plant Sci* **15**: 266–274. doi: 10.1016/j.tplants.2010.02.003

Christinet L, Burdet F, Zaiko M (2004) Characterization and functional identification of a novel plant 4, 5-extradiol dioxygenase involved in betalain pigment biosynthesis in *Portulaca grandiflora*. *Plant Physiol* **134**: 265–274. doi: 10.1104/pp.103.031914.sis

Clement JS, Mabry TJ (1996) Pigment evolution in the caryophyllales: A systematic overview. *Bot Acta* **109**: 360–367. doi: 10.1111/j.1438-8677.1996.tb00584.x

Cong L, Ran FA, Cox D, Lin S, Barretto R, Habib N, Hsu PD, Wu X, Jiang W, Marraffini LA, et al. (2013) Multiplex genome engineering using CRISPR/Cas system. *Science* **339**: 819–824. doi: 10.1126/science.1231143 RNA-Guided

Crisp P, Walkey DGA, Bellman E, Roberts E (1975) A mutation affecting curd colour in cauliflower (*Brassica oleracea* L. var. *Botrytis* DC). *Euphytica* **24**: 173–176. doi: 10.1007/BF00147182

Cuttriss AJ, Mimica JL, Howitt CA, Pogson BJ (2007) Carotenoids. In: Wise RR, Hoober JK (eds) The structure and functions of plastidstructure and function of plastids. Springer Netherlands, Dordrecht, pp 315–334

Davies KM, Bloor SJ, Spiller GB, Deroles SC (1998) Production of yellow colour in flowers: Redirection of flavonoid biosynthesis in *Petunia*. *Plant J* **13**: 259–266. doi: 10.1046/j.1365-313X.1998.00029.x

DeLoache WC, Russ ZN, Narcross L, Gonzales AM, Martin VJJ, Dueber JE (2015) An enzyme-coupled biosensor enables (*S*)-reticuline production in yeast from glucose. *Nat Chem Biol* **11**: 465–471. doi: 10.1038/nchembio.1816

Des Marais DL, Rausher MD (2008) Escape from adaptive conflict after duplication in an anthocyanin pathway gene. *Nature* **454**: 762–765. doi: 10.1038/nature07092

Doench JG, Fusi N, Sullender M, Hegde M, Vaimberg EW, Donovan KF, Smith I, Tothova Z, Wilen C, Orchard R, et al. (2016) Optimized sgRNA design to maximize activity and minimize off-target effects of CRISPR-Cas9. *Nat Biotechnol* **34**: 1–12. doi: 10.1038/nbt.3437

Dooner HK, Robbins TP, Jorgensen RA (1991) Genetic and developmental control of anthocyanin biosynthesis. *Annu Rev Genet* **25**: 173–199. doi: 10.1146/annurev.ge.25.120191.001133

Edwards K, Johnstone C, Thompson C (1991) A simple and rapid method for the preparation of plant genomic DNA for PCR analysis. *Nucleic Acids Res* **19**: 1349. doi: 10.1093/nar/19.6.1349

Fauser F, Schiml S, Puchta H (2014) Both CRISPR/Cas-based nucleases and nickases can be used efficiently for genome engineering in *Arabidopsis thaliana*. *Plant J* **79**: 348–359. doi: 10.1111/tpj.12554

Feng Z, Mao Y, Xu N, Zhang B, Wei P, Yang D-L, Wang Z, Zhang Z, Zheng R, Yang L, et al. (2014) Multigeneration analysis reveals the inheritance, specificity, and patterns of

CRISPR/Cas-induced gene modifications in *Arabidopsis*. *Proc Natl Acad Sci USA* **111**: 4632–4637. doi: 10.1073/pnas.1400822111

Forkmann G (1991) Flavonoids as flower pigments: The formation of the natural spectrum and its extension by genetic engineering. *Plant Breed* **106**: 1–26. doi: 10.1111/j.1439-0523.1991.tb00474.x

Forkmann G, Martens S (2001) Metabolic engineering and applications of flavonoids. *Curr Opin Biotechnol* **12**: 155–160. doi: 10.1016/S0958-1669(00)00192-0

Fraser PD, Truesdale MR, Bird CR, Schuch W, Bramley PM (1994) Carotenoid biosynthesis during tomato fruit sevelopment (Evidence for tissue-specific gene expression). *Plant Physiol* **105**: 405–413. doi: 10.1104/pp.105.1.405

Fray RG, Wallace A, Fraser PD, Valero D, Hedden P, Bramley PM, Grierson D (1995) Constitutive expression of a fruit phytoene synthase gene in transgenic tomatoes causes dwarfism by redirecting metabolites from the gibberellin pathway. *Plant J* **8**: 693–701. doi: 10.1046/j.1365-313X.1995.08050693.x

Fu Y, Foden JA, Khayter C, Maeder ML, Reyon D, Joung JK, Sander JD (2013) High-frequency off-target mutagenesis induced by CRISPR-Cas nucleases in human cells. *Nat Biotechnol* **31**: 822–826. doi: 10.1038/nbt.2623

Fukada-Tanaka S, Inagaki Y, Yamaguchi T, Saito N, Iida S (2000) Colour-enhancing protein in blue petals. *Nature* **407**: 581. doi: 10.1038/35036683

Fukui Y, Tanaka Y, Kusumi T, Iwashita T, Nomoto K (2003) A rationale for the shift in colour towards blue in transgenic carnation flowers expressing the flavonoid 3′,5′-hydroxylase gene. *Phytochemistry* **63**: 15–23. doi: 10.1016/S0031-9422(02)00684-2

Galpaz N, Ronen G, Khalfa Z, Zamir D, Hirschberg J (2006) A chromoplast-specific carotenoid biosynthesis pathway is revealed by cloning of the tomato *white-flower* locus. *Plant Cell* **18**: 1947–1960. doi: 10.1105/tpc.105.039966

Giuliano G, Bartley GE, Scolnik PA (1993) Regulation of carotenoid biosynthesis during tomato development. *Plant Cell* **5**: 379–387. doi: 10.1105/tpc.5.4.379

Giuliano G, Tavazza R, Diretto G, Beyer P, Taylor MA (2008) Metabolic engineering of carotenoid biosynthesis in plants. *Trends Biotechnol* **26**: 139–145. doi: 10.1016/j.tibtech.2007.12.003

Gomez-Roldan V, Fermas S, Brewer PB, Puech-Pagès V, Dun EA, Pillot J-P, Letisse F, Matusova R, Danoun S, Portais J-C, et al. (2008) Strigolactone inhibition of shoot branching. *Nature* **455**: 189–194. doi: 10.1038/nature07271

Gonzalez-Jorge S, Ha S-H, Magallanes-Lundback M, Gilliland LU, Zhou A, Lipka AE, Nguyen Y-N, Angelovici R, Lin H, Cepela J, et al. (2013) *Carotenoid cleavage dioxygenase4* is a negative regulator of β-carotene content in *Arabidopsis* seeds. *Plant Cell* **25**: 4812–4826. doi: 10.1105/tpc.113.119677

Hatlestad GJ, Sunnadeniya RM, Akhavan NA, Gonzalez A, Goldman IL, McGrath JM, Lloyd AM (2012) The beet *R* locus encodes a new cytochrome P450 required for red betalain production. *Nat Genet* **44**: 816–820. doi: 10.1038/ng.2297

Hayama R, Agashe B, Luley E, King R, Coupland G (2007) A circadian rhythm set by dusk determines the expression of *FT* homologs and the short-day photoperiodic flowering response in Pharbitis. *Plant Cell* **19**: 2988–3000. doi: 10.1105/tpc.107.052480

Higuchi Y, Sage-Ono K, Kamada H, Ono M (2007) Isolation and characterization of novel genes controlled by short-day treatment in *Pharbitis nil*. *Plant Biotechnol* **24**: 201–207. doi: 10.5511/plantbiotechnology.24.201

Higuchi Y, Sage-Ono K, Sasaki R, Ohtsuki N, Hoshino A, Iida S, Kamada H, Ono M (2011) Constitutive expression of the *GIGANTEA* ortholog affects circadian rhythms and suppresses one-shot induction of flowering in *Pharbitis nil*, a typical short-day plant. *Plant Cell Physiol* **52**: 638–650. doi: 10.1093/pcp/pcr023

Hirschberg J (2001) Carotenoid biosynthesis in flowering plants. *Curr Opin Plant Biol* **4**: 210–218. doi: 10.1016/S1369-5266(00)00163-1

Hoshino A, Jayakumar V, Nitasaka E, Toyoda A, Noguchi H, Itoh T, Shin-I T, Minakuchi Y, Koda Y, Nagano AJ, et al. (2016) Genome sequence and analysis of the Japanese morning glory *Ipomoea nil*. *Nat Commun* **7**: 13295. doi: 10.1038/ncomms13295

Huala E, Sussex IM (1993) Determination and cell interactions in reproductive meristems. *Plant Cell* **5**: 1157–1165. doi: 10.1105/tpc.5.10.1157

Huang F-C, Molnár P, Schwab W (2009) Cloning and functional characterization of carotenoid cleavage dioxygenase 4 genes. *J Exp Bot* **60**: 3011–3022. doi: 10.1093/jxb/erp137

Iida S, Hoshino A, Johzuka-Hisatomi Y, Habu Y, Inagaki Y (1999) Floricultural traits and transposable elements in the Japanese and common morning glories. *Ann N Y Acad Sci* **870**: 265–274. doi: 10.1111/j.1749-6632.1999.tb08887.x

Ilg A, Yu Q, Schaub P, Beyer P, Al-Babili S (2010) Overexpression of the *rice carotenoid cleavage dioxygenase 1 gene* in Golden Rice endosperm suggests apocarotenoids as substrates *in planta*. *Planta* **232**: 691–699. doi: 10.1007/s00425-010-1205-y

Imai Y (1931) Analysis of flower colour in *Pharbitis Nil*. *J Genet* **24**: 203–224. doi: 10.1007/BF02983854

Imai Y (1938) Genetic literature of the Japanese morning glory. *Japanese J Genet* **14**: 91–96. doi: 10.1266/jjg.14.91

Imamura S (1967) Photoperiodic induction and the floral stimulus. In: Physiology of flowering in *Pharbitis nil*. Japanese Society of Plant Physiologists, Tokyo, pp 15–28

Inagaki Y, Hisatomi Y, Iida S (1996) Somatic mutations caused by excision of the transposable element, *Tpn1*, from the *DFR* gene for pigmentation in sub-epidermal layer of periclinally chimeric flowers of Japanese morning glory and their germinal transmission to their progeny. *Theor Appl Genet* **92**: 499–504. doi: 10.1007/BF00224550

Inagaki Y, Hisatomi Y, Suzuki T, Kasahara K, Iida S (1994) Isolation of a *Suppressor-mutator/Enhancer*-like transposable element, *Tpn1*, from Japanese morning glory bearing variegated flowers. *Plant Cell* **6**: 375–383. doi: 10.1105/tpc.6.3.375

Inagaki Y, Johzuka-Hisatomi Y, Mori T, Takahashi S, Hayakawa Y, Peyachoknagul S, Ozeki Y, Iida S (1999) Genomic organization of the genes encoding dihydroflavonol 4-reductase for flower pigmentation in the Japanese and common morning glories. *Gene* **226**: 181–188. doi: 10.1016/S0378-1119(98)00571-X

Ito Y, Nishizawa-Yokoi A, Endo M, Mikami M, Toki S (2015) CRISPR/Cas9-mediated mutagenesis of the *RIN* locus that regulates tomato fruit ripening. *Biochem Biophys Res Commun* **467**: 76–82. doi: 10.1016/j.bbrc.2015.09.117

Iwasaki M, Nitasaka E (2006) The *FEATHERED* gene is required for polarity establishment in lateral organs especially flowers of the Japanese morning glory (*Ipomoea nil*). *Plant Mol Biol* **62**: 913–925. doi: 10.1007/s11103-006-9066-2

Jefferson RA, Kavanagh TA, Bevan MW (1987) GUS fusions: beta-glucuronidase as a sensitive and versatile gene fusion marker in higher plants. *EMBO J* **6**: 3901–3907

Jeknić Z, Jeknić S, Jevremović S, Subotić A, Chen THH (2014) Alteration of flower color in *Iris germanica* L. "Fire Bride" through ectopic expression of phytoene synthase gene (*crtB*) from *Pantoea agglomerans*. *Plant Cell Rep* **33**: 1307–1321. doi: 10.1007/s00299-014-1617-4

Jez JM, Bowman ME, Dixon RA, Noel JP (2000) Structure and mechanism of the evolutionarily unique plant enzyme chalcone isomerase. *Nat Struct Biol* **7**: 786–791. doi: 10.1038/79025

Katsumoto Y, Fukuchi-Mizutani M, Fukui Y, Brugliera F, Holton TA, Karan M, Nakamura N, Yonekura-Sakakibara K, Togami J, Pigeaire A, et al. (2007) Engineering of the rose flavonoid biosynthetic pathway successfully generated blue-hued flowers accumulating delphinidin. *Plant Cell Physiol* **48**: 1589–1600. doi: 10.1093/pcp/pcm131

Kawalleck P, Somssich IE, Feldbrügge M, Hahlbrock K, Weisshaar B (1993) Polyubiquitin gene expression and structural properties of the *ubi*4-2 gene in *Petroselinum crispum*. *Plant Mol Biol* **21**: 673–684. doi: 10.1007/BF00014550

Kikuchi R, Sage-Ono K, Kamada H, Ono M (2005) Efficient transformation mediated by *Agrobacterium tumefaciens* with a ternary plasmid in *Pharbitis nil*. *Plant Biotechnol* **22**: 295–302. doi: 10.5511/plantbiotechnology.22.295

Kim J, Smith JJ, Tian L, DellaPenna D (2009) The evolution and function of carotenoid hydroxylases in Arabidopsis. *Plant Cell Physiol* **50**: 463–479. doi: 10.1093/pcp/pcp005

Kim SH, Ahn YO, Ahn MJ, Jeong JC, Lee HS, Kwak SS (2013) Cloning and characterization of an *Orange* gene that increases carotenoid accumulation and salt stress tolerance in

transgenic sweetpotato cultures. *Plant Physiol Biochem* **70**: 445–454. doi: 10.1016/j.plaphy.2013.06.011

Kishimoto S, Ohmiya A (2009) Studies on carotenoids in the petals of compositae plants. *J Jpn Soc Hortic Sci* **78**: 263–272. doi: 10.2503/jjshs1.78.263

Kishimoto S, Ohmiya A (2006) Regulation of carotenoid biosynthesis in petals and leaves of chrysanthemum (*Chrysanthemum morifolium*). *Physiol Plantrum* **128**: 436–447. doi: 10.1111/j.1399-3054.2006.00761.x

Kishimoto S, Sumitomo K, Yagi M, Nakayama M, Ohmiya A (2007) Three routes to orange petal color via carotenoid components in 9 compositae species. *J Jpn Soc Hortic Sci* **76**: 250–257. doi: 10.2503/jjshs.76.250

Kitazawa D, Hatakeda Y, Kamada M, Fujii N, Miyazawa Y, Hoshino A, Iida S, Fukaki H, Morita MT, Tasaka M, et al. (2005) Shoot circumnutation and winding movements require gravisensing cells. *Proc Natl Acad Sci USA* **102**: 18742–18747. doi: 10.1073/pnas.0504617102

Kloer DP, Schulz GE (2006) Structural and biological aspects of carotenoid cleavage. *Cell Mol Life Sci* **63**: 2291–2303. doi: 10.1007/s00018-006-6176-6

Kumar S, Stecher G, Tamura K (2016) MEGA7: Molecular evolutionary genetics analysis version 7.0 for bigger datasets. *Mol Biol Evol* **33**: 1870–1874. doi: 10.1093/molbev/msw054

Lätari K, Wüst F, Hübner M, Schaub P, Beisel, Kim G, Matsubara S, Beyer P, Welsch R, Beisel, Kim G, Matsubara S, et al. (2015) Tissue-specific apocarotenoid glycosylation contributes to carotenoid homeostasis in Arabidopsis leaves. *Plant Physiol* **168**: 1550–1562. doi: 10.1104/pp.15.00243

Lei Y, Lu L, Liu HY, Li S, Xing F, Chen LL (2014) CRISPR-P: A web tool for synthetic single-guide RNA design of CRISPR-system in plants. *Mol Plant* **7**: 1494–1496. doi: 10.1093/mp/ssu044

Leitner-Dagan Y, Ovadis M, Shklarman E, Elad Y, Rav David D, Vainstein A (2006) Expression and functional analyses of the plastid lipid-associated protein CHRC suggest its role in chromoplastogenesis and stress. *Plant Physiol* **142**: 233–244. doi: 10.1104/pp.106.082404

Li L, Lu S, Cosman KM, Earle ED, Garvin DF, O'Neill J (2006) β-Carotene accumulation induced by the cauliflower *Or* gene is not due to an increased capacity of biosynthesis. *Phytochemistry* **67**: 1177–1184. doi: 10.1016/j.phytochem.2006.05.013

Li L, Yuan H (2013) Chromoplast biogenesis and carotenoid accumulation. *Arch Biochem Biophys* **539**: 102–109. doi: 10.1016/j.abb.2013.07.002

Li X, Jiang DH, Yong K, Zhang DB (2007) Varied transcriptional efficiencies of multiple *Arabidopsis U6* small nuclear RNA genes. *J Integr Plant Biol* **49**: 222–229. doi: 10.1111/j.1744-7909.2007.00393.x

Liu J, Yu J, McIntosh L, Kende H, Zeevaart JA (2001) Isolation of a *CONSTANS* ortholog from *Pharbitis nil* and its role in flowering. *Plant Physiol* **125**: 1821–1830. doi: 10.1104/pp.125.4.1821

Livak KJ, Schmittgen TD (2001) Analysis of relative gene expression data using real-time quantitative PCR and the $2^{-\Delta\Delta C}{}_T$ method. *Methods* **25**: 402–408. doi: 10.1006/meth.2001.1262

Lu S, Van Eck J, Zhou X, Lopez AB, O'Halloran DM, Cosman KM, Conlin BJ, Paolillo DJ, Garvin DF, Vrebalov J, et al. (2006) The cauliflower *Or* gene encodes a DnaJ

cysteine-rich domain-containing protein that mediates high levels of β-carotene accumulation. *Plant Cell* **18**: 3594–3605. doi: 10.1105/tpc.106.046417

Ly T, Fukuoka H, Otaka A, Hoshino A, Iida S, Nitasaka E, Watanabe N, Kuboyama T (2012) Development of EST-SSR markers of *Ipomoea nil*. *Breed Sci* **62**: 99–104. doi: 10.1270/jsbbs.62.99

Marin E, Nussaume L, Quesada A, Gonneau M, Sotta B, Hugueney P, Frey A, Marion-Poll A (1996) Molecular identification of zeaxanthin epoxidase of *Nicotiana plumbaginifolia*, a gene involved in abscisic acid biosynthesis and corresponding to the *ABA* locus of *Arabidopsis thaliana*. *EMBO J* **15**: 2331–2342. doi: 10.1002/j.1460-2075.1996.tb00589.x

Matsui T, Sawada K, Takita E, Kato K (2015) Compatibility of translational enhancers with various plant species. *Plant Biotechnol* **32**: 309–316. doi: 10.5511/plantbiotechnology.15.1103a

Mendel G (1950) Gregor Mendel's letters to Carl Nägeli, 1866-1873. *Genetics* **35**: 1–29

Meyer P, Heidmann I, Forkmann G, Saedler H (1987) A new petunia flower colour generated by transformation of a mutant with a maize gene. *Nature* **330**: 677–678. doi: 10.1038/330677a0

Mikami M, Toki S, Endo M (2015) Comparison of CRISPR/Cas9 expression constructs for efficient targeted mutagenesis in rice. *Plant Mol Biol* **88**: 561–572. doi: 10.1007/s11103-015-0342-x

Misawa N, Masamoto K, Hori T, Ohtani T, Boger P, Sandmann G (1994) Expression of an *Erwinia* phytoene desaturase gene not only confers multiple resistance to herbicides

interfering with carotenoid biosynthesis but also alters xanthophyll metabolism in transgenic plants. *Plant J* **6**: 481–489. doi: 10.1046/j.1365-313X.1994.6040481.x

Misawa N, Nakagawa M, Kobayashi K, Yamano S, Izawa Y, Nakamura K, Harashima K (1990) Elucidation of the *Erwinia uredovora* carotenoid biosynthetic pathway by functional analysis of gene products expressed in *Escherichia coli*. *J Bacteriol* **172**: 6704–6712. doi: 10.1128/jb.172.12.6704-6712.1990

Misawa N, Yamano S, Linden H, Felipe MR, Lucas M, Ikenaga H, Sandmann G (1993) Functional expression of the *Erwinia uredovora* carotenoid biosynthesis gene *crtI* in transgenic plants showing an increase of β-carotene biosynthesis activity and resistance to the bleaching herbicide norflurazon. *Plant J* **4**: 833–840. doi: 10.1046/j.1365-313X.1993.04050833.x

Moehs CP, Tian L, Osteryoung KW, DellaPenna D (2001) Analysis of carotenoid biosynthetic gene expression during marigold petal development. *Plant Mol Biol* **45**: 281–293. doi: 10.1023/A:1006417009203

Mol J, Cornish E, Mason J, Koes R (1999) Novel coloured flowers. *Curr Opin Biotechnol* **10**: 198–201. doi: 10.1016/S0958-1669(99)80035-4

Morita Y, Takagi K, Fukuchi-Mizutani M, Ishiguro K, Tanaka Y, Nitasaka E, Nakayama M, Saito N, Kagami T, Hoshino A, et al. (2014) A chalcone isomerase-like protein enhances flavonoid production and flower pigmentation. *Plant J* **78**: 294–304. doi: 10.1111/tpj.12469

Murashige T, Skoog F (1962) A revised medium for rapid growth and bio assays with tobacco tissue cultures. *Physiol Plantrum* **15**: 473–497. doi: 10.1111/j.1399-3054.1962.tb08052.x

Naito Y, Hino K, Bono H, Ui-Tei K (2015) CRISPRdirect: Software for designing CRISPR/Cas guide RNA with reduced off-target sites. *Bioinformatics* **31**: 1120–1123. doi: 10.1093/bioinformatics/btu743

Nakayama T (2002) Enzymology of aurone biosynthesis. *J Biosci Bioeng* **94**: 487–491. doi: 10.1016/S1389-1723(02)80184-0

Nakayama T, Yonekura-Sakakibara K, Sato T, Kikuchi S, Fukui Y, Fukuchi-Mizutani M, Ueda T, Nakao M, Tanaka Y, Kusumi T, et al. (2000) Aureusidin synthase: A polyphenol oxidase homolog responsible for flower coloration. *Science* **290**: 1163–1166. doi: 10.1126/science.290.5494.1163

Nisar N, Li L, Lu S, Khin NC, Pogson BJ (2015) Carotenoid metabolism in plants. *Mol Plant* **8**: 68–82. doi: 10.1016/j.molp.2014.12.007

Nishihara M, Nakatsuka T (2011) Genetic engineering of flavonoid pigments to modify flower color in floricultural plants. *Biotechnol Lett* **33**: 433–441. doi: 10.1007/s10529-010-0461-z

Nishihara M, Nakatsuka T, Yamamura S (2005) Flavonoid components and flower color change in transgenic tobacco plants by suppression of chalcone isomerase gene. *FEBS Lett* **579**: 6074–6078. doi: 10.1016/j.febslet.2005.09.073

Nishimasu H, Ran FA, Hsu PD, Konermann S, Shehata SI, Dohmae N, Ishitani R, Zhang F, Nureki O (2014) Crystal structure of Cas9 in complex with guide RNA and target DNA. *Cell* **156**: 935–949. doi: 10.1016/j.cell.2014.02.001

Nitasaka E (2003) Insertion of an *En/Spm*-related transposable element into a floral homeotic gene *DUPLICATED* causes a double flower phenotype in the Japanese morning glory. *Plant J* **36**: 522–531. doi: 10.1046/j.1365-313X.2003.01896.x

Niyogi KK (1999) PHOTOPROTECTION REVISITED: Genetic and Molecular Approaches. *Annu Rev Plant Physiol Plant Mol Biol* **50**: 333–359. doi: 10.1146/annurev.arplant.50.1.333

Niyogi KK (2000) Safety valves for photosynthesis. *Curr Opin Plant Biol* **3**: 455–460. doi: 10.1016/S1369-5266(00)00113-8

Noda N, Aida R, Kishimoto S, Ishiguro K, Fukuchi-Mizutani M, Tanaka Y, Ohmiya A (2013) Genetic engineering of novel bluer-colored chrysanthemums produced by accumulation of delphinidin-based anthocyanins. *Plant Cell Physiol* **54**: 1684–1695. doi: 10.1093/pcp/pct111

Noda N, Yoshioka S, Kishimoto S, Nakayama M, Douzono M, Tanaka Y, Aida R (2017) Generation of blue chrysanthemums by anthocyanin B-ring hydroxylation and glucosylation and its coloration mechanism. *Sci Adv* **3**: e1602785. doi: 10.1126/sciadv.1602785

Noman A, Aqeel M, Deng J, Khalid N, Sanaullah T, Shuilin H (2017) Biotechnological advancements for improving floral attributes in ornamental plants. *Front Plant Sci* **8**: 530. doi: 10.3389/fpls.2017.00530

Ohmiya A (2009) Carotenoid cleavage dioxygenases and their apocarotenoid products in plants. *Plant Biotechnol* **26**: 351–358. doi: 10.5511/plantbiotechnology.26.351

Ohmiya A, Kishimoto S, Aida R, Yoshioka S, Sumitomo K (2006) Carotenoid cleavage dioxygenase (CmCCD4a) contributes to white color formation in chrysanthemum petals. *Plant Physiol* **142**: 1193–1201. doi: 10.1104/pp.106.087130

Ohmiya A, Sumitomo K, Aida R (2009) “Yellow Jimba”: Suppression of carotenoid cleavage dioxygenase (*CmCCD4a*) expression turns white chrysanthemum petals yellow. *J Jpn Soc Hortic Sci* **78**: 450–455. doi: 10.2503/jjshs1.78.450

Ohmiya A, Toyoda T, Watanabe H, Emoto K, Hase Y, Yoshioka S (2012) Mechanism behind petal color mutation induced by heavy-ion-beam irradiation of recalcitrant chrysanthemum cultivar. *J Jpn Soc Hortic Sci* **81**: 269–274. doi: 10.2503/jjshs1.81.269

Ono E, Fukuchi-Mizutani M, Nakamura N, Fukui Y, Yonekura-Sakakibara K, Yamaguchi M, Nakayama T, Tanaka T, Kusumi T, Tanaka Y (2006) Yellow flowers generated by expression of the aurone biosynthetic pathway. *Proc Natl Acad Sci USA* **103**: 11075–11080. doi: 10.1073/pnas.0604246103

Ono M, Sage-ono K, Kawakami M, Hasebe M, Ueda K, Masuda K, Inoue M, Kamada H (2000) *Agrobacterium*-mediated regeneration and transformation of *Pharbitis nil*. *Plant Biotechnol* **17**: 211–216. doi: 10.5511/plantbiotechnology.17.211

Paine JA, Shipton CA, Chaggar S, Howells RM, Kennedy MJ, Vernon G, Wright SY, Hinchliffe E, Adams JL, Silverstone AL, et al. (2005) Improving the nutritional value of Golden Rice through increased pro-vitamin A content. *Nat Biotechnol* **23**: 482–487. doi: 10.1038/nbt1082

Park S, Kim HS, Jung YJ, Kim SH, Ji CY, Wang Z, Jeong JC, Lee H-S, Lee SY, Kwak S-S (2016) Orange protein has a role in phytoene synthase stabilization in sweetpotato. *Sci Rep* **6**: 33563. doi: 10.1038/srep33563

Polturak G, Breitel D, Grossman N, Sarrion-Perdigones A, Weithorn E, Pliner M, Orzaez D, Granell A, Rogachev I, Aharoni A (2016) Elucidation of the first committed step in

betalain biosynthesis enables the heterologous engineering of betalain pigments in plants. *New Phytol* **210**: 269–283. doi: 10.1111/nph.13796

Polturak G, Grossman N, Vela-Corcia D, Dong Y, Nudel A, Pliner M, Levy M, Rogachev I, Aharoni A (2017) Engineered gray mold resistance, antioxidant capacity, and pigmentation in betalain-producing crops and ornamentals. *Proc Natl Acad Sci USA* **114**: 9062–9067. doi: 10.1073/pnas.1707176114

Puchta H (2017) Applying CRISPR/Cas for genome engineering in plants: the best is yet to come. *Curr Opin Plant Biol* **36**: 1–8. doi: 10.1016/j.pbi.2016.11.011

Puchta H, Fauser F (2014) Synthetic nucleases for genome engineering in plants: Prospects for a bright future. *Plant J* **78**: 727–741. doi: 10.1111/tpj.12338

Rodrigo MJ, Alquézar B, Alós E, Medina V, Carmona L, Bruno M, Al-Babili S, Zacarías L (2013) A novel carotenoid cleavage activity involved in the biosynthesis of *Citrus* fruit-specific apocarotenoid pigments. *J Exp Bot* **64**: 4461–4478. doi: 10.1093/jxb/ert260

Römer S, Fraser PD, Kiano JW, Shipton CA, Misawa N, Schuch W, Bramley PM (2000) Elevation of the provitamin A content of transgenic tomato plants. *Nat Biotechnol* **18**: 666–669. doi: 10.1038/76523

Sage-Ono K, Ono M, Harada H, Kamada H (1998) Accumulation of a clock-regulated transcript during flower-inductive darkness in *Pharbitis nil*. *Plant Physiol* **116**: 1479–1485. doi: 10.1104/pp.116.4.1479

Saito N, Cheng J, Ichimura M, Yokoi M, Abe Y, Honda T (1994) Flavonoids in the acyanic flowers of *Pharbitis nil*. *Phytochemistry* **35**: 687–691. doi: 10.1016/S0031-9422(00)90588-0

Saitou N, Nei M (1987) The neighbor-joining method: a new method for reconstructing phylogenetic trees. *Mol Biol Evol* **4**: 406–425. doi: 10.1093/oxfordjournals.molbev.a040454

Sandmann G, Römer S, Fraser PD (2006) Understanding carotenoid metabolism as a necessity for genetic engineering of crop plants. *Metab Eng* **8**: 291–302. doi: 10.1016/j.ymben.2006.01.005

Sasaki N, Wada K, Koda T, Kasahara K, Adachi T, Ozeki Y (2005) Isolation and characterization of cDNAs encoding an enzyme with glucosyltransferase activity for *cyclo*-DOPA from four o'clocks and feather cockscombs. *Plant Cell Physiol* **46**: 666–670. doi: 10.1093/pcp/pci064

Satina S, Blakeslee AF, Avery AG (1940) Demonstration of the three germ layers in the shoot apex of datura by means of induced polyploidy in periclinal chimeras. *Am J Bot* **27**: 895–905. doi: 10.2307/2436558

Satoh J, Kato K, Shinmyo A (2004) The 5'-untranslated region of the tobacco *alcohol dehydrogenase* gene functions as an effective translational enhancer in plant. *J Biosci Bioeng* **98**: 1–8. doi: 10.1263/jbb.98.1

Schliemann W, Kobayashi N, Strack D (1999) The decisive step in betaxanthin biosynthesis is a spontaneous reaction. *Plant Physiol* **119**: 1217–1232. doi: 10.1104/pp.119.4.1217

Schreier PH, Seftor EA, Schell J, Bohnert HJ (1985) The use of nuclear-encoded sequences to direct the light-regulated synthesis and transport of a foreign protein into plant chloroplasts. *EMBO J* **4**: 25–32

Schwartz SH, Qin X, Zeevaart JAD (2003) Elucidation of the indirect pathway of abscisic acid biosynthesis by mutants, genes, and enzymes. *Plant Physiol* **131**: 1591–1601. doi: 10.1104/pp.102.017921

Schwartz SH, Qin X, Zeevaart JAD (2001) Characterization of a novel carotenoid cleavage dioxygenase from plants. *J Biol Chem* **276**: 25208–25211. doi: 10.1074/jbc.M102146200

Schwartz SH, Tan BC, Gage DA, Zeevaart JAD, McCarty DR (1997) Specific oxidative cleavage of carotenoids by VP14 of maize. *Science* **276**: 1872–1874. doi: 10.1126/science.276.5320.1872

Schwinn KE (2016) The dope on L-DOPA formation for betalain pigments. *New Phytol* **210**: 6–9. doi: 10.1111/nph.13901

Shan Q, Wang Y, Li J, Zhang Y, Chen K, Liang Z, Zhang K, Liu J, Xi JJ, Qiu J-L, et al. (2013) Targeted genome modification of crop plants using a CRISPR-Cas system. *Nat Biotechnol* **31**: 686–688. doi: 10.1038/nbt.2650

Shewmaker CK, Sheehy JA, Daley M, Colburn S, Ke DY (1999) Seed-specific overexpression of phytoene synthase: Increase in carotenoids and other metabolic effects. *Plant J* **20**: 401–412. doi: 10.1046/j.1365-313X.1999.00611.x

Shibuya K, Shimizu K, Niki T, Ichimura K (2014) Identification of a NAC transcription factor, EPHEMERAL1, that controls petal senescence in Japanese morning glory. *Plant J* **79**: 1044–1051. doi: 10.1111/tpj.12605

Shimada N, Nakatsuka T, Nishihara M, Yamamura S, Ayabe S, Aoki T (2006) Isolation and characterization of a cDNA encoding polyketide reductase in *Lotus japonicus*. *Plant Biotechnol* **23**: 509–513. doi: 10.5511/plantbiotechnology.23.509

Solymosi K, Keresztes A (2012) Plastid structure, diversification and interconversions II. Land plants. *Curr Chem Biol* **6**: 187–204. doi: 10.2174/2212796811206030003

Sprink T, Eriksson D, Schiemann J, Hartung F (2016) Regulatory hurdles for genome editing: process- vs. product-based approaches in different regulatory contexts. *Plant Cell Rep* **35**: 1493–1506. doi: 10.1007/s00299-016-1990-2

Sternberg SH, Redding S, Jinek M, Greene EC, Doudna JA (2014) DNA interrogation by the CRISPR RNA-guided endonuclease Cas9. *Nature* **507**: 62–67. doi: 10.1038/nature13011

Strack D, Vogt T, Schliemann W (2003) Recent advances in betalain research. *Phytochemistry* **62**: 247–269. doi: 10.1016/S0031-9422(02)00564-2

Sunnadeniya R, Bean A, Brown M, Akhavan N, Hatlestad G, Gonzalez A, Symonds VV, Lloyd A (2016) Tyrosine hydroxylation in betalain pigment biosynthesis is performed by cytochrome P450 enzymes in beets (*Beta vulgaris*). *PLoS One* **11**: e0149417. doi: 10.1371/journal.pone.0149417

Suzuki S, Nishihara M, Nakatsuka T, Misawa N, Ogiwara I, Yamamura S (2007) Flower color alteration in *Lotus japonicus* by modification of the carotenoid biosynthetic pathway. *Plant Cell Rep* **26**: 951–959. doi: 10.1007/s00299-006-0302-7

Suzuki Y, Saso K, Fujioka S, Yoshida S, Nitasaka E, Nagata S, Nagasawa H, Takatsuto S, Yamaguchi I (2003) A dwarf mutant strain of *Pharbitis nil*, Uzukobito (*kobito*), has defective brassinosteroid biosynthesis. *Plant J* **36**: 401–410. doi: 10.1046/j.1365-313X.2003.01887.x

Takeno K (2016) Stress-induced flowering: The third category of flowering response. *J Exp Bot* **67**: 4925–4934. doi: 10.1093/jxb/erw272

Tan BC, Joseph LM, Deng WT, Liu L, Li QB, Cline K, McCarty DR (2003) Molecular characterization of the Arabidopsis 9-*cis* epoxycarotenoid dioxygenase gene family. *Plant J* **35**: 44–56. doi: 10.1046/j.1365-313X.2003.01786.x

Tan BC, Schwartz SH, Zeevaart JAD, McCarty DR (1997) Genetic control of abscisic acid biosynthesis in maize. *Proc Natl Acad Sci USA* **94**: 12235–12240. doi: 10.1073/pnas.94.22.12235

Tanaka Y, Aida R (2009) Genetic engineering in floriculture. In: Jain SM, Brar DS (eds) Molecular Techniques in Crop Improvement. Springer Netherlands, Dordrecht, pp 695–717

Tanaka Y, Katsumoto Y, Brugliera F, Mason J (2005) Genetic engineering in floriculture. *Plant Cell Tissue Organ Cult* **80**: 1–24. doi: 10.1007/s11240-004-0739-8

Tanaka Y, Ohmiya A (2008) Seeing is believing: engineering anthocyanin and carotenoid biosynthetic pathways. *Curr Opin Biotechnol* **19**: 190–197. doi: 10.1016/j.copbio.2008.02.015

Tanaka Y, Sasaki N, Ohmiya A (2008) Biosynthesis of plant pigments: anthocyanins, betalains and carotenoids. *Plant J* **54**: 733–749. doi: 10.1111/j.1365-313X.2008.03447.x

Tian L, Musetti V, Kim J, Magallanes-Lundback M, DellaPenna D (2004) The *Arabidopsis LUT1* locus encodes a member of the cytochrome p450 family that is required for carotenoid epsilon-ring hydroxylation activity. *Proc Natl Acad Sci USA* **101**: 402–407. doi: 10.1073/pnas.2237237100

Trabelsi N, Petit P, Manigand C, Langlois d'Estaintot B, Granier T, Chaudière J, Gallois B (2008) Structural evidence for the inhibition of grape dihydroflavonol 4-reductase by

flavonols. *Acta Crystallogr Sect D Biol Crystallogr* **64**: 883–891. doi: 10.1107/S0907444908017769

Trezzini GF, Zryd J-P (1990) *Portulaca grandiflora*: A model system for the study of the biochemistry and genetics of betalain synthesis. *Acta Hortic* **280**: 581–585. doi: 10.17660/ActaHortic.1990.280.95

Tzuri G, Zhou X, Chayut N, Yuan H, Portnoy V, Meir A, Sa'Ar U, Baumkoler F, Mazourek M, Lewinsohn E, et al. (2015) A "golden" SNP in *CmOr* governs the fruit flesh color of melon (*Cucumis melo*). *Plant J* **82**: 267–279. doi: 10.1111/tpj.12814

Umehara M, Hanada A, Yoshida S, Akiyama K, Arite T, Takeda-Kamiya N, Magome H, Kamiya Y, Shirasu K, Yoneyama K, et al. (2008) Inhibition of shoot branching by new terpenoid plant hormones. *Nature* **455**: 195–200. doi: 10.1038/nature07272

Vallabhaneni R, Bradbury LMT, Wurtzel ET (2010) The carotenoid dioxygenase gene family in maize, sorghum, and rice. *Arch Biochem Biophys* **504**: 104–111. doi: 10.1016/j.abb.2010.07.019

van der Fits L, Deakin EA, Hoge JHC, Memelink J (2000) The ternary transformation system: constitutive *virG* on a compatible plasmid dramatically increases Agrobacterium-mediated plant transformation. *Plant Mol Biol* **43**: 495–502. doi: 10.1023/A:1006440221718

Vishnevetsky M, Ovadis M, Itzhaki H, Levy M, Libal-Weksler Y, Adam Z, Vainstein A (1996) Molecular cloning of a carotenoid-associated protein from *Cucumis sativus* corollas: homologous genes involved in carotenoid sequestration in chromoplasts. *Plant J* **10**: 1111–1118. doi: 10.1046/j.1365-313X.1996.10061111.x

Vogt T, Grimm R, Strack D (1999) Cloning and expression of a cDNA encoding betanidin 5-*O*-glucosyltransferase, a betanidin- and flavonoid-specific enzyme with high homology to inducible glucosyltransferases from the Solanaceae. *Plant J* **19**: 509–519. doi: 10.1046/j.1365-313X.1999.00540.x

Waibel F, Filipowicz W (1990) RNA-polymerase specificity of transcription of *Arabidopsis* U snRNA genes determined by promoter element spacing. *Nature* **346**: 199–202. doi: 10.1038/346199a0

Walter MH, Floss DS, Strack D (2010) Apocarotenoids: Hormones, mycorrhizal metabolites and aroma volatiles. *Planta* **232**: 1–17. doi: 10.1007/s00425-010-1156-3

Wei Y, Wan H, Wu Z, Wang R, Ruan M, Ye Q, Li Z, Zhou G, Yao Z, Yang Y (2016) A comprehensive analysis of carotenoid cleavage dioxygenases genes in *Solanum lycopersicum*. *Plant Mol Biol Report* **34**: 512–523. doi: 10.1007/s11105-015-0943-1

Willems E, Leyns L, Vandesompele J (2008) Standardization of real-time PCR gene expression data from independent biological replicates. *Anal Biochem* **379**: 127–129. doi: 10.1016/j.ab.2008.04.036

Winter D, Vinegar B, Nahal H, Ammar R, Wilson GV, Provart NJ (2007) An "electronic fluorescent pictograph" browser for exploring and analyzing large-scale biological data sets. *PLoS One* **2**: 1–12. doi: 10.1371/journal.pone.0000718

Wise RR, Hoober JK (2006) The structure and function of plastids. Springer Netherlands, Dordrecht

Yamada T, Ichimura K, Kanekatsu M, Van Doorn WG (2007) Gene expression in opening and senescing petals of morning glory (*Ipomoea nil*) flowers. *Plant Cell Rep* **26**: 823–835. doi: 10.1007/s00299-006-0285-4

Yamamizo C, Kishimoto S, Ohmiya A (2010) Carotenoid composition and carotenogenic gene expression during *Ipomoea* petal development. *J Exp Bot* **61**: 709–719. doi: 10.1093/jxb/erp335

Yamazaki Y, Akashi R, Banno Y, Endo T, Ezura H, Fukami-Kobayashi K, Inaba K, Isa T, Kamei K, Kasai F, et al. (2009) NBRP databases: Databases of biological resources in Japan. *Nucleic Acids Res* **38**: D26-32. doi: 10.1093/nar/gkp996

Ye X, Al-Babili S, Klöti A, Zhang J, Lucca P, Beyer P, Potrykus I (2000) Engineering the provitamin A (beta-carotene) biosynthetic pathway into (carotenoid-free) rice endosperm. *Science* **287**: 303–305. doi: 10.1126/science.287.5451.303

Yuan H, Owsiany K, Sheeja T, Zhou X, Rodriguez C, Li Y, Welsch R, Chayut N, Yang Y, Thannhauser TW, et al. (2015a) A single amino acid substitution in an ORANGE protein Promotes carotenoid overaccumulation in Arabidopsis. *Plant Physiol* **169**: 421–431. doi: 10.1104/pp.15.00971

Yuan H, Zhang J, Nageswaran D, Li L (2015b) Carotenoid metabolism and regulation in horticultural crops. *Hortic Res* **2**: 15036. doi: 10.1038/hortres.2015.36

Zhang B, Liu C, Wang Y, Yao X, Wang F, Wu J, King GJ, Liu K (2015) Disruption of a *CAROTENOID CLEAVAGE DIOXYGENASE 4* gene converts flower colour from white to yellow in *Brassica species*. *New Phytol* **206**: 1513–1526. doi: 10.1111/nph.13335

Zhang B, Yang X, Yang C, Li M, Guo Y (2016a) Exploiting the CRISPR/Cas9 system for targeted genome mutagenesis in petunia. *Sci Rep* **6**: 20315. doi: 10.1038/srep20315

Zhang D, Li Z, Li JF (2016b) Targeted gene manipulation in plants using the CRISPR/Cas technology. *J Genet Genomics* **43**: 251–262. doi: 10.1016/j.jgg.2016.03.001

Zhang H, Zhang J, Wei P, Zhang B, Gou F, Feng Z, Mao Y, Yang L, Zhang H, Xu N, et al. (2014) The CRISPR/Cas9 system produces specific and homozygous targeted gene editing in rice in one generation. *Plant Biotechnol J* **12**: 797–807. doi: 10.1111/pbi.12200

Zhou X, Welsch R, Yang Y, Álvarez D, Riediger M, Yuan H, Fish T, Liu J, Thannhauser TW, Li L (2015) *Arabidopsis* OR proteins are the major posttranscriptional regulators of phytoene synthase in controlling carotenoid biosynthesis. *Proc Natl Acad Sci USA* **112**: 3558–3563. doi: 10.1073/pnas.1420831112

Zhu C, Naqvi S, Breitenbach J, Sandmann G, Christou P, Capell T (2008) Combinatorial genetic transformation generates a library of metabolic phenotypes for the carotenoid pathway in maize. *Proc Natl Acad Sci USA* **105**: 18232–18237. doi: 10.1073/pnas.0809737105

Acknowledgements

I wish to express my sincere appreciation to Associate professor Michiyuki Ono (University of Tsukuba) for invaluable suggestions and encouragement throughout the course of my research.

I also wish to express my sincere appreciation to Drs. Chihiro Oda-Yamamizo and Akemi Ohmiya at Institute of Vegetable and Floriculture Science, National Agriculture and Food Research Organization (NARO) for invaluable suggestions, HPLC analysis and providing the *GPcLC* vector. I thank to Drs. Masaki Endo and Seiichi Toki at Plant Genome Engineering Research Unit, Institute of Agrobiological Sciences, NARO for invaluable suggestions and providing the vectors; pDeCas9-Kan, pMR203, pMR204 and pMR205. I owe a very important debt to Ms. Anna Kobayashi and Dr. Kimiyo Sage-Ono at University of Tsukuba for enormous contribution.

I'm grateful to the National BioResource Project (NBRP) "Morning glory," which is supported by the Agency for Medical Research and Development (AMED) Japan, for supplying the seeds of *I. nil* and information on the DNA sequence of *I. nil*. I also thank to Aomori Green BioCenter for providing the *Chrysanthemum F3H* promoter and pBI121 binary vector. I also thank to Dr. Ko Kato at Nara Institute of Science and Technology for providing sequences of tobacco *ADH* 5' UTR enhancer and *Arabidopsis HSP* terminator. I also express thanks to Mrs. Kazuyuki Onda and Shingo Ogata for their preliminary studies. I also thank Drs. Holger Puchta, Friedrich Fauser and Simon Schiml at the Karlsruhe Institute of Technology for providing the FFCas9 construct used in this study.

This work was partially financially supported by a Cooperative Research Grant of the Plant Transgenic Design Initiative (PTraD), Gene Research Center, T-PIRC, the University of Tsukuba.

I am grateful to the late Professor Hiroshi Kamada for advice on genome editing research and express my condolences.

List of publication

Watanabe Kenta, Oda-Yamamizo Chihiro, Sage-Ono Kimiyo, Ohmiya Akemi and Ono Michiyuki, Alteration of flower colour in *Ipomoea nil* through CRISPR/Cas9-mediated mutagenesis of *carotenoid cleavage dioxygenase 4*. *Transgenic Research* (in press). doi: 10.1007/s11248-017-0051-0.

Watanabe Kenta, Oda-Yamamizo Chihiro, Sage-Ono Kimiyo, Ohmiya Akemi and Ono Michiyuki, Overexpression of carotenogenic genes in the Japanese morning glory *Ipomoea* (*Pharbitis*) *nil*. *Plant Biotechnology* (in press). doi: 10.5511/plantbiotechnology.17.1016a.

Watanabe Kenta, Kobayashi Anna, Endo Masaki, Sage-Ono Kimiyo, Toki Seiichi and Ono Michiyuki (2017) CRISPR/Cas9-mediated mutagenesis of the *dihydroflavonol-4-reductase-B (DFR-B)* locus in the Japanese morning glory *Ipomoea (Pharbitis) nil*. *Scientific Reports* **7**:10028. doi:10.1038/s41598-017-10715-1.